Akademiya Nauk SSSR

V. A. Bronshten, Editor

THE PLANET JUPITER

Translated from Russian

Published for the National Aeronautics and Space Administration
and the National Science Foundation, Washington, D.C.
by the Israel Program for Scientific Translations

AKADEMIYA NAUK SSSR. VSESOYUZNOE ASTRONOMO-GEODEZICHESKOE OBSHCHESTVO
Academy of Sciences of the USSR. All-Union Astronomical and Geodetic Society

V. A. Bronshten, Editor

THE PLANET JUPITER

(Issledovaniya planety Yupiter)

Izdatel'stvo "Nauka"
Moskva 1967

Translated from Russian

Israel Program for Scientific Translations
Jerusalem 1969

NASA TT F-563
TT 69-55026

Published Pursuant to an Agreement with
THE NATIONAL AERONAUTICS AND SPACE ADMINISTRATION
and
THE NATIONAL SCIENCE FOUNDATION, WASHINGTON, D.C.

IPST Cat. No. 5442

Translated by A. Moscona
Edited by Z. Lerman

Printed in Jerusalem by IPST Press
Binding: Wiener Bindery Ltd., Jerusalem

Available from the
U.S. DEPARTMENT OF COMMERCE
Clearinghouse for Federal Scientific and Technical Information
Springfield, Va. 22151

VIII/16/3

Table of Contents

MOLECULAR ABSORPTION OF LIGHT IN JUPITER'S ATMOSPHERE AND THE SURFACE STRUCTURE OF THE PLANETARY CLOUD LAYER

V. G. TEIFEL'
Astrophysical Institute, Kazakh Academy of Sciences

INTRODUCTION

Jupiter's atmosphere may be described in broad outline by the following model:

a) the outer atmosphere, which is the gas layer above the surface of the continuous cloud cover around the planet;

b) the condensation zone or cloud layer, which is a mixture of gas and aerosols, comprising solid particles (crystals of substances with a relatively high melting point) in the upper part of the layer and liquid drops in the lower part;

c) the lower atmosphere, which is a high-pressure region where the gas is greatly compressed;

d) the transition zone, which is a relatively thin layer of matter in a semiliquid state, overlying the solid mantle of Jupiter.

The outer atmosphere apparently contains one or several ionized layers which form Jupiter's ionosphere, under which there may be a roughly isothermal stratosphere, and within a few kilometers above the cloud layer there may be an adiabatic troposphere. The cloud layer itself is probably in moist-adiabatic equilibrium, and the changes occurring on the visible surface of Jupiter, that of the cloud layer, are probably a reflection of circulation processes of much higher intensity which take place in the lower atmosphere. According to De Marcus /1/, under isothermal conditions the density in highly compressed hydrogen varies much more slowly than when the gas is under moderate pressure. Compressed hydrogen resembles a liquid, and the lower regions of Jupiter's atmosphere have been appropriately called a hydrogen "ocean."

For the time being only the outer atmosphere and the surface of the cloud layer are accessible to direct observation and study. The character of the deeper-lying layers of Jupiter's atmosphere may be deduced only from theoretical calculations, whose accuracy depends on the available observational data for the outer atmosphere and on the particular equations of state used for the pressures and temperature which presumably prevail in the lower layers of Jupiter's gaseous envelope. Unfortunately, the available information on Jupiter's outer atmosphere is quite inadequate for constructing a reliable model of the entire atmosphere of the planet. Thus, to date we have no exact knowledge of the quantitative chemical composition of the

atmosphere. Existing estimates of the hydrogen content are greatly divergent (~5 km-atm according to Zabriskie /2/, ~ 27 km-atm according to Spinrad and Trafton /3/, while Foltz and Rank /4/ assume on the basis of calculations and laboratory experiments an even higher content of H_2, without giving an exact value). The content of methane and ammonia, the other two easily detectable gases, is based only on Kuiper's findings /5/ dating from 1947, which have not been checked since.

Kuiper found a methane content of 15,000 cm-atm, and an ammonia content of 700 cm-atm. The estimates given in the literature for the relative content of helium in Jupiter's atmosphere are at wide variance with each other. The values normally adopted for the contents of H_2, CH_4, and NH_3 are taken to apply solely to the outer atmosphere, overlying the cloud surface which acts as a continuous reflecting veil.

Recently various investigators /6—8/ have expressed doubts in the validity of the assumption that the observed molecular absorption bands of the gases in Jupiter's atmosphere (as in the atmospheres of the other giant planets and Venus) originate exclusively in the part of the atmosphere above the cloud layer. In point of fact, the cloud layer consists of aerosol particles suspended in a gaseous medium. Due to multiple scattering by the aerosol particles, the light quanta traverse fairly long optical paths in the gas before emerging from the cloud layer, and they thus experience not only some absorption by the particles but also absorption by the gas molecules at certain wavelengths. No exact theory of this process, which could be directly applied to the interpretation of observational results, has yet been developed, but even rough calculations show that the optical path of a light ray in a gas-aerosol cloud medium, at the wavelengths corresponding to the molecular absorption bands, may be larger than the path in the clear gaseous atmosphere above the clouds. It thus seems that the existing quantitative estimates on the contents of gases in Jupiter's atmosphere, which usually refer to the outer atmosphere, will have to be revised.

A point which has not been properly elucidated is the structure of the cloud surface. Strictly speaking, this surface is not a geometrical concept, since it is impossible to draw a clearcut boundary between the clouds and the clear gaseous atmosphere. There apparently exists a certain zone of unknown thickness Δh where the density of the dispersed phase (the concentration of cloud particles) drops to zero. This zone may be level, overlying Jupiter's mantle at the same height throughout, it may show a regular variation in altitude from the equator to the poles or from the subsolar point to the limb, or else it may be distorted due to differences in the circulation conditions in the night and day halves of Jupiter. Variations in the altitude of the summits of the cloud layer (i. e., of the altitude of the zone where the density of the dispersed phase falls off to zero) cannot be detected by direct observations, either visual or photographic, because even with ideal instrumental resolution (0".02) we can only observe altitude differences of not less than 60 km. In actual practice atmospheric turbulence restricts the resolution to 0".1—0".2, so that altitude differences of hundreds of kilometers on Jupiter are just barely discernible. However, spectrophotometric measurements of the intensity of molecular absorption bands detect differences as small as 2—3 km in the altitude of the cloud summits, since the intensity of the methane and ammonia absorption bands is highly sensitive to small variations in the thickness of the gas layer above the clouds.

The investigation of the high-altitude structure of the visible surface of Jupiter's cloud cover is of interest in relation to the atmospheric circulation of the planet. There is total lack of agreement even concerning the nature of the dark belts on Jupiter's disk. According to V. G. Fesenkov /9/, the belts are produced by dark substances which are lifted up to the visible cloud surface, though normally they condense at a much lower level. Urey /10/ conversely maintains that the dark belts are regions of descending atmospheric currents and "clear sky", free from condensation products, i.e., cloud particles.

INTENSITY DISTRIBUTION OVER JUPITER'S DISK IN THE CONTINUOUS SPECTRUM AND IN THE ABSORPTION BANDS

The strongest absorption band in the visible spectrum of Jupiter is the 6190 Å band of methane. According to the author's observations of 1959–1962 its equivalent width is 19 ± 1 Å, and the residual intensity at the center of the band (relative to the continuous spectrum) $I_b/I_c = 0.79 \pm 0.01$.

From spectrograms of 1949, Hess /11/ found for this band an equivalent width of 16.2 ± 1.9 Å at Jupiter's equator. He also studied the spectra at latitude zones 10, 30, and 60° and on the planet's limb at the equator. He found that the absorption in the methane band does not increase toward the limb, as could be expected, but remains nearly constant and even somewhat decreases poleward. Under the assumption that absorption occurs only in the outer layer, Hess postulated that the summit of the cloud layer rises toward the limb (by about 10 km), and the optical thickness of the clear gaseous atmosphere correspondingly decreases, thus compensating for the increased absorption due to the oblique passage of light through the atmosphere near the limb. Hess associated the uplift of the effective cloud summit at the limb with a stronger evaporation of ammonia crystals near the subsolar point of Jupiter's disk and with the lower temperature on the morning and evening limb. Squires /12/ has shown, however, that such an assumption is not realistic, because the solar heat influx during 1.5–2 hours is sufficient for evaporating a mass of not more than 0.01 g/cm^2 of condensed ammonia and thus is much too low for the required effect (evaporation of at least 0.43 g/cm^2 NH_3 during the same time). Squires advanced another hypothesis according to which the upper part of Jupiter's cloud cover consists of cumulus clouds whose tops rise about 20–30 km above the main surface of the cloud layer. The line of sight reaches the base of the cumuli only near the center of the disk, and toward the limb the effective scattering level rises because the cloud bases are screened by the nearby cloud summits.

However, Squires' hypothesis is also debatable. Photometric studies show that the brightness decreases from the center to the limb approximately according to Lambert's law, the only difference being a slightly smaller gradient of limb darkening. This difference is due to the fact that in the case of Jupiter we are dealing not with a perfectly white matte surface but with a cloud layer, where both scattering and true absorption occurs. The observed intensity distribution along Jupiter's equator is in good agreement

with that theoretically calculated from Ambartsumyan's formulas /13/, originally derived for a layer of infinite optical thickness where the ratio between scattering and true absorption is expressed by

$$\tilde{\omega}_\lambda = \frac{\sigma_\lambda}{\sigma_\lambda + \varkappa_\lambda}, \tag{1}$$

where σ_λ is the scattering coefficient, and $\varkappa_\lambda$ is the coefficient of true absorption. The intensity of radiation reflected in any given direction by a layer with $\tau \to \infty$ and isotropic scattering properties is given by

$$I_\lambda(\eta, \xi) = \frac{\tilde{\omega}_\lambda}{4} S_\lambda \frac{\xi}{\eta + \xi} \varphi(\eta)\varphi(\xi). \tag{2}$$

Here $\eta = \cos i$; $\xi = \cos \varepsilon$ (i is the angle of incidence and ε is the angle of reflection); S_λ is the intensity of the incident radiation; $\varphi(\eta)$ and $\varphi(\xi)$ are auxiliary functions tabulated by Ambartsumyan and Chandrasekhar /14/.

At opposition ($\eta = \xi$) the relative intensity distribution over the disk will be

$$\frac{I}{I_0} = \left[\frac{\varphi(\eta)}{\varphi(1)}\right]^2. \tag{3}$$

$\varphi(\xi)$ and $\varphi(\eta)$ depend on the value of $\tilde{\omega}_\lambda$, and thus Jupiter's limb darkening is different at different wavelengths. Spectophotometric observations /15—17/ show that in the continuous spectrum true absorption increases at shorter wavelengths. This leads to the observed difference in the brightness distribution over the disk for different wavelengths—the blue-light curves, corresponding to a smaller $\tilde{\omega}_\lambda$, are flatter than those in orange light (Figure 1). In the dark belts the difference is more pronounced, in agreement with the observable increase in contrast between the dark and light belts as one passes from red to blue.

Thus the observed intensity distribution over Jupiter's disk is in fairly good agreement with the theoretical distribution, derived by assuming a flat planar scattering layer. If the cloud surface of Jupiter consisted of columnar cumulus-type cloud formations, in which the ratio between the height and the base diameter $\frac{h}{d} > 1$, the brightness distribution would follow a completely different pattern. Indeed, on approaching the limb we would not have an even surface inclined at the certain angle to the incident light but an aggregate of cumuliform surface elements each with its own slope, and effective reflection would take place from the cumulus flanks almost perpendicular to the incident light. Clearly, in that case the limb darkening would be much less than observed.

On the other hand if it is assumed in Squires' hypothesis that $\frac{h}{d} < 1$ or that the distance between the clouds $l \ll d$, the decrease produced by such cloud formations in the optical depth of the effective reflecting layer would be too small to offset the increased absorption in the methane band toward the limb due to the oblique propagation of light.

The intensities of the CH_4 6190 Å and 5430 Å bands in various sections of Jupiter's disk, as measured in 1958—1961, are given in /7, 18/. According

to the measurements, the absorption remains virtually constant over the entire disk. An additional study of the variation of the equivalent width of the CH_4 6190 Å band with the latitude on Jupiter's disk was performed in 1963 on an AZT-7 200-mm meniscus telescope. An ASP-9 spectrograph (dispersion 143 Å/mm for H_γ) was used to photograph the spectra of eight latitude zones. Jupiter's image was projected on the spectrograph slit by means of an enlarger, which gave the system an equivalent focal distance of 12 m. On these spectrograms the contours of the absorption band in the areas near the central meridian of the planet were measured photometrically. A total of 136 spectrograms were analyzed. The contours were used to determine the equivalent band width W_b and the band depth $R_b = 1 - \frac{I_b}{I_c}$, where I_b/I_c is the residual intensity at the center of the band, referred to the intensity of the continuous spectrum. The values of W_b and R_b are given in Table 1 for each of the latitude zones. The mean square error of one W_b measurement is $\sigma = \pm 1.6$ Å, and the average error of W_b for each zone is $\sigma_\varphi = \pm 0.4$ Å; n is the number of spectrograms.

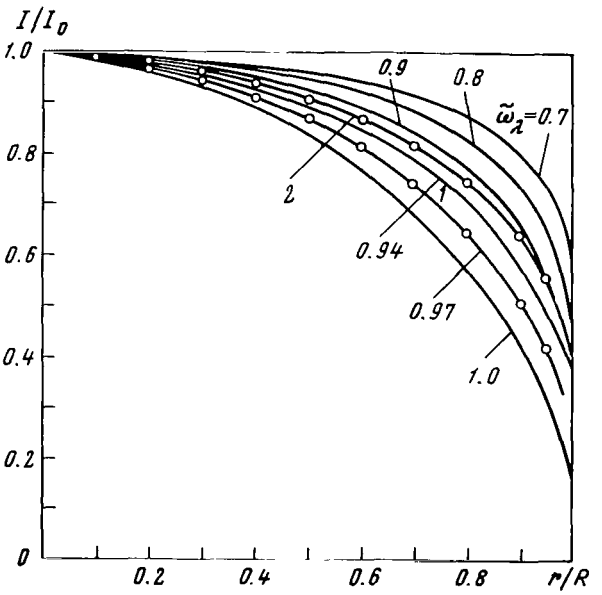

FIGURE 1. Limb darkening curves calculated by Ambartsumyan's formula for a planet with an atmosphere of infinite optical thickness, and the limb darkening along Jupiter's equator observed on 10–11 October 1963:

1–orange filter; 2–blue filter.

As may be seen from the table, the equivalent width of the CH_4 6190 Å absorption band is almost independent of the location on the disk and varies between 18.3 and 20.4 Å, i. e., by as little as ± 1 Å. If methane absorption

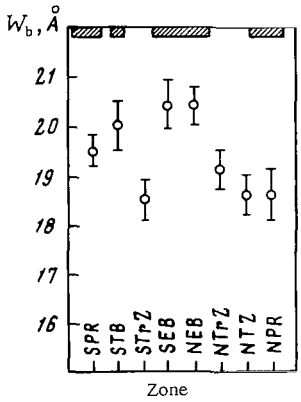

FIGURE 2. Equivalent width of the CH_4 6190 Å absorption band in various latitude zones on Jupiter. Vertical bars mark the probable range of error.

took place only in the outer layer of the atmosphere, the equivalent width of the absorption band at a latitude of about 50° should be twice as large as that at the equator, which is not the case.

A small biased difference is observed in the W_b for the belts and the zones (Figure 2). In the equatorial and south temperate belts the equivalent width is slightly larger than in the corresponding zones. If this difference is significant and is taken as an indication of differences in the level of the cloud layer summit, one can determine the difference in summit altitude in the belts and zones. This might also provide the means of finding whether Jupiter's belts are in fact breaks in the cloud layer or whether they are darker cloud areas with pigmented particles. First, however, we should analyze the possible causes for the observed constancy in the intensity of the absorption bands on Jupiter's disk, and also to ascertain if this constancy holds true for all the bands.

TABLE 1. Equivalent width and depth of the CH_4 6190 Å absorption band at various Jovian latitudes

Zone	Latitude range φ, degrees	W_b, Å	R_b	n
South polar region	-50 — -80	19.5	0.218	17
South temperate belt	-20 — -30	20.0	0.222	17
South tropical zone	-10 — -20	18.5	0.212	17
Southern equatorial belt	0 — -10	20.4	0.231	17
Northern equatorial belt	0 — +15	20.4	0.229	17
North tropical zone	+15 — +25	19.1	0.217	17
North temperate zone	+25 — +35	18.6	0.215	17
North polar region	+50 — +80	18.3	0.221	17

A SIMPLIFIED TWO-LAYER MODEL OF JUPITER'S ABSORBING ATMOSPHERE

Let us assume, as was done earlier in /7/ that true absorption by methane molecules (or some other absorbing gas) occurs not only in the outer atmosphere, which apparently consists mainly of clear gas, but also in Jupiter's cloud layer. In the clear gaseous atmosphere the true absorption lowers the value of $\tilde{\omega}_\lambda$, which in the absence of true absorption is equal to unity, and increases the optical thickness τ_b of the gas layer in discrete molecular bands. In the cloud layer, where besides light scattering by aerosol particles there is also continuous true absorption by pigmented particles, $\tilde{\omega}_\lambda$ is always somewhat smaller than unity. If the gas in which

the cloud particles are suspended also absorbs, we have inside the molecular absorption bands

$$\tilde{\omega}_b = \frac{\sigma}{\sigma + \varkappa + \varkappa_b}, \tag{4}$$

while outside the bands

$$\tilde{\omega}_c = \frac{\sigma}{\sigma + \varkappa}. \tag{5}$$

Clearly, $\tilde{\omega}_b < \tilde{\omega}_c$. If there were no clear gas layer above the cloud layer (which floats in a methane atmosphere), we would still observe the methane absorption band in Jupiter's spectrum. The same applies to the other gases in Jupiter's atmosphere. Actually, $\tilde{\omega}$ determines the albedo A of any planet surrounded by a cloud layer or by a gaseous atmosphere of infinite optical thickness, i.e.,

$$A = 1 - \varphi(\xi)\sqrt{1-\tilde{\omega}}. \tag{6}$$

Now since $\tilde{\omega}_b < \tilde{\omega}_c$, the reflectance of the cloud layer at the wavelength corresponding to the absorption band will be lower than the reflectance near the band, where $\varkappa_b = 0$, and the spectrum will show an absorption band whose intensity at any point is defined by the corresponding value of $\tilde{\omega}_b$, i.e.,

$$\frac{I_b}{I_c} = \frac{\tilde{\omega}_b}{\tilde{\omega}_c}\left[\frac{\varphi_b(\eta)}{\varphi_\pi(\eta)}\right]^2 \tag{7}$$

Calculations show that the observed absorption band should grow fainter toward the limb. If above the cloud layer there is a gas layer with an optical thickness τ_b in the absorption band, then, discounting multiple-scattering effects in the clear gas layer, we can write the following expression for the residual intensity at any point of the absorption band:

$$\frac{I_b}{I_c} = \frac{\tilde{\omega}_b}{\tilde{\omega}_c}\left[\frac{\varphi_b(\eta)}{\varphi_c(\eta)}\right]^2 e^{-\frac{2\tau_b}{\eta}}. \tag{8}$$

The optical thickness of the outer atmosphere in the continuous spectrum is taken equal to zero. Since Jupiter's atmosphere consists mainly of hydrogen and helium, which have low scattering coefficients, and the concentration of methane and ammonia is a fraction of a percent, the optical thickness of the outer atmosphere $\tau_c < 0.01$ over the entire visible range of the spectrum, and for $\lambda > 6000$ Å, $\tau_c < 0.001$.

Using (8) we can show that, given a certain ratio between the absorption in the outer atmosphere and in the cloud layer, the intensity of the absorption band will remain virtually constant over the disk almost to the limb. Since the absorption bands of methane, ammonia, and molecular hydrogen lie mainly in the red and infrared regions of the spectrum, we may approximately take $\tilde{\omega}_c$ equal to 0.97, in accordance with photometric data for Jupiter's disk (see Figure 1). Depending on the intensity of the absorption band, or on the intensity of its individual components, $\tilde{\omega}_b$ may assume

different values. The curves in Figure 3 show the calculation results for I_b / I_c from (8) using $\tilde{\omega}_b$ from 0.80 to 0.96, and τ_b values near which this equation yields a constant I_b/I_c ratio at least up to $r/R = 0.85 - 0.90$.

From these curves we can find the optical thickness of Jupiter's outer atmosphere at the center of the CH_4 6190 Å absorption band. In the one-layer model (methane absorption in the outer atmosphere only), τ_b is obtained from measurements of the absorption band, and is equal to 0.12. In the two-layer model we use the observed residual intensity I_b/I_c in the band and the fact that this intensity remains constant over the disk. According to the 1963 observations, $I_b/I_c = 0.78$. The closest fit with observational results is obtained with curve b, Figure 3, for $\tilde{\omega}_b = 0.95$ and $\tau_b = 0.03$. The curve is almost perfectly horizontal up to $r/R = 0.90$, and only beyond that point does the residual intensity start to decrease, i.e., the absorption increases. Since it is very difficult to perform spectroscopic observations near the limb—the slit must be placed nearly tangent to the limb and this gives a very narrow spectrogram—it is not clear how the molecular absorption behaves near the limb.

If the two-layer model of the absorbing atmosphere is correct, a comparison of observations with the theory shows that the quantity of methane above the cloud layer is much less than is normally assumed. We obtained for the optical thickness of the outer atmosphere in the 6190 Å methane band a value four times smaller than that obtained from the one-layer model. Thus depending on whether the growth curve (which relates the equivalent widths of the absorption lines and bands to the number of absorbing molecules) is a linear or a square-law function, the mass of methane above the cloud layer will have to be about 2.7 g/cm^2 or 5.4 g/cm^2, but not 10.7 g/cm^2 as was assumed by Kuiper /5/. This result must, of course, be used with considerable reservations, since it entails a radical revision of the relative and absolute composition of Jupiter's atmosphere, and accordingly requires new models for the vertical structure of the atmosphere.

With the exception of Hess's measurements, which are not sufficiently reliable, there are as yet no data on the variation of ammonia absorption over Jupiter's disk. In 1964 Münch and Younkin were reported /19/ to have found that the intensity of the quadrupole absorption line of molecular hydrogen was constant over Jupiter's disk. Further observations with high-dispersion spectrographs are required, in order to enable the individual components of the absorption bands to be studied.

To check the validity of the two-layer model, we need the behavior of the absorption band in the infrared. The infrared absorption of CH_4 is considerably stronger than that in the visible spectrum. Is the intensity of the infrared methane bands constant over Jupiter's disk?

The increase in the absorption band intensity results from an increase in $\varkappa_b$; the optical thickness τ_b of Jupiter's outer atmosphere varies with $\varkappa_b$ as

$$\tau_b = \varkappa_b H , \qquad (9)$$

where H is the scale height, and $\tilde{\omega}_b$ is related to this coefficient by equation (4). Let us examine the relative variation of the optical thickness τ_b and the factor $\tilde{\omega}_b$.

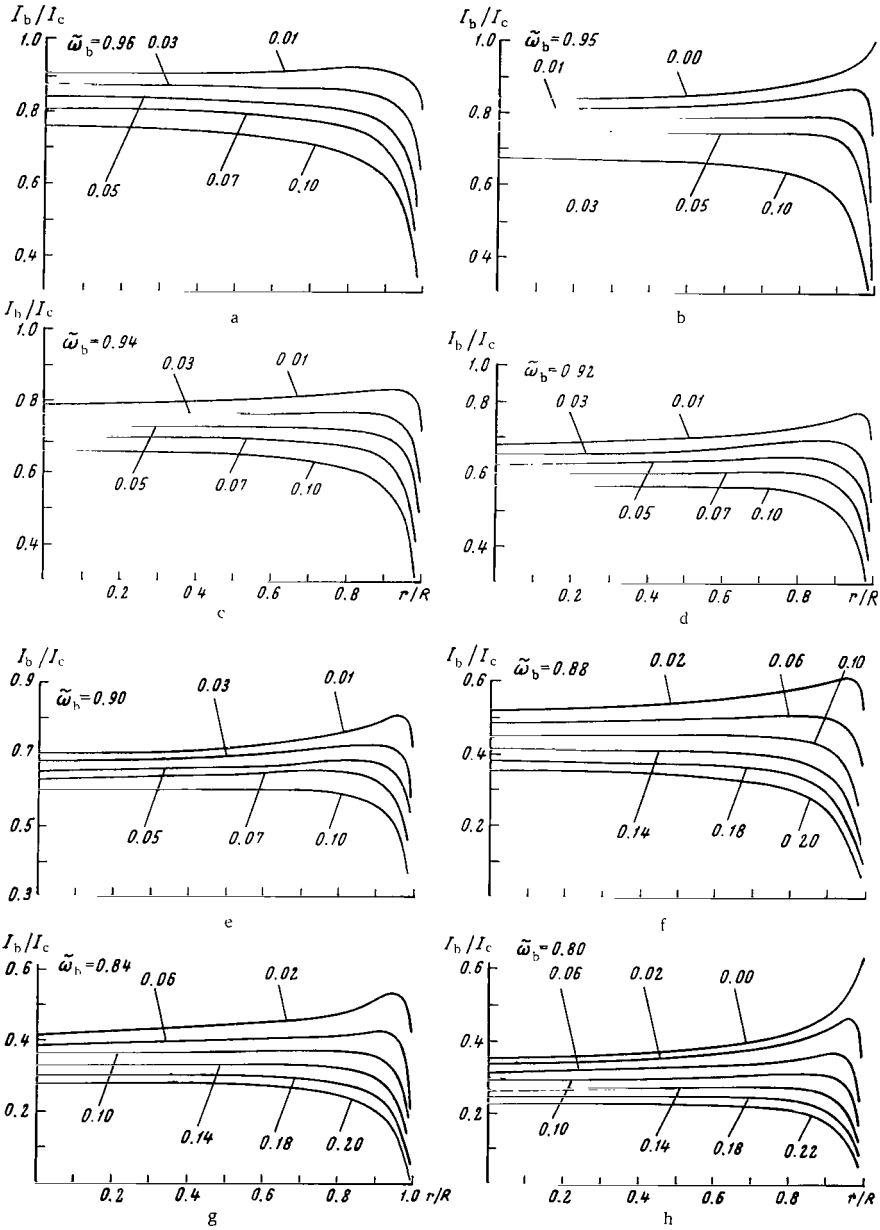

FIGURE 3. Curves of the residual intensities in the absorption bands for different values of $\tilde{\omega}_b$ and τ_b (a—h), in accordance with formula (8).

We rewrite (4) in the form

$$\tilde{\omega}_b = \frac{1}{1+\frac{\varkappa}{\sigma}+\frac{\varkappa_b}{\sigma}} = \frac{1}{\frac{1}{\tilde{\omega}_c}+\frac{\varkappa_b}{\sigma}} = \frac{1}{\frac{1}{\tilde{\omega}_c}+\frac{\tau_b}{H\sigma}}. \tag{10}$$

This gives the relation between $\tilde{\omega}_b$ and τ_b, if the product $H\sigma$ is known. This product can be approximately evaluated from the above values of $\tilde{\omega}_b$ and τ_b for the CH_4 6190 Å band. Thus

$$H\sigma = \frac{\tilde{\omega}_H \tilde{\omega}_b \tau_b}{\tilde{\omega}_c - \tilde{\omega}_b} = \frac{0.97 \cdot 0.95 \cdot 0.03}{0.97 - 0.95} \cong 1.4. \tag{11}$$

Then

$$\tilde{\omega}_b = \frac{1}{1.03 + 0.71\tau_b}. \tag{12}$$

It is assumed that the scattering coefficient is independent of the wavelength in the near infrared. Figure 4 gives τ_b as a function of $\tilde{\omega}_b$ (curve 1). Figure 3 shows, however, that the values of τ_b for which the absorption band intensity remains constant up to $r/R = 0.9$ are related to $\tilde{\omega}_b$ by a different function, shown in Figure 4 by curve 2. This curve is not as reliable as curve 1, because within the measurement accuracy we can observe a constant band intensity on the disk at values of τ_b differing by ± 0.01 to ± 0.02 from those corresponding to curve 2. Even so curves 1 and 2 greatly diverge for $\tilde{\omega}_b < 0.90$. This means that in the two-layer model the strong absorption bands of methane (and other gases) with residual intensity at the center $I_b/I_c < 0.6$ cannot have constant intensity over the disk. These bands require an outer atmosphere of much higher optical thickness than that needed for maintaining the intensity constant. Accordingly, as may be seen from Figure 3, the intensity of the strong bands should increase toward the limb. According to /19/, Münch and Younkin found by photoelectric scanning of Jupiter's disk in the infrared absorption bands of methane and ammonia up to λ 10,400 Å that these bands increased in intensity toward the poles, except the CH_4 8892 Å band which became lighter in the polar regions. The latter phenomenon still needs to be checked and explained. It is further necessary to carry out measurements on the equivalent width of the infrared bands of methane and ammonia, both as a function of latitude and at various distances from the central meridian. In order to test the validity of the two-layer model, it is important to investigate the band intensity over the disk as a function of $(I_b/I_c)_{\eta=1}$ and to compare the observations with the theoretical dependence.

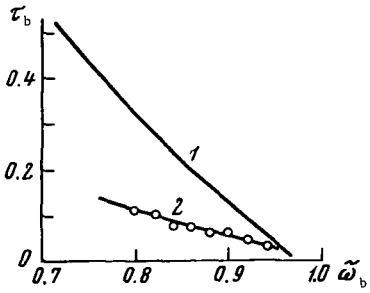

FIGURE 4. τ_b vs. $\tilde{\omega}_b$.

THE NATURE OF THE DARK BELTS AND THE POLAR REGIONS

Without going into the possible causes for the formation of the belts on Jupiter's disk (this belongs to the domain of hydrodynamics), let us consider, on the basis of photometric and spectroscopic observations, whether the belts can be areas of cloud-free atmosphere, as is assumed by Urey /10/ and Öpik /20/.

Photometry of Jupiter at different wavelengths shows that the contrast between the belts and the zones increases as one advances toward the shorter wavelengths (Table 2).

TABLE 2. Relative intensity of the equatorial belt on Jupiter's disk at different wavelengths

Filter	λ_{eff}, mμ	I_d / I_z		
		1962	1963	1964
KS-10 (red)	625	0.85	0.89	0.94
ZS-1 (green)	530	0.73	0.84	0.87
SS-5 (blue)	420	0.60	0.72	0.73
FS-7 (violet)	360	0.50	0.71	0.72

The contrast between the belts and the zones varies within wide limits from year to year, but the belts always appear darker in blue and violet light than in red and green. This indicates that the belts must be colored red or yellow against the light zones in Jupiter's cloud layer. Thus, the belts cannot be clear gas. As is known, scattering by gas molecules increases toward the shorter wavelengths. In that case the contrast of the belts should decrease as we pass from red to violet light. Öpik tried to avoid the inconsistency by introducing strong continuous true absorption in the deeper-lying layers of Jupiter's gaseous atmosphere. He did not explain, however, what could produce such absorption. Any gas showing strong true absorption must be different from all the currently known components of Jupiter's atmosphere. Up until now the attempts to discover by spectroscopic means any chemical compounds in Jupiter's atmosphere other than the known ones have failed, so that the presence of a strongly absorbing gas in Jupiter's atmosphere is debatable.

Still, let us assume that the dark belts are actually gaps in the cloud layer, through which shows the deeper-lying atmosphere which contains some absorbing gas with absorption increasing toward the shorter wavelengths. In red light, where the molecular absorption bands of methane, ammonia, and hydrogen are observed, the continuous true absorption cannot be very large, since the relative brightness of the belts $I_d \geqslant 0.85\, I_z$. This means that in red light we simply observe the deep-lying gaseous atmosphere. Obviously, since the clear gaseous atmosphere above the cloud layer has a small optical thickness in the continuous spectrum, the direct solar radiation should penetrate through the gas far below the top of the cloud layer, and accordingly there should be back-scattered radiation coming from the deeper-lying regions. As a result, due to the absorption of both the direct and the back-scattered radiation, the molecular absorption band in the cloud gaps ought to be stronger than in the light zones of the cloud cover.

If the gaseous atmosphere is adiabatic, the variation of the pressure with depth is given by

$$P = P_0\left(1 - \frac{\Gamma_a h}{T_0}\right)^{\frac{\bar{\mu} g}{R\Gamma_a}}, \qquad (13)$$

where $\Gamma_a = -\frac{dT}{dh}$ is the adiabatic lapse rate; $\bar{\mu}$ is the mean molecular weight of the atmosphere, g is the gravitational acceleration, P_0 and T_0 are the temperature and pressure at some reference level, R is the gas constant, and h is the height (taken with a minus sign in the direction of the planet's surface). Since the pressure is proportional to the number N of gas molecules in an atmospheric column of unit cross section, and since methane does not condense under Jupiter's atmospheric conditions, the number of absorbing molecules also varies with depth according to formula (13). We will assume that the CH_4 6190 Å absorption band falls on the linear part of the growth curve. The optical thickness $\tau_b \sim N$, and it thus varies with the depth in the same way as N. The residual intensity in the absorption band will accordingly vary in a similar manner. The rate of change depends on the model adopted for Jupiter's atmosphere, i.e., on the values of Γ_a, T_0 and $\bar{\mu}$, or, ultimately, on the chemical composition of the atmosphere. Figure 5 shows the curves of the residual intensity I_b/I_c at the center of the absorption band as a function of depth of the cloud surface, for two models of the atmosphere, which constitute the two extreme cases:

Model I:	$\bar{\mu} = 3.26$	$\Gamma_a = 3.44$ deg/km,	$T_0 = 160$ °K
Model II:	$\bar{\mu} = 4.02$	$\Gamma_a = 4.70$ deg/km,	$T_0 = 160$°K

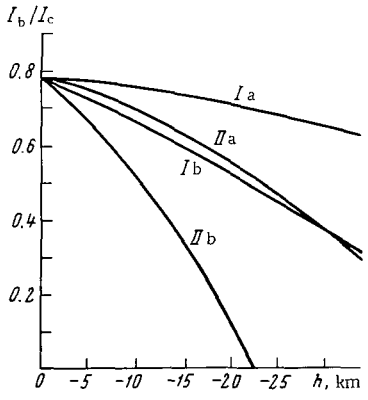

FIGURE 5. The residual intensity in the CH_4 6190 Å band as a function of depth of the cloud surface, for two different models of Jupiter's atmosphere:

Ia—model I, $\tau_b = 0.03$; Ib—model I, $\tau_b = 0.12$; IIa—model II, $\tau_b = 0.03$; IIb—model II, $\tau_b = 0.12$.

Suppose that the direct radiation penetrates through the gaps in the cloud layer only to a depth of 20 km below the cloud surface, and that further on diffusely scattered and reflected radiation becomes dominant. When the optical thickness of the outer atmospheric layer in the absorption band is $\tau_b = 0.03$, the residual intensity in model I changes by 0.08, i.e., by an amount which can easily be detected spectrophotometrically. If we take $\tau_b = 0.12$ (methane absorption in the outer atmosphere only), the residual intensity changes by 0.26. In model II the variation of the residual intensity with depth is even larger.

Now since the absorption toward the limb in a gas atmosphere increases proportionately to the secant of the angular distance from the center of the planetary disk, the absorption band should appear stronger toward the limb

in the belts, where the optical thickness for direct radiation is larger than in the zones; this is so because, in red light, $\tilde{\omega}_{c,d} \simeq \tilde{\omega}_{c,r}$ while $\tau_{b,d} > \tau_{b,r}$. Actually, however, the author /7/ has earlier observed that the methane absorption at λλ 6190 and 5430 Å remains constant also in the belts, whatever the distance from the center of the disk. The belts therefore apparently consist of the same cloud formations as the zones, but they contain darker particles which possibly differ from the lighter ones not only in coloration but also in size. The belt tops occurs nearly at the same altitude as the zone tops. Figure 5 and Table 1 enable us to fix the upper limit for the difference in altitude of the belt and zone tops in Jupiter's atmosphere. The observed difference of the residual density in the CH_4 6190 Å absorption band does not exceed 0.02, which yields according to curve Ia a maximum altitude difference of not more than 8 km, and by theother curves as little as 1—4 km.

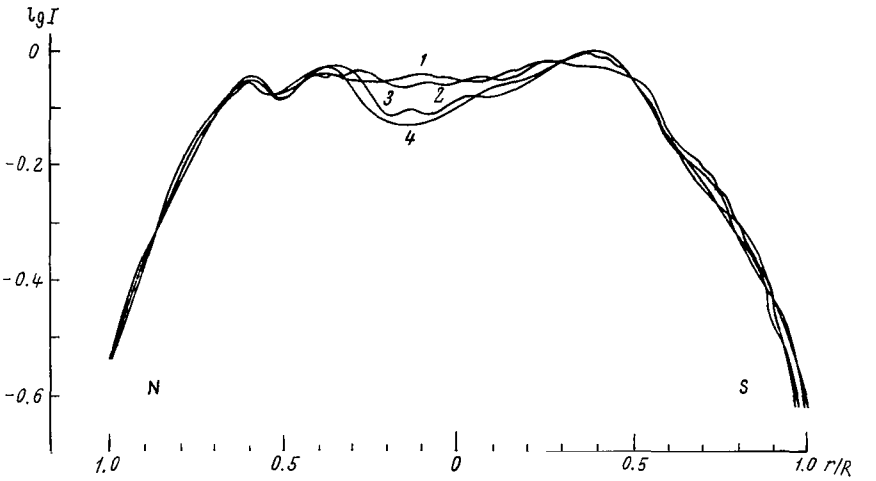

FIGURE 6. Limb darkening along Jupiter's central meridian in orange (1), green (2), blue (3), and violet (4) light, from photographs of 10—11 October 1963. In the polar regions the curves virtually coincide.

The same may be said of Jupiter's polar regions, which show a gray coloration. In recent years the northern polar region appears very dark, and it begins as far south as 30° lat. The dark matter in the polar regions has probably slightly different optical properties from the matter in the belts, because, according to 1963 photometric measurements, the brightness decrease toward Jupiter's poles was exactly the same both in red and in violet light (Figure 6), whereas in the equatorial belt there was a distinct difference in the limb darkening at different wavelengths (Figure 1).

It is known that Jupiter's polar regions display an anomalously high polarization, up to 6—7 %. Lyot /21/ and Gehrels and Teska /22/ account for it by assuming that over Jupiter's polar regions there is either no cloud cover at all, or else it lies at a much greater depth than at the temperate latitudes. The polarization then results from multiple scattering in the

outer gas layer, for which Gehrels and Teska derive an estimated optical thickness of 0.4—0.8 at λ 5500 Å. This is a very high value for the clear gaseous atmosphere. If it is correct, the optical thickness in the CH_4 6190 Å band should be at least 3 times larger, i.e., in the polar regions we should have $\tau_b > 1$, which is inconsistent with observations. The anomalous polarization may apparently be attributed to cloud particles of different size and shape than those in the clouds of the temperate zones, or to the presence of very fine particles in the outer atmosphere, which produce near-Rayleigh scattering that compensates the increased absorption by the dark matter in the short-wave region. This can also explain why the pole darkening is observed to be independent of the wavelength in the visible spectrum.

The author is indebted to L. V. Vetryachenko, A. N. Aksenov and V. F. Kartashov for assistance with the calculations.

Bibliography

1. De Marcus.—Astron. J., 58(2):36—37. 1953.
2. Zabriskie, F. R.—Astron. J., 67(3):168—170. 1962.
3. Spinrad, H. and L. M. Trafton.—Icarus, 2(1):19—28. 1963.
4. Foltz, J. W. and D. H. Rank.—Astrophys. J., 138(4): 1319—1321. 1963.
5. Kuiper, G. P. Atmospheres of Earth and Planets, Chicago. 1952.
6. Rozenberg, G. V.—Doklady AN SSSR, 148(2):300—302. 1963.
7. Teifel', V. G.—Izvestiya Komissii po Fizike Planet, 1:93—104. 1959.
8. Chamberlain, J. W. and G. P. Kuiper. Astrophys. J., 124(2): 399—405. 1956.
9. Fesenkov, V. G.—Izvestiya Astrofizicheskogo Instituta AN Kaz SSR, 1(1/2):239—251. 1955
10. Urey, H. C.—Handbuch der Physik, 52:363—418. 1959.
11. Hess, S. L.—Astrophys. J., 118(1):150—160. 1953.
12. Squires, P.—Astrophys. J., 126(1):185—194. 1957.
13. Ambartsumyan, V. A.—Nauchnye Trudy, 1:206—262. 1960.
14. Chandrasekar, S. Transfer of Radiant Energy [Russian translation. 1953].
15. Younkin, R. L. and G. Münch. La physique des planetes, pp. 125—136, Liège. 1963.
16. Teifel', V. G.—Izvestiya Astrofizicheskogo Instituta AN Kaz. SSR, 13:54—61. 1963.
17. Teifel', V. G.—Izvestiya AN Kaz. SSR, Seriya Fiziko-Matematicheskikh Nauk, Astrofizika, 16:74—77. 1963.
18. Teifel', V. G. and N. V. Priboeva.—Izvestiya AN Kaz. SSR, Seriya Fiziko-Matematicheskikh Nauk, Astrofizika, 16:61—73. 1963.
19. Sky and Telescope, 28(3):133. 1964.
20. Öpik, E. J.—Icarus, 1(3):200—257. 1962.
21. Lyot, B.—Ann. Observ. Paris (Sect. Meudon), 8, No. 1. 1929.
22. Gehrels, T. and T. M. Teska.—Communs Lunar and Planet. Lab., 1(22):167—177. 1962.

TENTATIVE PHOTOMETRY OF JUPITER'S ATMOSPHERIC ACTIVITY

A. N. AKSENOV
Astrophysical Institute, Kazakh Academy of Sciences

INTRODUCTION

The purpose of the present paper is to bring out a short-term periodicity in the activity fluctuations of Jupiter's atmosphere. Most authors have given only a qualitative description of the changes occurring in the planetary cloud envelope. The first quantitative study of the atmospheric activity was done by Shapiro /1/. Later on Focas and Banos /2/, in analyzing 1952—1963 Jupiter's photographs, introduced a quantitative measure for the activity of Jupiter's atmosphere, the activity coefficient R.

The only visible manifestation of the atmospheric activity are the changes in Jupiter's cloud envelope—the appearance of dark belts and light zones parallel to the planet's equator. The width and intensity of the belts and zones may be used as a quantitative activity characteristic of Jupiter's atmosphere.

According to Fokas and Banos /2/ the parameters of the belts depend on the amplitude of the turbulence function and the amplitude of the difference in the angular velocity between the equator and the poles. The instability of convective currents, the mixing of currents flowing with different velocities, and the drag between adjacent cells give rise to vertical motions which transfer condensed dark matter from the interior of the atmosphere to the top of the cloud layer. Thus, the atmospheric activity results in the concentration of dark matter on the visible surface of the planet. Fokas and Banos correspondingly define the overall activity coefficient R as the ratio of the total intensity of the belt areas to the total intensity of the spherical zone of brightness I. The photometric study of the activity of Jupiter's atmosphere accordingly amounts to measuring the intensity of the apparent surface features, as it varies with time.

All the negatives used by Fokas and Banos were obtained in yellow light with the 25- and 16-inch refractors at the National Observatory in Athens. Jupiter's photographs were on a scale of 4—5" to 1 mm. Fokas and Banos used 17 plates for the period of 1952—1953, of which 8 were taken in 1962. The remaining plates covered 1 year each. It is thus obvious that Fokas and Banos could not reveal the short-time variations in the activity of Jupiter's atmosphere.

OBSERVATIONAL DATA

In 1964 the Group for Planetary Studies of the Astrophysical Institute of the Kazakh Academy of Sciences launched a photographic survey of Jupiter. One of its aims was photometry of the active processes in the cloud layer of the planet.

The author analyzed 50 series of photographs of Jupiter, taken between August and November 1954 (observers: A. N. Aksenov, V. P. Kudashkin, N. V. Priboeva, V. G. Teifel'). The observations were made on the AZT-7 meniscus telescope ($D = 200$ mm) with ocular magnification ($f_{oc} = 10$ mm), fitted with an MFN-3 microphotographic attachment. The equivalent focal length of the system was 26.3 m, which gave images 5 — 6 mm in diameter. The photographs were taken on RF-3 film. Five spectral regions were covered, using light filters whose characteristics are listed in Table 1.

TABLE 1. Characteristics of the light filters

Filter	Transmission band	λ_{eff}, mμ	Exposure, sec
KS-10 (red)	590 — 660	610	20 and 15
OS-12 (orange)	540 — 650	600	5 and 3
ZS-1 (green)	470 — 600	520	15 and 10
SS-5 (blue)	360 — 510	420	5 and 3
FS-7 (violet)	280 — 460	360	10 and 7

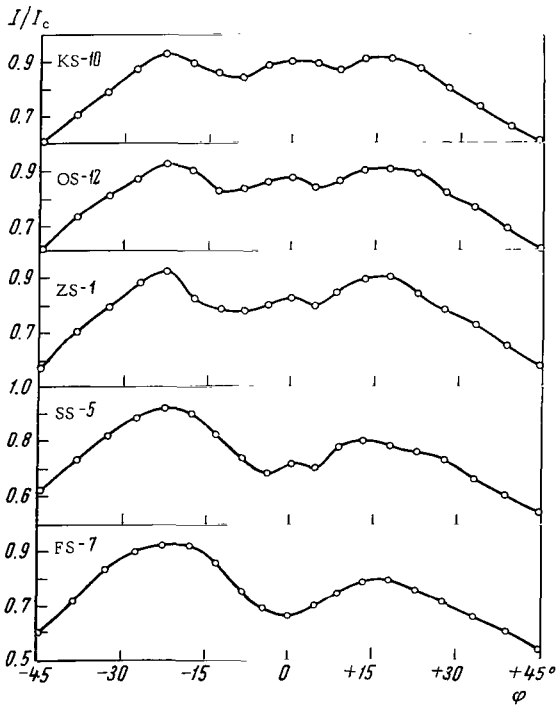

FIGURE 1. The photometric profile of Jupiter along the central meridian for different filters.

The negatives were calibrated with an FSR-1 step-wedge sensitometer (21 steps) and SS-5 (blue) and KS-10 (red) filters. The films were developed under carefully controlled conditions.

The photometry of the negatives was made on an MF-4 microphotometer. Photometric sections were taken along Jupiter's central meridian, and the intensity was measured at intervals of 0.1 mm.

The three best images in each series with each filter were used for photometry. The photometric profiles of Jupiter were plotted in log I vs. r coordinates, where r is the linear distance of the point on the photograph from the planetary equator, and I is the intensity at that point.

The profiles were graphically averaged over 3 photographs. The averaged profiles were used to determine the relative intensities I/I_c, where I is the intensity of a given point on the profile, and I_c is the intensity of the brightest point, reduced to the center of the planetary disk using Lambert's law.

The results were plotted as a function of the latitude (Figure 1). The activity coefficient can be reliably determined only within the zone between -45 and $+45°$ lat. The regions beyond these limits should not be included, as the brightness markedly decreases toward the poles and there are no clearly marked belts in those regions.

DETERMINATION OF THE ACTIVITY COEFFICIENT

The activity coefficient is defined as the ratio of the area occupied by the belts on the plot to the total area of the plot, and is given by

$$R = \frac{1}{C}\int_{-45°}^{+45°}\left(1 - \frac{I(\varphi)}{I_c}\right)d\varphi,$$

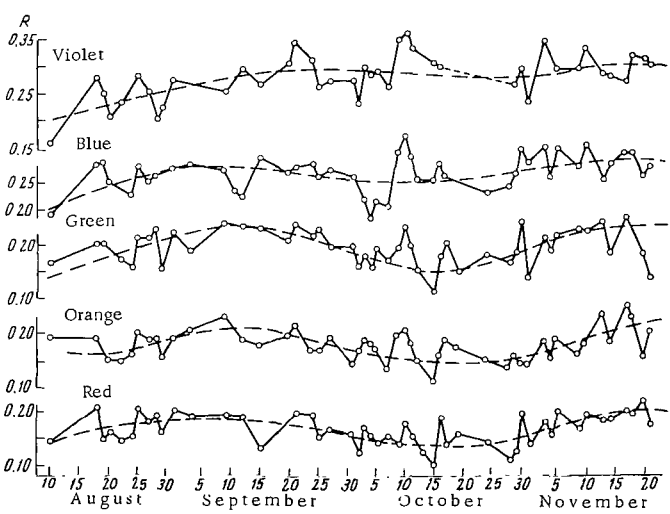

FIGURE 2. Activity variations of Jupiter during August-November 1964.

where φ is the latitude, $I(\varphi)/I_c$ is the relative intensity of a point lying inside the measured latitude range, and C is the total area of the plot.

The calculation results are summarized in Table 2 and plotted in Figure 2.

TABLE 2. The activity coefficient R

Date	Filter					Date	Filter				
	Red	Orange	Green	Blue	Violet		Red	Orange	Green	Blue	Violet
Aug.						Oct.					
10	0.145	0.196	0.164	0.192	0.160	10	0.178	0.204	0.229	0.328	0.354
18	0.205	0.189	0.198	0.279	0.274	11	0.147	0.181	0.193	0.290	0.328
19	0.148	—	0.201	0.283	0.246	12	0.120	0.149	0.149	0.254	—
20	0.159	0.150	—	0.251	0.203	15	0.096	0.106	0.109	0.250	0.300
22	0.143	0.147	0.172	0.233	0.231	16	0.183	0.155	0.175	0.283	0.296
24	0.150	0.161	0.156	0.223	—	17	0.134	0.185	0.199	0.260	—
25	0.204	0.200	0.209	0.276	0.279	19	0.155	0.171	0.146	—	—
27	0.182	0.186	0.211	0.247	0.246	24	0.141	0.145	0.176	0.226	—
28	0.188	0.190	0.227	0.260	0.197	28	0.106	0.136	0.161	0.238	—
29	0.160	0.155	0.154	—	0.219	29	0.122	0.155	0.178	0.260	0.262
31	0.202	0.191	0.221	0.274	0.270	30	0.193	0.141	0.236	0.305	0.292
Sept.						31	0.133	0.136	0.136	0.278	0.229
3	0.187	0.203	0.186	0.282	—	Nov.					
9	0.192	0.227	0.233	0.269	0.247	3	0.179	0.180	0.205	0.308	0.340
12	0.187	0.185	0.227	0.220	0.289	4	0.155	0.146	0.180	0.255	—
15	0.137	0.174	0.224	0.288	0.260	5	0.198	0.185	0.210	0.308	0.288
20	—	0.194	0.200	0.263	0.302	9	0.165	0.152	0.222	0.271	0.290
21	0.197	0.214	0.235	0.274	0.338	10	0.191	0.177	0.218	0.312	0.326
24	0.191	0.164	0.207	0.280	0.304	13	0.180	0.228	0.236	0.250	0.282
25	0.150	0.164	0.220	0.256	0.256	14	0.180	0.177	0.177	0.289	0.278
27	0.165	0.189	0.189	0.265	0.268	17	0.195	0.246	0.242	0.298	0.265
Oct.						18	0.188	0.224	0.222	0 302	0.314
1	0.156	0.141	0.193	0.257	0.269	20	0.215	0.149	0.175	0.256	0.310
2	0.120	0.166	0.155	0.249	0.224	21	0.171	0.195	0.133	0.273	0.295
3	0.171	0.185	0.174	0.215	0.296						
4	0.156	0.178	0.156	0.182	0.280						
5	0.142	0.170	0.190	0.214	0.287						
7	0.152	0.132	0.164	0.202	0.258						
9	0.137	0.193	0.188	0.301	0.342						

We tried to detect a correlation between the activity coefficient and the photographic quality of the images. The difference between the activity coefficients obtained from photographs of varying quality in the same period was found to lie within the measurement error.

VARIATION OF THE ACTIVITY COEFFICIENT

Figure 2 shows the variations in the atmospheric activity of Jupiter during August-November 1964. Maximum activity is noted in the first half of September. At that time the concentration of dark matter raised by atmospheric processes from the deeper-lying layers to the visible surface of the planet was the lightest.

In the second half of September, the activity starts declining, and the dark matter in the belts either sinks into the lower-lying layers of the

atmosphere or is mixed with lighter matter. As a result the contrast between the belts and the zones diminishes.

Minimum activity is noted in the second half of October. At that time the system of belts is fainter. Then there is another rise in activity, accompanied by the emergence of additional dark matter onto the cloud surface. The activity variations in Jupiter's atmosphere thus display a certain periodicity with a cycle of about 3 months. To what extent this periodicity is significant can be determined only after the observational material of 1964—1965 has been fully processed.

In conclusion it should be noted that the "jumps" in the activity coefficient are due not only to errors, but also to the fact that the observations were taken with the central meridian at different longitudes. Since the belts are of nonuniform intensity in longitude, there was a certain inhomogeneity in the observational material, which caused the "jumps."

The author is indebted to V. G. Teifel' for supervising the work.

Bibliography

1. Shapiro, R.—J. Meteorol., 10(5):350 - 355. 1953.
2. Focas, J. H. and C. J. Banos.- Ann. Astrophys., 27(1): 36—45. 1964.

LONG-TERM VARIATIONS IN THE WIDTH OF JUPITER'S BELTS

V. A. BRONSHTEN, A. N. SEDYAKINA, AND Z. A. STREL'TSOVA
All-Union Astronomical and Geodetic Society, Moscow Branch,
Department of Planets and the Moon

The width of the dark belts observed on Jupiter's disk undergoes constant, irregular variations. Many attempts have been made to detect some kind of periodicity in these variations, and possibly some connection with solar activity. However, no conclusive results have been obtained to date.

The Department of Planets and the Moon has been conducting since 1929 systematic visual observations of Jupiter's belts with a view to studying the changes which occur in them. The results of yearly observations were published in the form of tables listing the latitudes of the belt boundaries and graphs plotting their variations.

The visual observations and drawings of the position of Jupiter's belts were usually done by fairly inexperienced observers using 3 to 8" instruments, and their accuracy is not very high. However, the reduction method which averages the data of dozens of observations, lowers the mean square error to ± 0.5°. Also, by averaging the observations of different observers, the biased errors are eliminated or minimized.

The yearly observations of Jupiter's belts were processed by the grouping method, described in /1/.

Back in 1948, V. A. Bronshten tried to generalize the observations of Jupiter's belts for 1876—1937, using not only the Moscow observation series, but also other series of observations published in the astronomical literature. The data for 1876—1890 were discredited, however, because the observers (Russell, Hough, and de Boll) measured micrometrically only the latitude of the belt center. After 1894 there were series of micrometric measurements of the width of Jupiter's belts, taken by Nijland, Gledhill, Lamp, Hough, Mollesworth, and L. Struve, and a long series of measurements by Law (1905—1915). Further there were series of measurements from drawings made by A. N. Volokhov in 1916—1920 and by the Moscow Society of Amateur Astronomers in 1922—1925, and also a continuous series for 1929—1937 by the Department of Planets and the Moon.

A preliminary report of the results of 1894—1937 observations was given by Bronshten at the First All-Union Conference on Planetary Physics in May 1949 /2/. The width of the belts was seen to vary with a period of 3—5 years; the northern tropical belt was at maximum width when the southern was at its minimum, and vice versa. No correlation with solar activity was observed.

In 1963 the work was continued by A. N. Sedyakina and Z. A. Strel'tsova, on the basis of the observations for 1938, 1942, and an almost continuous

series for 1948—1961. Accordingly, the overall series of observations covers a period of 67 years (1894—1961), with some gaps (of up to 6 years).

All the observations used are summarized in Table 1.

TABLE 1. List of observations

Years	Observer	Method of observation	Number of observations	Source
1894—1899	A. Nijland	Micrometry	150	/3/
1896—1899	J. Gledhill	"		/4/
1896—1899	Hough	"		/5/
1896	E. Lamp	"		/6/
1903	P. Mollesworth	"		/7/
1903—1910	L. Struve, H. Lau	"		/8/
1913—1915	H. Lau	"		/9/
1916—1920	A.N. Volokhov	Drawings	96	/10/
1922	Moscow Society of Amateur Astronomers	"	42	/11/
1924—1925	Mirgorod amateur group	"	58	/12/
1929—1930	Moscow Society of Amateur Astronomers	"	198	/13/
1931	The same	"	96	/14/
1932	" "	"	50	/15/
1933—1935	MOVAGO* observation team	"	392	/16—18/
1936	The same	"	72	/19/
1937	A.M. Bakharev et al.	"	58	/20/
1938	MOVAGO* observation team	"	112	/21/
1942	Asenkov	"	22	/22/
1948	MOVAGO Department of Planets	"	104	/23/
1949	The same	"	102	/24/
1950	" "	"	104	/25/
1951	" "	"	130	/26/
1953—1954	" "	"	87	/27/
1955	" "	"	52	/28/
1956	" "	"		/29/
1957	" "	"	98	/30/
1958	" "	"	110	/31/
1959	" "	"	140	/32/
1960	G.K. Katagarov, V.A. Baranenko, et al.	"	146	/33/
1961	MOVAGO* Department of Planets	"		/34/

* [Moscow Branch of the All-Union Astronomical and Geodetic Society.]

The measurement results are given in Table 2 and plotted in Figures 1 and 2. They show the variations in the width of the northern and southern tropical belts (NTB and STB).

From an analysis of the graphs we can conclude the following:

1. The width of Jupiter's two tropical belts undergoes appreciable variations over 2—4 years, with an amplitude sometimes reaching 16° (1918—1920, STB). Normally, however, the amplitude of the variations is within 5—8°.

2. The STB width ranged during the relevant period within 5—16° (with the exception of a sharp narrowing in 1920), and the NTB width varied

within 4—16°. Between 1894 and 1932 the STB was almost always wider than the NTB; the widths subsequently equalized, and after 1950 the NTB became wider than the STB, though not considerably so.

TABLE 2. Width of Jupiter's tropical belts

Year	NTB	STB	ΣTB	Year	NTB	STB	ΣTB
1895	10.0	14.0	24.0	1929—1930	10.4	10.8	21.2
1896	4.0	13.0	17.0	1931	10.2	12.4	22.6
1897	14.7	15.4	30.1	1932	14.3	13.7	28.0
1898	4.7	13.1	17.8	1933	13.2	7.4	20.6
1899	12.9	13.0	25.9	1934	9.8	14.6	24.4
1903	5.6	8.6	14.2	1935	13.1	12.8	25.9
1904	—	10.6		1936	15.0	5.0	20.0
1905	—	13.3	—	1937	13.7	7.7	21.4
1907	—	13.6	—	1938	10.0	11.3	21.3
1908	—	13.5	—	1942	11.9	10.2	22.1
1909	—	12.5	—	1948	11.5	11.9	23.4
1910	—	14.1	—	1949	9.8	7.8	17.6
1913	—	12.8	—	1950	9.5	11.4	20.9
1914	—	12.2	—	1951	8.3	5.8	14.1
1915	9.6	9.2	18.8	1953—1954	13.4	11.1	24.5
1916—1917	13.6	14.2	27.8	1955	10.2	7.6	17.8
1918	7.1	16.3	23.4	1956	8.8	8.6	17.4
1919	10.3	7.6	17.9	1957	7.8	5.0	12.8
1920	9.0	12.2	21.2	1958	11.5	6.3	17.8
1921	4.0	13.0	17.0	1959	15.4	15.4	30.8
1922	10.6	13.2	23.8	1960	10.8	8.5	19.3
1924	12 7	14.1	26.8	1961	5.9	6.4	12.3
1925	8.9	13.4	22.3				
				Average	10.33	11.21	21.54

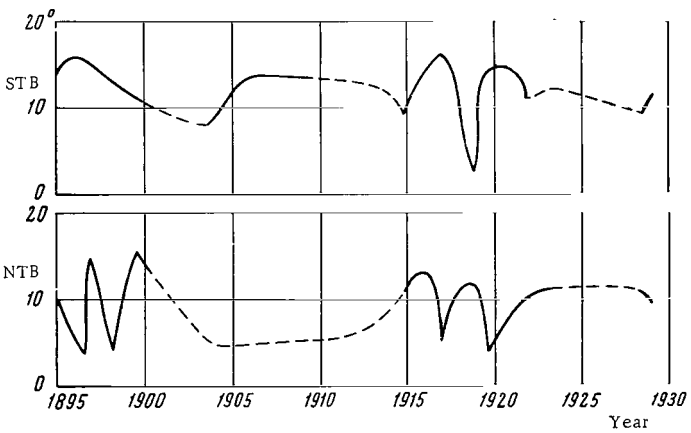

FIGURE 1. Variations in the width of Jupiter's tropical belts during 1895—1930.

3. During the periods of 1915—1924 and 1929—1939, which are well covered by observations, there is a clearly marked alternation of the maxima and minima in the width of the two belts which, as mentioned

previously, occur in cycles of about 3.5 years. The maxima are flat and the minima are sharp, maximum width of one belt corresponding to a minimum of the other.

4. During 1948—1951 the width of the belts showed variations with a mean period of 4.1 years, but in this case the maxima of the two belts occur at the same time and have sharper peaks.

5. Over this period the NTB width on the whole increases, and the STB width decreases: thus, the variations in the width of Jupiter's belts again occur in opposite directions in the two hemispheres.

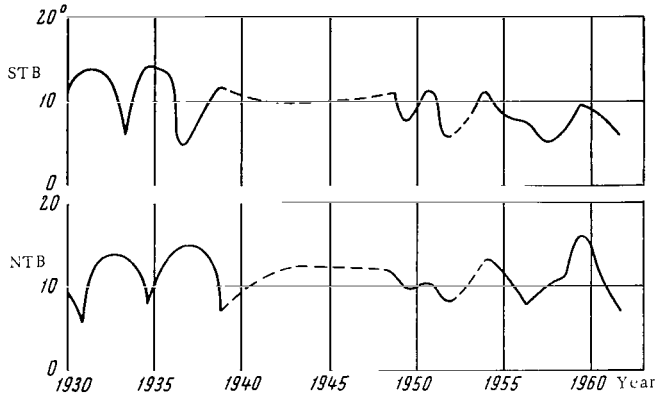

FIGURE 2. Variations in the width of Jupiter's tropical belts during 1930—1961.

In 1962 the two tropical belts merged near the equator /35/, and it was therefore impossible to follow any further the variations in the width of each belt separately.

6. The combined width of Jupiter's tropical belts varies within 15—30°, and does not display any periodicity. No connection is noted between the belt width variations and solar activity.

Bibliography

1. Bronshten, V.A. Planety i ikh nablyudenie (Planets and their Observation).—Gostekhizdat. 1957.
2. Bronshten, V.A. Konferentsiya po fizike planet (Conference on the Physics of Planets).—Byulleten' VAGO, No. 7(14). 1949.
3. Nijland, A.—Recherches astronomiques de l'Observatoire d'Utrecht, 4:18. 1911.
4. Gledhill, J. Measures of the Position of the Principal Belts of Jupiter.—MN, 56(9):478.1896; 57(9):648.1897; 60(1):45.1899.
5. Hough.—MN, 60(8):564. 1900.
6. Lamp, E.—AN, 140:169, 189.
7. Mollesworth, P.B.— MN, 65(7):702. 1905.
8. Lau, H.F.—AN, 171, No. 4097. 1906.

9. Lau, H. E. — AN, 195, Nos. 4673, 4708, 4796, 4943, 19...
10. Zateishchikov, G. O. Yupiter v 1916—1920 gg (Jupiter in 1916—1920). — Byulleten' KN VAGO, No. 45. 1937.
11. Shreider, A. A. Yupiter v 1922 g. (nablyudeniya so svetofil'trami) (Jupiter in 1922. (Observations with Light Filters)). — Byulleten' KN MOLA, No. 15. 1932.
12. Fedynskii, V. V. Yupiter v 1924g. (Jupiter in 1924). -- Byulleten' KN MOLA, No. 4. 1925; Yupiter v 1925g. (Jupiter in 1925). — Byulleten' KH MOLA, No. 7. 1926.
13. Pikel'ner, S. B. Yupiter v 1929—1930 gg. (Jupiter in 1929—1930). — Byulleten' VAGO, No. 4. 1939.
14. Bronshten, V. A. and T. D. Aristova. Yupiter v 1931g. (Jupiter in 1931). — Byulleten' KN VAGO, No. 42. 1937.
15. Bronshten, V. A. Yupiter v 1932g. (Jupiter in 1932). — Arkhiv VAGO.
16. Bronshten, V. A. Yupiter v 1933g. (Jupiter in 1933). — Byulleten' KN VAGO, No. 33. 1935.
17. Bronshten, V. A. Yupiter v 1934g. (Jupiter in 1934). — Byulleten' KN VAGO, No. 34. 1935.
18. Bronshten, V. A. Yupiter v 1935g. (Jupiter in 1935). — Byulleten' KN VAGO, No. 37. 1936.
19. Zateishchikov, G. O. Yupiter v 1936 g. (Jupiter in 1936). — Byulleten' VAGO, No. 1. 1939.
20. Bakharev, A. M. Yupiter v 1937 g. (Jupiter in 1937). — Byulleten' VAGO, No. 1. 1939.
21. Klyakotko, M. A. Yupiter v 1938 g. (Jupiter in 1938). — Byulleten' VAGO, No. 18(25). 1956.
22. Kurt, V. G. Yupiter v yanvare-fevrale 1942g. (Jupiter in January-February 1942). — Byulleten' VAGO, No. 12(19). 1952.
23. Shneider, R. G. and I. A. Shcherbo. Yupiter v 1948g. (Jupiter in 1948). — Byulleten' VAGO, No. 11(18). 1952.
24. Otdel planet i Luny MOVAGO, Yupiter v 1949g. (Department of Planets and the Moon MOVAGO, Jupiter in 1949). — Byulleten' VAGO, No. 18(25). 1956.
25. Margolina, V. L. and M. N. Stroganova. Yupiter v 1950g. (Jupiter in 1950). — Byulleten'. VAGO, No. 18 (25). 1956.
26. Fishkis, M. Ya. and G. F. Glagoleva. Yupiter v 1951g. (Jupiter in 1951). — Byulleten' VAGO, No. 18(25). 1956.
27. Shterenshtein, Zh. B. Yupiter v 1953—1954gg. (Jupiter in 1953—1954). — Byulleten' VAGO, No. 21(28). 1958.
28. Rutkovskaya, M. Ya. Yupiter v 1955g. (Jupiter in 1955). — Byulleten' VAGO, No. 25(32). 1959.
29. Vlasov, Yu. P. and I. T. Zotkin. Fotografirovanie Yupitera s okulyarnym uvelicheniem (Photographing of Jupiter with Ocular Magnification). — Byulleten' VAGO, No. 24 (31). 1959.
30. Tsvetkov, V. I. Polozhenie polos i detalei na Yupitere v 1957 g. (Location of the Belts and Other Features on Jupiter in 1937). — Byulleten' VAGO, No. 27(34). 1960.
31. Rutkovskaya, M. Ya. Polozhenie polos i detalei na Yupitere v 1958 g. (Location of the Belts and Other Features on Jupiter in 1958). — Byulleten' VAGO, No. 28(35). 1960.

32. Tsvetkov, V.I. Osnovnye polosy i detali na Yupitere v 1959 g.(Main Belts and Other Features on Jupiter in 1959).—Byulleten' VAGO, No. 34. 1963.
33. Baranenko, V.A. and F.K.Katagarov. Nablyudeniya Yupitera v 1960g.(Observations of Jupiter in 1960).—Byulleten' VAGO, No. 31 (38). 1962.
34. Strel'tsova, Z.A. Yupiter v 1961 g. (Jupiter in 1961).—Arkhiv VAGO.
35. Vsekhsvyatskii, S.K. Burnye protsessy na Yupitere (Violent Processes on Jupiter).—Astronomicheskii Tsirkulyar, No. 232. 1962; see also this collection, p. 30.

THE BELTS AND OTHER FEATURES ON JUPITER IN 1960

V. A. EGOROV
The V. I. Lenin Moscow State Teachers' Training College,
Moscow Branch of the All-Union Astronomical and
Geodetic Society

In 1960 the Department of Planets organized regular observations of Jupiter, with the participation of the amateur astronomers of the Moscow Planetarium. A 5-inch Zeiss refractor was used. The observations lasted from 22 June to 24 September, during which period 41 drawings of the planet were made. The drawings showed the intensity as well as the position of the features. About half of the drawings were prepared by experienced observers.

The latitudes of the belt edges, the polar caps, and other features were measured to within 1° by means of a graticule /1/. The drawings were divided into 7 groups, each containing 3 to 15 specimens drawn at about the same time. The mean latitude of the belts and the caps and the mean date of observation were calculated for each individual group. The intensity of the features was reduced in a similar manner.

The mean latitudes of the belts and the caps and the mean intensity of the features were calculated with allowance for the statistical weight of the measurements; thus, values which showed large deviations were assigned a lower weight.

The joviographic coordinates of the belts and other features were calculated from the measured coordinates, using the apparent coordinates of the disk center and of the central meridian /2/.

The intensity of the belts and the features was evaluated on a relative scale, in which 6 corresponds to the intensity of the satellite shadow on Jupiter's disk, and 0 corresponds to the intensity of the equatorial zone. The darkest spots can have an intensity of 5, and the brightest an intensity of -1 /1/. This evaluation is not very precise, though, because its accuracy is affected by the observational conditions and the observer's skill (Table 1).

The results were used to plot the variations in the latitude (Figure 1) and the intensity (Figure 2) of the belts and the caps.

Figure 1 plots the variations in the width of the polar caps, the two tropical belts, and the South Temperate Belt. The polar belts and the North Temperate Belt were hardly observable at all. The South Polar Cap and the South Temperate and Tropical belts do not extend over the entire time axis since the points with a question mark in Table 1 were omitted. We see that during the period of observation there were no appreciable variations in the width of the belts and the caps. The only exception is the North Polar Cap, whose width changed by as much as 6°.

The points in Figure 2 show a considerable spread due to the effect of observational conditions. The decrease in intensity on 13 August or the

increase on 23 September relative to the average occur simultaneously for most features. On the whole, the maximum variation in the intensity of the features does not exceed 1.5.

TABLE 1. Mean latitudes and intensities

Feature	Edge	Mean date						
		24 June	12 July	27 July	5 Aug	13 Aug	28 Aug	23 Sept
South Polar Cap	Northern	−40°	−39°	−39°	−39°	−42°	−44°?	
	I	2.3	2.3	2.1	2.4	2.2	2.2	
South Temperate Belt	Southern	−32?	−39	−39	−36?		−39?	
	Northern	−24?	−29	−29	−26?		−31?	
	I	3.4	3.6	2.8	3.0		3.5?	
South Tropical Belt	Southern	−10?	−16	−13	−8?	−13	−14	−14°
	Northern	−5?	−7	−7	−2?	−6	−7	−6
	I	3.0	3.0	3.1	2.8	2.0?	2.5	2.9
North Tropical Cap	Southern	5	4	4	5	1?	5	4
	Northern	14	13	14	16	9?	14	14
	I	3.7	3.9	3.5	3.7	2.8	3.5	4.3
North Polar Cap	Southern	32	33	30	33	32	36	32
	I	1.8	2.1	1.8	2.1	1.4	2.2	2.5

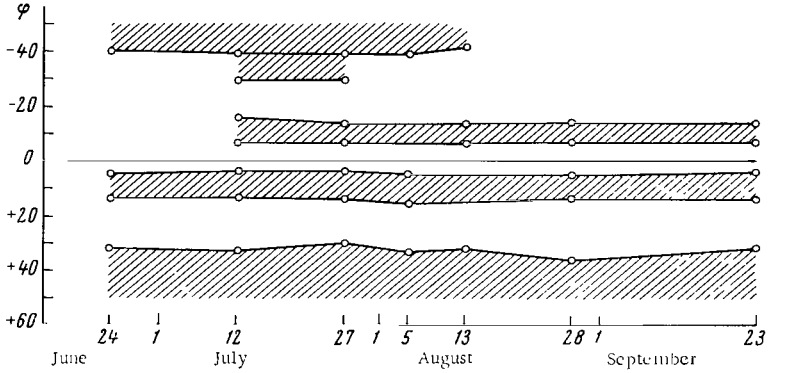

FIGURE 1. Variation in the position and the width of Jupiter's belts during June – September 1960

Among the features marked on the drawings, 4 were identified as permanent, and their mean coordinates and intensities were calculated. The features are shown in the drawings of N. V. Kirpichnikov (Figure 3), and their mean coordinates and intensities are given in Table 2.

The inaccuracies in the determination of the position, the size, and particularly the intensity of Jupiter's features are a serious shortcoming of the observations. It is therefore desirable to seek more effective methods of observation. Fairly good results were obtained by I. T. Zotkin, Yu. P. Vlasov, A. V. Zasov, and L. M. Ozernyi /3/, who photographed Jupiter with ocular magnification. This technique gives satisfactory

photographs which provide almost as much detail as drawings, even with small instruments. Microphotometric measurements may then be made on the photographs, supplying more objective and accurate results than can be obtained by the reduction of planetary drawings of the planet.

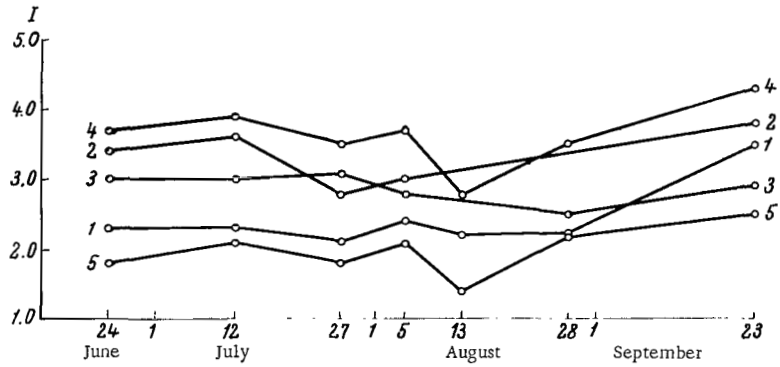

FIGURE 2. Variation in the intensity of Jupiter's belts during June—September 1960:

1—Southern Polar Cap; 2—South Temperate Belt; 3—South Tropical Belt; 4—North Tropical Belt; 5—North Polar Cap.

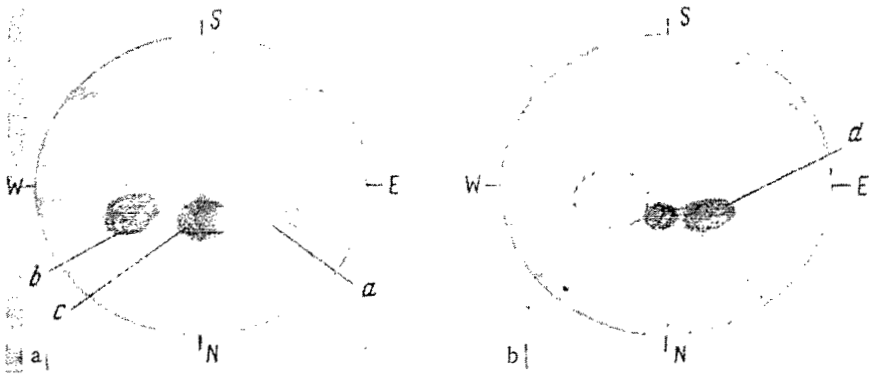

FIGURE 3. Drawings of Jupiter:

a—14 July (T_0 = 18 hrs 58.5 min); b—23 July (T_0 = 18 hrs 44 min). Observer N. V. Kirpichnikov. Features: a—light bridge, b, c, d—dark spots.

TABLE 2. Mean coordinates and intensity of features

Permanent feature	Mean Jovian latitude		Mean Jovian longitude		Mean intensity
	S-edge	N-edge	W-edge	E-edge	
Light bridge (a) (NTB)	+6°	+19°	21°	30°	0.8
Dark spot (b) (NTB)	+3	+16	320	339	3.9
Dark spot (c) (NTB)	+4	+16	356	10	3.8
Dark spot (d)	+3	+15	5	71	4.3

Bibliography

1. Bronshten, V.A. Planety i ikh nablyudeniya (Planets and their Observation).— Gostekhizdat. 1957.
2. Tsvetkov, V.I. Polozhenie detalei i polos na Yupitere v 1957g. (Location of Belts and Other Features on Jupiter in 1957).— Byulleten' VAGO, No. 27(34). 1960.
3. Vlasov, Yu.P. and I.T. Zotkin. Fotografirovanie Yupitera s okulyarnym uvelicheniem (Photographing of Jupiter with Ocular Magnification). — Byulleten' VAGO, No. 24(31). 1957.

VISUAL OBSERVATIONS OF JUPITER DURING THE FLARE OF 1961—1964

S. K. VSEKHSVYATSKII

1. In the course of three years (1961—1964) Jupiter's surface displayed some exceptionally rapid and radical changes /1—3/, which led to an adjustment of our current notions of the processes occurring on this planet.

From an analysis of a series of visual observations for the period of 1857—1962 (mainly by Lose, the observers of the British Astronomical Association, and Law, Plakidis, and Focas), and from Pic du Midi photographs and polarimetric observations in Athens, Focas concluded that the activity of the planet showed periodic variation with a cycle of about 20—22 years /4/.

The initial stage of activity is cataclysmic, leading to the formation of bright white spots, and also pairs and clusters of spots. This is followed by the appearance of dark nodules, which usually trail after the bright spots. The nodules eject dark filamentary streaks, which move toward the poles in the direction opposite to the sense of planetary rotation. The streaks develop into persistent bands and this stage marks the maximum activity. After the maximum, the dark bands, or belts, slowly grow fainter. The dark condensations and belts become lighter and narrower, as if showing through a semitransparent medium of steadily increasing thickness. The results of polarimetric measurements are consistent with a hypothesis of descending motion of dark matter. Focas suggests that the visible dark matter is produced by the atmospheric activity of the planet.

Activity minima (attenuation of the belts, general clearing of the planetary surface) occur, according to Focas, every 20—22 years; in the course of this cycle isolated regions may go through one or two activity maxima. During the century the activity in the Southern Hemisphere was higher than in the Northern.

2. According to Focas, 1961 was supposed to be a year near a minimum of activity. The actual planetary processes, however, disproved this prediction, as well as the presumed 11-year or 22-year periodicity in Jupiter's atmospheric circulation. In the second half of 1961 a radical change took place in the aspect of the planet. A wide and very dark equatorial girdle formed over the equatorial zone, with the concurrent disappearance of the usual South and North Equatorial Belts. These tremendous changes were accompanied by a strong increase in the brightness and color of the Red Spot and the onset of extremely active processes in both hemispheres.

A similar dark equatorial girdle was observed in 1872 (it may be seen in the drawings of Copeland, Flammarion, and Lose); at the same time the Red Spot flared up and was "rediscovered." The equatorial girdle persisted

for over 8 years (1872—1880). The violent changes of 1961 indicate a possible cycle of 80—90 years for planetary activity.

3. It would have been worth determining how and when the changes of 1961 actually took place. Unfortunately, at that time Jupiter had a large south declination and evening observations were difficult to perform in the Northern Hemisphere. Certain conclusions may nevertheless be drawn.

From the observations of 1960 /5, 6/, it is possible to note a descent of the South Equatorial Belt toward the equator (joviographic latitude -8 to -9°) and a strong activity in the area of the North Equatorial Belt. A unique photograph, taken by Marin at the Pic du Midi on 4 August 1961 /5/, shows the South Equatorial Belt even closer to the equator (- 7°), and the Equatorial Zone is crossed by dark streaks issuing from the NEB. It was apparently then that the Equatorial Zone first started filling up with dark matter. On 8 August 1961, photographs taken by Anderson with a 12-inch reflector /7/ show the Equatorial Zone completely filled with dark matter, forming a wide equatorial girdle, asymmetric with respect to the equator. The Red Spot, which flared up for a few days, is also distinct. The dark equatorial girdle persists, changing its appearance only in 1962 and 1963; it remains a distinctive feature on the surface of the planet to this day (1965).

Thus, Jupiter's previously light equatorial zone filled with dark matter during the short period between 4 and 8 August 1951; it should be noted that this could have been produced only by a catalysm of immense force, which apparently involved all longitudes of the Equatorial Zone.

4. Systematic visual observations of Jupiter were begun in Kiev on 25 December 1962, with an AZT-7 telescope (130 ×), and continued until 1 January 1963. The observations were resumed on 4 October 1963 and continued until 20 March 1964. During the first period the equatorial girdle showed a reddish-brown color, and the Red Spot was bright pink-red. The observations covered the development of a strong ejection in the South Temperate Zone. In Athens the beginning of the process was noted on 30 August 1962 /2/ at $\lambda_{II} = 220°$, and at the beginning of September at $\lambda_{II} = 140 - 240°$. Our observations showed how the light spot on the southern boundary of the equatorial girdle became framed with dark streaks, which were ejected at an angle of 70—80° to the parallel and then turned in the direction opposite to the sense of diurnal rotation. The geometry of the currents shows that the initial velocity of the dark matter should be at least several kilometers per second. In October and November the discharges in the South Temperate Zone stretched out into a belt which girdled the entire planet, crossed the South Temperate Zone at an angle, and ran into the Red Spot. Far from the ejection center, at the latitudes of 350—100°, the new belt broke down into distinct condensations, apparently due to large-scale turbulence.

At the same time on the northern boundary of the equatorial girdle and in the North Temperate Zone there appeared yellowish fog and isolated clouds, which must have concealed the dark areas of the equatorial girdle.

In 1963 there was very high activity in the North Temperate Zone, where an ejection produced a belt that almost touched the northern boundary of the equatorial girdle. During several weeks, the entire Northern Hemisphere and the Polar Cap remained appreciably darker than the Southern Hemisphere and the Polar Cap (outside the belt). The width of the equatorial girdle increased somewhat in 1963, though its intensity decreased

considerably; the width of the girdle varied between 0.22 and 0.25 of the polar diameter, and accordingly the girdle took up 0.32 of the area of the planetary disk.

5. From the first observations of Jupiter's surface in 1962 it became evident that the dark matter in the equatorial girdle must have considerably reduced the total brightness of the planet.

In 1962, 1963, and 1964 the ephemeris stellar magnitude of Jupiter was as follows:

	1962	1963	1964
24 October	$-2^m.2$	$-2^m.4$	–
25 November	-2.0	-2.3	–
27 December	-1.8	-2.1	–
14 January	–	–	$-1^m.9$

Jupiter's brightness was measured on 25 October 1962, and on 12, 13, and 23 January 1964. The observations were made by the reversed-binoculars method, whereby the reduced image of the planet (seen through the objective of the binoculars) is compared with stars observed with the unaided eye. Considerable experience has been gained in similar observations of lunar eclipses, and this made it possible to rely on the accuracy of the results. The following rules were carefully observed: 1) the reference stars were viewed with one eye, usually the left, while the right eye was covered with the binoculars; 2) the reference stars were chosen to be similar in color and at the same elevation as the planet; 3) the instrumental constant of the binoculars was measured in every observation, mainly using the zenith stars.

Use was made of low-power opera glasses, and its instrumental constant was found using the stars of Auriga and also those of Lyra and Cygnus; it proved to be 2 .33 (for the appropriate combinations of left and right eyes). Jupiter's brightness was compared with that of the stars in Orion, Auriga, and Taurus, when they were at the same elevation as the planet. The following results were obtained: 25 October 1962, $m_J = -1^m.8 \pm 0.15$; 12 January 1964, $m_J = -1^m.49 \pm 0.06$; 13 January 1964, $m_J = -1^m.60 \pm 0.08$; 23 January 1964; $m_J = -1^m.52 \pm 0.05$.

The brightness reduction due to the formation of the dark girdle was found to be $\Delta m = 0^m.35$, with an error not exceeding $\pm 0^m.05$.

Taking Allen's value for the mean albedo of the planet /8/ $a_{av} = 0.41$, and given the ratio of the area of the equatorial girdle to the disk area, we can find the albedo of the dark matter in the girdle. In fact, if I/I_0 is the ratio of the observed to the average brightness of the planet, we have

$$\frac{I}{I_0} = 2.512^{-\Delta m} = 1 - \frac{S_g}{S_0} + \frac{S_g}{S_0}\frac{a_g}{a_{av}}, \qquad (1)$$

where a_g is the sought albedo of the girdle, and S_g/S_0 is the ratio of the girdle area to the total disk area. In our case ($\Delta m = 0^m.35$, $S_g/S_0 = 0.32$) we obtain

$$a_g = \frac{0.045}{0.32} a_{av} \approx 0.06.$$

Even if $\Delta m = 0^m.25$ (and this is definitely lower than what our determination gives), $a_g = 0.14$. Accordingly, the dark material forming the equatorial girdle and the other belts of the planet have a reflectance of 0.06—0.1, the same as that of solid particles with the characteristics of terrestrial ash.

Significant variations in Jupiter's brightness, beyond all possible margin of error, had been noted before. In the course of 100 years the absolute magnitude of the planet fluctuated by $0^m.45$ during oppositions. Harris /9/ considered these fluctuations to be significant. A sharp decrease in Jupiter's brightness during the 1870's, in 1887—1890 and in 1916—1918 was associated with periods of maximum activity on the planet.

Taking into account the albedo of the dark matter in the belt and the activity pattern on the planet, we conclude that the belts are made up of ash particles injected into the upper layers of Jupiter's atmosphere by recurrent volcanic eruptions. The suspected periodicity of the processes on Jupiter (e.g., the 11-year or 20- to 22-year periodicity according to forecasts, the 4- to 5-year periodicity in the evolution of the North Equatorial Belt /10/, and the manifest 90-year interval between the cataclysmic processes on the planet) must reflect a periodicity in the evolution of volcanic processes, which is probably associated with the peculiarities of the planet's motion and the enhancement or weakening of tidal forces.

Consequently, continuous recording of the brightness with modern photoelectric equipment, in conjunction with observations of the surface, will make it possible to study the evolution of volcanic processes on Jupiter.

6. An analysis of the evolutionary pattern of Jupiter's belts leads to the following conclusions:

a) The belts on the planet mark the position of the centers of volcanic activity, which erupt during the entire time that the belt persists.

b) The latitudinal migration of the belts must be due to the appearance of new centers of volcanic activity. The formation of the equatorial girdle (1872, 1961) may be attributed only to the onset of tremendous volcanic processes in the equatorial zone or to the production of an ash ring around the planet due to the activity of its satellite. It is reasonable to assume that the concurrent disappearance of the North and the South Equatorial belts is due to an interaction between the gaseous masses accumulating in the coastal layer.

c) During an increase in volcanic activity on Jupiter (and undoubtedly on the other giant planets, as well) the integrated brightness may change not only because of the swelling and darkening of the belts, but also because of an overall pollution of the atmosphere with ash.

d) During the outbursts of activity the ash in the belts is apparently distributed above the mean level of the cloud cover. As the volcanic activity subsides and the injection of ash in a given area diminishes, the dark matter gradually settles through the cloud cover into the lower atmospheric layer. Accordingly, a minimum of volcanic activity should correspond to a general clearing of the atmosphere and a reduction of contrast between the zones and the belts.

7. It can be assumed that the ash particles on Jupiter are similar to the terrestrial ash particles and are comparable with the known types of ash. There are grounds to believe that the ash produced from liquid magma sprayed by a fast-moving jet of gas is subject to similar conditions both on Earth and on Jupiter; we may thus try to evaluate the minimum

amount of ash that would reduce the integrated brightness by $\Delta m = 0^m.45$, during a regular activity maximum.

By means of (1) we find that the area of the completely obscured regions constitutes $S/S_0 = 0.39$ of the total area of the planetary disk, which for Jupiter's ellipsoid corresponds to 0.31 of the spheroid surface area, or $0.9 \cdot 10^{20}$ cm^2. The size of terrestrial ash particles varies between wide limits; we may use the measurements for ash particles from the Caucasian system of Post-Tertiary deposits in South Moldavia /11/. For 80% of the particles, the size was 0.005—0.0005 cm (specific gravity 2.41, bulk density 0.8). According to Dolfus /12/, polarimetric studies of ash from Vesuvius gave a particle size between 0.03 and 0.4 cm.

The mass absorption coefficient K (cm^2/g) at $\lambda = 4400$ Å, of dielectric and metal dust particles with the above diameters has the following values /13/:

Particle size, cm	0.005 - 0.0005	0.4—0.03
Dielectric dust	500 - 5000	7—60
Metal particles	30 - 250	0.5—5

We take $\tau = 10$ for the optical thickness of the ash-saturated medium on Jupiter, which is not an exaggeration, considering the overall opacity in regions of terrestrial volcanic eruptions. In that case $M = \frac{\tau}{K}$ g/cm^2 gives the quantity of matter above 1 cm^2 of the planetary surface. Given the maximum values of K above, we obtain $M = 4$ to 4000 g/cm^2 or on the average 10 to 100 g/cm^2. Taking the entire area S of the ash-saturated region, we obtain the following estimate for the minimum amount of ash in Jupiter's atmosphere at times of peak activity:

$$S \cdot M = 1.9 \cdot 10^{20} \cdot (10^1 - 10^2)\,\text{g} \approx 2 \cdot 10^{21} - 2 \cdot 10^{22}\,\text{g}.$$

During the eruption of the Tambora in 1815, the total amount of dust which fell out within a radius of 1000 kilometers amounted to about 200 km^3. Taking the particle density equal to unity we find that $2 \cdot 10^{17}$ g were lifted over an area of $3 \cdot 10^{15}$ cm^2. Assuming that similar conditions prevail over the equatorial girdle on Jupiter, we obtain for the total amount of ash on the planet

$$\frac{1.9 \cdot 10^{20}}{3 \cdot 10^{15}} \cdot 2 \cdot 10^{17}\,\text{g} \approx 1.3 \cdot 10^{21}\,\text{g},$$

i.e., a figure of the same order as above. Admittedly, this fit could be accidental, considering that we have no data on the height of the Jovian atmosphere, the velocity of motion and the turbulence of the atmospheric masses, and the degree of mixing between the warm and cold parts of the atmosphere (which probably contain ice crystals and ammonia "snow"). Our calculation can be taken only as a rough approximation to the minimum amount of ash present in Jupiter's atmosphere.

Further study of the changes in Jupiter's belts, together with accurate photometric recording of the integrated brightness of the planet, would make it possible to determine the conditions in the atmosphere and down on the surface, which is apparently hot (as indicated by the presence of a

gaseous atmosphere), and also to ascertain if and how the ash particles precipitate from the atmosphere.

BASIC FINDINGS FROM THE OBSERVATIONS OF 1962—1964

1. The observations of Jupiter, which were begun in Kiev in September 1962 (in 1961 no observations could be carried out in Kiev due to the low position of the planet), showed the presence of a dark equatorial girdle (EG) and the STeB, which were the most prominent features on the disk. The EG was brick-brown, its color differing from that of the Red Spot (bright pink-red) and the STeB. Violent activity developed in the South Tropical Zone at 220—240° longitude (II) and further on down to 140° (September—October). From an observed attenuation of $0^m.35$ in Jupiter's brightness the albedo of the EG was bound to be $A = 0.06$, which led to the conclusion that the girdle consisted of volcanic ash.

2. On 5—7 October 1962 the sharp northern boundary of the EG became covered with lighter diffuse clouds (II 120—200°). On 8—10 October the northern boundary could again be clearly distinguished at these latitudes, and by 17 October it became perfectly sharp. The EG is not symmetric with respect to the planetary equator and is displaced to the north. Beginning from 13 October another strong rise in activity was observed on the southern boundary of the EG and in the South Tropical Zone (II 160—200°). The whole Northern Hemisphere grew darker and remained so for a long time, the darkening still being noticeable at the beginning of 1965. At the end of October a South Tropical Belt formed in the active zone, in the form of separate condensations running at an angle to the parallel. By the beginning of November, the whole South Tropical Zone became filled with dark streaks all along the southern boundary of the EG within the range II 220—80°, and these grew to a maximum in the first week of December 1962. During that time the STeB showed the highest saturation and darkness. The northern boundary of the EG became indistinct again, and the darkening of the Northern Hemisphere was particularly marked. At that time a thin stripe could be observed on the EG slightly north of the disk center, resembling a shadow of Jupiter's hypothetical ring. In October—December 1962 photometric observations showed a decrease of $0.3—0^m.4$ in Jupiter's brightness.

3. The observations were interrupted at the end of December 1962 and resumed again at the beginning of October 1963. The South Tropical Zone then showed a general darkening, which persisted until the middle of December 1963. The North Tropical Zone, which was clear in October, became obscure after the middle of November by some kind of dark veil, The Red Spot was almost invisible throughout the period from September 1963 to February 1964 (according to Japanese observational data and the observations of V. A. Zinov'ev in Volgograd); it could be barely distinguished on 15 February 1964, and then it gradually cleared and recovered its bright pink-red color. The fading of the Red Spot was no doubt due to a high dust content in the upper atmosphere, probably produced by eruptive processes in the South Tropical Zone. During the same period (toward the middle of January 1964) there was a pronounced rise in the density (darkness) of

the EG, though the STeB was still the darkest feature on the disk. From this time on the Northern Hemisphere remained appreciably darker than the southern and showed a yellowish-brown tinge, unlike the Southern Hemisphere which was a greyish-white.

4. The processes which started in December 1963 on the northern boundary of the EG developed at the end of January 1964 into a gigantic disturbance at II 140—180°, which gave rise to a North Tropical Belt running to the east. During that time, the northern boundary of the EG at II 320—360° and the whole northern hemisphere were completely blurred. In February 1964 the whole EG was violently agitated, broken up by strongly disturbed dark and light areas and gaps. The disturbances penetrated into the North Tropical Zone, which displayed dark streaks at an angle to the parallels. The whole Northern Hemisphere did not show during that time any belts, which were probably concealed by a thick layer of volcanic mass. Segments of belts began appearing only at the end of February 1964, and in the first half of March the North Tropical Belt appeared in full.

5. At the end of 1962, in 1963 and the beginning of 1964 the EG was not symmetric with respect to the equator but slightly shifted to the north, because although it lay exactly across the middle of the apparent planetary surface, the disk center itself was at a north joviographic latitude. In the second half of 1964 the FG moved off to the south, possible due to a lower activity in its northern part and a resultant decrease in its width. In September 1964 there was a brightening in the central part of the EG in visible light, though in the photographic range the absorption still remained high. The STeB appeared consistently as the darkest feature on the disk, but the overall contrast of the features dropped appreciably. At the end of December the northern hemisphere showed traces of the usual belts (NTeB, NNTeB), as if the belts were seen through a fog. The EG continuously displayed a brick-reddish color, markedly different from the brownish tinge of the STeB. Besides the brightening in its central part, the EG also showed in its southern part a darkening and the formation of a narrow stripe extending across the whole disk. This suggests that what we may be observing (with the disk center at +3°.4 joviographic latitude) is the rim and shadow of a ring forming sufficiently high above the planetary surface (approximately at a distance of one planetary radius).

6. In August and September 1964 the South Tropical Zone became covered near the Red Spot with chocolate-colored streaks, which were apparently part of the usual South Tropical Belt. The color of this feature is distinctly different from the brick-red color of the EG. In October 1964 the EG still remained strongly disturbed at II 80—150° (I 200—260°). In that area the STeB faded away and could be seen only as an extremely faint double stripe. The whole part of the STeB east of the Red Spot gradually receded, as if it were sinking under a cloud layer. The southern boundary of the EG consisted of two belts—the inner brick-colored, and the outer bluish.

In November 1964 the STeB began approximately at II 200° and passed above the Red Spot, touching it. From the beginning of January 1965 on, the whole part of the STeB east of the Red Spot disappeared and the belt narrowed down and ran into the Red Spot. The "dustiness" of the Northern Hemisphere decreased, and the regular belts of the hemisphere showed clearly in the telescope and were photographed.

The appearance of the planet in January 1965 is shown in Figures 1 and 2 in the next article, taken with the large astrograph of the Kiev Astronomical Observatory. The dark equatorial girdle can be distinguished in Figure 1, and the Red Spot is clearly visible in Figure 2.

APPENDIX

THE OBSERVATIONS OF 1958—1965

The observation series of 1962—1965 was carried out using the AZT-7 miniscus telescope ($D = 20$ cm, $F_{eq} = 200$ cm) with 130 x principal magnification. The features of the planet were identified only after prolonged scrutiny, and whenever clear images were obtained, they were marked on special disk blanks 100 mm in diameter; before this, the surface markings were usually memorized by 10—15 minutes of continuous scrutiny. It normally took at least another 30—40 minutes for correcting the position of the features.

In order to compare and examine the distinctive characteristics of the radical changes on the planet, we have included some drawings made in 1968 from observation with the Kiev astrograph ($D = 25$ cm, $F = 435$ cm) under 150 x magnification. These observations were taken together with photographs of the planet, and showed that the drawings were much better for revealing the fine details.

The Appendix lists the relevant particulars of each drawing: longitude of the central meridian in Systems I and II, Universal Time, joviographic latitude B_0 of the disk center, seeing, and description of the features.

1. I 206°.7; II 227°.9. 22 May 1958, 18^h35^m; seeing good; $B_0 = -3°.3$.
2. I 139.8; II 130.8. 26 May 1958, 19^h10^m; seeing fair; $B_0 = -3°.3$.
3. I 154.0; II 345°.4. 16 June 1958, 18^h30^m; seeing fair; $B_0 = -3°.2$. Red Spot appears on the east.
4. I 345°.6; II 115°.9. 24 June 1958, 18^h45^m; seeing fair; $B_0 = -3°.1$.
5. I 36°.3; II 306°.7. 3 July 1958, 20^h40^m; seeing good; $B_0 = -3°.0$.
6. I 162°.9; II 320°.2. 18 July 1958, 18^h30^m; seeing fair; $B_0 = -3°.0$; Red Spot not visible, though should have been on eastern limb.
7. I 232°.6; II 310°.8. 17 August 1958, 19^h0^m; seeing fair; $B_0 = -2°.9$.
8. I 334°.3; II 128°.3. 25 September 1962, 18^h0^m; seeing occasionally excellent; $B_0 = +1°.3$. Equatorial girdle (henceforth denoted by EG) brick-brown throughout; the regular zones are white. STeB also showing, tinged with gray.
9. I 38°.2; II 154°.1. 30 September 1962, 17^h50^m; seeing poor; $B_0 = +1°.3$. Observed shortly before clouds developed. STeB charcoal gray, appreciably darker than EG.
10. I 177°.8; II 286°.2. 1 October 1962, 17^h30^m; seeing steady, the planet observed through a fine cloud haze; $B_0 = +1°.3$. Color of STeB markedly different from the brick color of EG.
11. I 132°.4; II 225°.4. 3 October 1962, 17^h18^m; $B_0 = +1°.3$. Seeing at first very unsteady, later improving. On the southern boundary of the EG, near the central meridian, light regions stand out above the dark areas; a dark streak issues there, forming a thin STeB. The S-cap is a greenish-red.
12. I 167°.2; II 259°.8. 3 October 1962, 18^h15^m; $B_0 = +1°.3$. Seeing good; inhomogeneities (dark and light spots) visible in EG.
13. I 312°.9; II 38°.1. 4 October 1962, 17^h55^m; $B_0 = +1°.2$. Seeing at first poor, later improving. Red Spot considerably redder than EG. Inhomogeneities visible in the STeB and a bright area in the STeZ. N-hemisphere appreciably grayer than the S-region over EG. N-cap also darker than S-cap.
14. I 340°.3; II 65°.3. 4 October 1962, 18^h40^m; $B_0 = +1°.2$. Seeing steady. Inhomogeneities seen in SSTeB.
15. I 101°.6; II 179°.2. 5 October 1962, 17^h40^m; $B_0 = +1°.2$. Seeing fair. Further darkening of N-hemisphere is noticeable, and the formation of fog over the western part of the EG, through which the northern boundary does not show. The S- and N-caps are markedly different. From 18^h45^m the foggy area moves to the western limb, and the N-boundary of the EG appears sharp at least up to 110° from the eastern limb.
16. I 63°.8; II 126°.4. 7 October 1962, 17^h50^m; $B_0 = +1°.2$. Seeing steady and sharp. The EG is a deep brick-red. Most of its northern boundary is blurred and seems to be obscured by fog. The Northern Hemisphere is grayer and darker than the Southern.
17. I 215°.6; II 270°.6. 8 October 1962, 17^h40^m; $B_0 = +1°.2$. Seeing good. The light recess in the northern region of the EG (seen before on 3 October) has sharp boundaries and does not look at all like the foggy area observed on 5 October. At 18^h42^m Ganymede started its transit along the S-boundary of the EG; the

satellite stands out clearly, and its brightness exceeds that of the EG by a factor of 5—6. At 19^h5^m the Red Spot appears on the east, colored a deep red.

18. I 286°.7; II 319°.0. 11 October 1962, 16^h30^m; $B_0 = +1°.2$. Seeing good. The fog in the N-cap dissipates, as the NTeB and NNTeB appear faintly; the EG shows many features and light areas. The N-hemisphere is appreciably darker than the S-hemisphere and has a brick-yellowish tinge.

19. I 246°.2; II 263°.0. 13 October 1962, 16^h35^m; $B_0 = +1°.2$. Seeing excellent. A tremendous disturbance develops in the S-tropical zone (220—190° II). Distinct condensations on the belt crossed the central meridian at $16^h59^m.1$ and $17^h21^m.8$. The protrusion in the N-boundary of the EG crossed at $16^h43^m.7$.

20. I 57°.1; II 50°.9. 16 October 1962, 18^h10^m; $B_0 = +1°.2$. Observed on the 6-inch guide of the double astrograph of the Kremenchug Astronomical Observatory. The dark S-boundary of the EG is clearly visible.

21. I 233°.3; II 219°.3. 17 October 1962, 18^h40^m; $B_0 = +1°.2$. Kremenchug Astronomical Observatory. Seeing very good. STB separated into distinct condensations.

22. I 348°.3; II 327°.2. 18 October 1962, 17^h30^m; $B_0 = +1°.2$. Kremenchug Astronomical Observatory. Seeing good. Inhomogeneities clearly visible in the STeB and STB. The N-hemisphere appears more bluish-gray than the S-hemisphere. The NTeB is lighter than the EG.

23. I 260°.1; II 208°.8. 22 October 1962, 17^h22^m; $B_0 = +1°.2$. Kiev AZT-7 telescope. Seeing good. The general blurring of the Northern Hemisphere reduced, and the NTeB and the NNTeB are showing. There is unusual activity south of the equatorial girdle—bright white spots and streaks on the southern boundary.

24. I 333°.8; II 259°.6. 25 October 1962, 16^h25^m; $B_0 = +1°.2$. Kiev, AZT-7. Seeing satisfactory only for brief intervals. Again apparent is the disturbance in the STZ and the composite structure of the STB.

25. I 147°.0; II 65°.0. 26 October 1962, 16^h50^m; $B_0 = +1°.2$. Seeing poor. The S-hemisphere is very bright and white, and the N-hemisphere is dark and blue-grey. The NTeB is barely visible. The disturbance on the N-boundary of the EG (200° I) has persisted for more than 3 weeks. The EG is a reddish-yellow with pink-brown spots and a few dark gray ones.

26. I 207°.9. II 167°.6. 29 October 1962, 17^h10^m; $B_0 = +1°.1$. Seeing poor. STB does not show.

27. I 16°.8; II 249°.1. 1 November 1962, 16^h55^m; $B_0 = +1°.1$. Seeing occasionally good. STZ disturbed throughout; bright areas visible over the N-boundary of the EG. The recess on the N-boundary of the EG crossed the CM at $17^h23^m.2$.

28. I 190°.1; II 54°.4. 2 November 1962, 17^h20^m; $B_0 = +1°.1$. Seeing good. NTeB not visible; the N-cap is dark. The EG has sharp boundaries. The Red Spot is distinctly redder than the EG. The light spot A on the EG crossed the CM at $17^h34^m.2$, moving much faster than System I.

29. I 270°.5; II 128°.9. 3 November 1962, 15^h12^m; $B_0 = +1°.1$. Seeing good. The North Polar Cap is appreciably darker than the South. The S-boundary of the EG is very sharp and deeper red; the N-boundary is less distinct. Occasionally traces of the NTeB can be seen. The light area in the EG crossed the CM at $15^h30^m.7$.

30. I 313°.8; II 171°.5. 3 November 1962, 16^h25^m; $B_0 = +1°.1$. Seeing good. STZ covered with streaks in the longitude range 323—0° I. Central transit of the western boundary at $16^h40^m.0$.

31. I 341°.9; II 198°.6. 3 November 1962, 17^h10^m; $B_0 = +1°.1$. Seeing satisfactory. The S-tropical streak blurred up.

32. I 65°.5; II 282°.3. 3 November 1962, 19^h25^m; $B_0 = +1°.1$. Seeing satisfactory. The N-cap is gray, with a bluish tinge; the S-cap is whiter. Condensations ("turbulent elements") appear clearly on the inclined NTB. Jupiter low; the image often blurs up.

33. I 78°.8; II 289°.0. 4 November 1962, 15^h31^m; $B_0 = +1°.1$. Seeing good. The pattern is almost identical to the previous, only the light area in the EG occurs appreciably higher. The STeB is considerably darker and wider than two weeks before. The dents on the N-boundary of the EG sometimes appear brighter than the NTeZ. The S-boundary of the EG is darker and redder than the N-boundary. The NNTeB is distinguished with difficulty. The inclined STB is full of condensations.

34. I 115°.4; II 324°.7. 4 November 1962, 15^h30^m; $B_0 = +1°.0$. Seeing very good. The S-boundary of the EG stands out sharply; the girdle itself is somewhat paler than in October. The Spot, although at the limb, is a brighter color than the EG. Occasionally a bridge can be seen between the STeB and the turbulent sloping belt running to the Spot.

35. I 236°.1; II 72°.6. 5 November 1962, 15^h30^m; $B_0 = +1°.1$. Seeing fairly steady. The EG is somewhat paler and looks a lighter brown; the NTZ is a clear purplish-gray. The S-cap is somewhat turbid and only slightly lighter than the N-cap. The SSTeZ disappeared. A disturbance is developing on the N-boundary of the EG (260°I).

36. I 46°.2; II 240°.9. 6 November 1962, 15^h50^m; $B_0 = +1°.1$. Seeing good. The inclined STB, emerging from an area of disturbance, is almost as wide as the STeB, but less dense and of cloudy structure. The S-boundary of the EG is darker and accentuated. At 15^h56^m Ganymede comes out of occultation; at

that time it is fainter than Europa by 2^m; at $16^h6^m.3$ they are equally bright; at 16^h10^m Ganymede is brighter by $0^m.6$. At 16^h16^m the center of the light area on the EG crosses the CM; at $16^h33^m.0$ the dent on the N-boundary of the EG crosses the CM.

37. I 305°.3; II 130°.8. 7 November 1962, 18^h30^m; $B_0 = +1°.1$. Observed through tenuous clouds, images sharp, contrast reduced. The N-hemisphere considerably darker; the N-boundary of the EG seems obscured by fog.

38. I 331°.4; II 150°.8. 8 November 1962, 15^h0^m; $B_0 = +1°.1$. Seeing exceptionally good. The EG is inhomogeneous in structure, as if made up of separate belts. It is a bleached brick color. There is a very thin dark stripe just north of the equator.

39. I 8°.0; II 187°.1. 8 November 1962, 16^h0^m; $B_0 = +1°.1$. Seeing very good. The western edge of the S-tropical disturbance is on the CM at $15^h31^m.8$. The dark stripe on the EG is clearly visible.

40. I 44°.6; II 223°.4. 8 November 1962, 17^h0^m; $B_0 = +1°.1$. Seeing very good. On the S-boundary of the EG near the CM there is a bright spot infront of a dark streak; the STB slants toward it. The contrast of all the features is weaker than in October.

41. I 81°.2; II 259°.7. 8 November 1962, 18^h0^m; $B_0 = +1°.1$. Seeing good. The protrusion in the N-boundary of the EG crosses the CM at 18^h10^m. Io is occulted slightly down of the center of the EG; when it was at the limb (for 8 minutes) its brightness was $1.5-2^m$ higher than that of the EG. The satellite then faded by $3-4^m$ and diminished in size, and eventually went out as a small pip on the limb.

42. I 202°.4; II 13°.5. 9 November 1962, 17^h0^m; $B_0 = +1°.1$. Seeing satisfactory. The EG is dim brick in color, but darker than the Red Spot by at least $1^m.5$. The eastern part of the S-cap is distinctly darker than the western. The N-cap is not darker than the S-cap, but shows a grayish tinge.

43. I 260°.0; II 325°.5. 23 November 1962, 17^h15^m; $B_0 = +1°.1$. Seeing satisfactory. Changes can be seen in the position and intensity of the S-tropical belt and the STeB.

44. I 156°.2; II 151°.8. 2 December 1962, 14^h57^m; $B_0 = +1°.1$. Seeing satisfactory at first. A peak of activity in STZ; the whole zone is darkened by streaks. The N-hemisphere seems to be shrouded in a bluish-gray fog. Io transits exactly along the southern boundary of the EG; it appears on the limb at $15^h17^m.2$. The surface brightness of the satellite is at least 2^m higher than that of the EG.

45. I 314°.6; II 303°.8. 3 December 1962, 15^h0^m; $B_0 = +1°.1$. Seeing poor. STB slants toward the STeB. High activity is noted in the STeZ. The S-cap is slightly darker than the N-cap. The Red Spot *emerged at the limb* at 15^h30^m.

46. I 121°.6; II 103°.0. 4 December 1962, 15^h15^m; $B_0 = +1°.1$. Seeing occasionally good. High activity in STZ and STeZ. The N-cap is appreciably grayer and darker than the S-cap. The EG and the blurry areas show a brownish tinge. The bright areas above the S-boundary of the EG are bluish-white.

47. I 283°.2; II 224°.8. 9 December 1962, 17^h45^m; $B_0 = +1°.1$. Seeing occasionally good. High activity and streaks over the whole STZ.

48. I 292°.4; II 233°.9. 9 December 1962, 18^h0^m; $B_0 = +1°.1$. Seeing occasionally good. STB is broadened and almost joins with the STeB.

49. I 62°.8; II 356°.9. 10 December 1962, 17^h15^m; $B_0 = +1°.1$. Seeing occasionally good. The EG shows a deeper brick coloration, while the STeB is dark and an ashy grayish-blue. The Red Spot cannot be seen.

50. I 222°.2; II 149°.1. 11 December 1962, 17^h20^m; $B_0 = +1°.1$. Seeing poor.

51. I 309°.3; II 229°.7. 12 December 1962, 15^h25^m; $B_0 = +1°.1$. Seeing occasionally good.

52. I 93°.5; II 246°.3. 29 December 1962, 15^h0^m; $B_0 = +1°.1$. Seeing poor. The S-hemisphere is grayer than the N-hemisphere. Bright areas are visible over the S-boundary of the EG. On 1 January 1963 (I 280°; II 49°), at $t = -20°C$, the Red Spot and some features of the EG were observed. It was difficult to make a detailed drawing.

53. I 333°.1; II 153°.8. 4 October 1963, 18^h40^m; $B_0 = +3°.0$. Seeing fair. The darkest part of the EG is on the N-boundary. STZ, which was clear in 1962, is filled with dark matter. On the other hand, the N-tropical zone (bordering on the N-boundary of the EG) is now the lightest. There are bright areas over the STeB. A persistent light region formed in the center of the EG, but much darker than the bright areas.

54. I 95°.7; II 162°.2. 19 October 1963, 19^h10^m; $B_0 = +2°.9$. Seeing satisfactory. There are considerable changes as compared with 4 October 1963. The brightest area is the S-temperate zone. The EG shows a grayer tinge. No features appear in the N-hemisphere.

55. I 223°.8; II 183°.0. 2 November 1963, 18^h20^m; $B_0 = +2°.8$. Seeing poor. The STeB is distinctly inhomogeneous. The EG, with the light gap in the middle, are brownish in color.

56. I 248°.2; II 207°.2. 2 November 1963, 19^h0^m; $B_0 = +2°.8$. Seeing steadier. The features appear more clearly.

57. I 93°.7; II 85°.3. 15 November 1963, 16^h10^m; $B_0 = +2°.7$. Seeing satisfactory. The whole EG is filled up, but its color is whitish, not deep as in 1962. The darkest feature is the STeB; the lightest area is the STeZ. The N-hemisphere looks hazy.

58. I 307°.2; II 52°.7. 13 November 1963, 17^h50^m; $B_0 = +2°.6$. Seeing good; $t = -9°C$. STZ changed its configuration: STB has approached the STeB; the whole zone is covered with dark haze. The Red Spot is not visible, though it should have been not far west of the CM. The N-hemisphere is lighter than the S-cap, and shows a stronger brown coloration.

59. I 21°.3; II 104°.1. 3 December 1963, 16^h45^m; $B_0 = +2°.6$. Seeing steady; $t = -8°C$. The EG is a light chocolate color; the S-hemisphere has a silvery tinge; the N-hemisphere is brownish. The light areas in the middle of the EG have shrunk and almost disappeared. The SSTeB is made up of separate condensations.

60. I 252°.7; II 326°.8. 4 December 1963, 17^h45^m; $B_0 = +2°.6$. Seeing unsteady; $t = -7°C$. The EG is faintly chestnut color; the N-hemisphere has a brownish tinge, while the N-tropical zone is bluish-gray. The southern boundary of the EG is sharp, and the N-boundary is blurred, especially in its western part.

61. I 191°.3; II 213°.1. 11 December 1963, 16^h24^m; $B_0 = +2°.6$. Seeing unsteady; observed on the guide of the astrograph of the Kremenchung Astronomical Observatory ($D = 25$ cm, $F = 430$ cm); $t = 16°C$. The S-boundary of the EG is blurred. The STZ is covered with haze. The N-polar cap has a bluish tinge. The occultation of Europa was observed.

62. I 209°.6; II 125°.7. 25 December 1963, 15^h35^m; $B_0 = +2°.5$. Seeing unsteady; $t = -8°C$. The STeB is the darkest feature; the STZ has become rather light.

63. I 343°.9; II 183°.2. 4 January 1964, 15^h30^m; $B_0 = +2°.5$. Seeing unsteady, and often blurry; $t = -3°.5$ C. The EG is dun colored with a reddish tinge. The STeB is a dense brown. The N-cap has a distinct yellowish tinge. The NTB is the lightest.

64. I 338°.8; II 108°.2. 13 January 1964, 15^h55^m; $B_0 = +2°.5$. Seeing often blurry; $t = -9°C$. The EG is definitely darker than in December 1963, with a distinct reddish tinge. Over the STZ there seem to be faint dark clouds.

65. I 180°.6; II 259°.7. 21 January 1964, 16^h28^m; $B_0 = +2°.5$. Seeing steady; $t = -6°C$. New developments: the whole N-hemisphere seems to be under a yellowish-brown fog; the N-cap is darker than the S-cap. The EG shows a brown coloration, and its N-boundary is blurred, especially on the east and west. The lightest region is the STZ. Europa is near the western limb (casting a shadow on the STeB), as well as Io before occultation.

66. I 72°.3; II 126°.8. 23 January 1964, 14^h43^m; $B_0 = +2°.5$. Seeing good; $t = -4°C$. The STeB is inhomogeneous, with a bright indentation which crossed the CM at $14^h55^m.6$. The S-tropical zone is appreciably lighter than the N-tropical zone, which is bluer in places. The N-boundary of the EG is sharper than the S-boundary, and much darker.

67. I 101°.3; II 155°.6. 23 January 1964, 15^h30^m; $B_0 = +2°.5$. Seeing at first satisfactory, later often blurry. An N-tropical band is very faintly discernible; traces of the NTeB appear on the east. At 16^h15^m a strong dark disturbance emerges from behind the limb, next to the N-boundary of the EG. At 17^h5^m the front of this new gigantic formation passes the CM (I 159°; II 213°); behind the light recess there is an intense dark protrusion which penetrates almost 6° latitude into the N-tropical zone, and beyond it the boundary of the EG is completely disturbed and there is a new dark band.

68. I 155°.0; II 209°.6. 23 January 1964; 17^h0^m; $B_0 = +2°.5$. Seeing good. The protrusion on the N-boundary of the EG is near the CM.

69. I 129°.0; II 145°.6. 28 January 1964, 14^h25^m; $B_0 = +2°.5$. Seeing fair; $t = -14°C$. The STeB is the darkest, as is also the part of the N-boundary of the EG in front of the large tropical disturbance. The boundary of the bulge crossed the CM at 14^h54^m; an N-tropical belt develops from the projection. The NTeB can be seen.

70. I 162°.5; II 178°.8. 28 January 1964, 15^h16^m; $B_0 = +2°.5$. Seeing satisfactory; $t = -14°C$. The N-tropical disturbance is near the CM; a dark band can be seen in the northern part of the EG on the east.

71. I 293°.0; II 301°.8. 29 January 1964, 14^h35^m; $B_0 = +2°.5$. Seeing occasionally good; $t = -9°C$. The STZ is lighter than the NTZ. The N-polar cap is appreciably darker than the S-cap. There are no signs of the Red Spot on the east.

72. I 335°.7; II 344°.1. 29 January 1964, 15^h45^m; $B_0 = +2°.5$. Seeing satisfactory, occasionally blurry; $t = 10°C$. The Red Spot showed up on the limb at 15^h10^m; at 16^h35^m its western boundary was on the CM. The Spot is considerably narrower than at the end of 1963, and paler than the STeB; it has a more delicate and redder tinge than the EG. There is a considerable rise in brightness in the STeZ over the Red Spot. The S-boundary of the EG is sharp; the N-boundary is completely diffuse and fades into the Polar Cap which is dark and blurred up. Io transits across the disk slightly south of the S-boundary of the EG. At 0.2 of the radius from the limb the satellite is approximately 2^m brighter than the background (the STZ).

73. I 184°.5; II 131°.7. 6 February 1964, 16^h30^m; $B_0 = +2°.5$. Seeing good; $t = -2°C$. The indentation in the STeB has persisted for more than 2 weeks. Slanting bands can be clearly seen on the EG. The N-cap is homogeneous without belts, but with a dark region inclined to the parallel.

74. I 295°.8; II 236°.7. 7 February 1964, 15^h15^m; $B_0 = +2°.5$. Seeing excellent; $t = -7°.5$C. The N-cap is appreciably darker than the S-cap; the N-boundary of the EG is thoroughly disturbed on the west, and as a result the girdle appears unusually wide. The shadow of Io is moving off the disk.

75. I 39°.3; II 316°.5. 10 February 1964, 15^h0^m; $B_0 = +2°.5$. Seeing fair; $t = -12$°C. The S-boundary of the EG is sharp, and the N-boundary is completely blurred. The N-cap is appreciably darker than the S-cap. The Red Spot is on the limb.

76. I 8°.5; II 274°.8. 12 February 1964, 15^h22^m; $B_0 = +2°.5$. Seeing very good; $t = -9$°C. The N-cap is tinged a greenish-yellow, and is distinctly darker than the S-cap. Along the middle of the EG there is a very fine perfectly homogeneous stripe. Disturbed areas are visible on the northern boundary of the EG.

77. I 44°.8; II 311°.4. 12 February 1964, 16^h20^m; $B_0 = +2°.5$. Seeing very good; $t = -8$°C. The EG is distinctly a reddish-brown, and it can be seen in very fine detail. The thin central stripe is visible at times throughout the length of the EG, while the band in the STZ has almost vanished. The N-cap appears yellowish.

78. I 356°.6; II 242°.8. 14 February 1964, 16^h15^m; $B_0 = +2°.5$. Seeing fair; $t = -12$°C. The gigantic disturbance on the northern boundary of the EG has spread to the west and given rise to an intense NTB. The N-polar cap is appreciably darker than the S-cap. The S-boundary of the EG is sharp, and the N-boundary is blurred. The satellite's shadow (Io) is much darker than the brick-red EG and the dark brown STeB.

79. I 111°.8; II 350°.8. 15 February 1964, 15^h10^m; $B_0 = +2°.5$. Seeing poor; $t = -8$°C. The Red Spot is clearly visible, but it does not stand out as it did in 1962 and 1963; it crossed the CM at 15^h48^m, and the eastern limb at 16^h7^m. The N-polar cap is almost as dark as the EG. The thin equatorial stripe running across the middle of the EG is clearly visible.

80. I 136°.2; II 15°.1. 15 February 1964, 16^h45^m; $B_0 = +2°.5$. Seeing improving; $t = -10$°C. The Red Spot is on the CM, and its coloration is quite different from that of the EG. The EG is visible only in the western part.

81. I 342°.0; II 213°.6. 16 February 1964, 17^h5^m; $B_0 = +2°.5$. Seeing very good; $t = -14$°C. The North Polar Cap is slightly yellower (with a brownish tinge) than the S-cap, and is almost like the EG.

82. I 317°.1; II 135°.1. 23 February 1964, 15^h45^m; $B_0 = +2°.5$. Seeing exceptional in steadiness, high resolution attainable; $t = -7$°C. Details are visible of the disturbance on the N-boundary of the EG, which rapidly developed at the end of January. The dark wedge crosses the CM at 15^h2^m. The EG is much darker than the N-cap which is now lighter than the S-cap at those longitudes, but the whole N-hemisphere is unmistakeably a brownish-yellow. The indentation in the STeB still persists (from the middle of January). At 17^h25^m the newly formed thin NTB stretches almost across the whole disk; the NTeB is made up of several selections.

83. I 153°.7; II 321°.7. 24 February 1964, 16^h48^m; $B_0 = +2°.5$. Seeing poor, appearing only for brief intervals; $t = -13 - 15$°C. The N-boundary of the EG is blurred, and there is no light area in the middle; the N-polar cap is darker than the S-cap and seemed to form a whole with the EG. There are traces of the Red Spot on the eastern limb. The darkest formation is the STeB.

84. I 76°.7; II 158°.4. 6 March 1964, 16^h25^m; $B_0 = +2°.6$. Seeing fair, often blurry; elevation of planet only 20°; $t = -17$°C. The S-boundary of the EG is dark, the N-boundary is blurred, disturbance developing. The EG is clearly asymmetric with respect to the disk center. The whole N-hemisphere is dark, and distinctly yellowish.

85. I 138°.8; II 189°.7. 11 March 1964, 16^h25^m; $B_0 = 2°.6$. Seeing satisfactory, occasionally good; $t = -2$°C. The whole N-hemisphere is dark, tinged a brownish-yellow. There is a thin north belt across the disk. The shadow of Ganymede is on the S-cap.

86. I 107°.5; II 140°.2. 13 March 1964, 16^h45^m; $B_0 = +2°.6$. Seeing good. The Northern Hemisphere is very dark, as before. The N-boundary of the EG is blurred. There are large inhomogeneities in the EG; the southern boundary of the EG is not parallel to the SSTeB.

87. I 329°.0; II 315°.7. 19 March 1964, 16^h35^m; $B_0 = +2°.6$. Seeing poor; $t = -5$°C. Jupiter low. The features are blurry, but the thin NTB shows clearly. The whole N-hemisphere is under dark fog.

88. I 118°.6; II 98°.0. 20 March 1964, 16^h25^m; $B_0 = +2°.6$. Seeing occasionally good; $t = -4$°C. The whole N-hemisphere is obscured by dense turbidity; the N-tropical zone cannot be distinguished. The dark stripe is visible in the middle of the EG.

89. I 338°.2; II 306°.7. 26 September 1964, 19^h46^m; $B_0 = +3°.3$. These and the following observations were taken on the guide of the astrograph of the Kremenchug Astronomical Observatory ($D = 25$ cm, $F = 430$ cm); $t = +16$°C. The N-hemisphere is darker and looks hazy; it has a brownish color. The STeB and SSTeB are the finest details, and can be seen with difficulty. There are some light formations on the eastern end of the N-boundary of the EG.

90. I 80°.3; II 25°.1. 29 September 1964, 19^h26^m; $B_0 = +3°.3$. Exceptionally good seeing; $t = +15°C$. There are tremendous changes in the STZ and on the S-boundary of the EG between March and September, due to the appearance of a dense dark region which obscured the STZ. The N-hemisphere is tinged with brown. The Red Spot is a clear red, totally unlike the brown color of the EG.

91. I 192°.2; II 114°.8. 2 October 1964, 19^h22^m; $B_0 = +3°.3$. Seeing very poor. It is however possible to note the disappearance of the STeB over the range II 80—200°. The N-hemisphere is appreciably darker than the S-hemisphere. The central regions of the EG have a distinct reddish color; its south and north borders are brown with a bluish-gray tinge.

92. I 107°.7; II 359°.6. 6 October 1964, 19^h27^m; $B_0 = +3°.3$. Seeing poor at first, later improving; $t = +11°C$. The STeB is very attenuated; below the STeB, east of the Red Spot, there are some bright light areas. The Red Spot is a vivid red, quite different from the grayish-brown of the equatorial regions. The whole N-hemisphere looks slightly lighter than before. The center of the Red Spot crossed the CM at 19^h59^m.

93. I 248°.8; II 133°.6. 7 October 1964, 19^h0^m; $B_0 = +3°.3$. Seeing steady; $t = +13°C$. The boundary of the EG is blurred; the bright spot on the S-boundary of the EG crosses the CM at 19^h20^m. The boundary of the EG has a greenish-blue fringe. The STeB barely shows as a faint double band. The northern part of the EG is strongly disturbed.

94. I 302°.9; II 80°.6. 21 October 1964, 19^h4^m; $B_0 = +3°.4$. In spite of some light cirrus, seeing occasionally good; $t = +11°.5C$. The S-boundary of the EG has moved up to the South, and has become darker and bluer; the former boundary, tinged with brown, can be seen 3—5° below. The N-cap is a yellowish-brown considerably darker than the rest of the region. The STeB ends abruptly near the CM, and just barely shows to the east split into two.

95. I 23°.7; II 139°.0. 24 October 1964, 18^h8^m; $B_0 = +3°.4$. Seeing often blurry; $t = +11°C$. The STeB is virtually invisible, only a very faint trace can barely be seen. The whole S-hemisphere is light; the N-hemisphere is dark and yellowish. The shadow of Io runs over the bluish border above the distinct brown region of the EG; the N-region of the EG is inhomogeneous. A thin NTB and the NTeB are showing.

96. I 314°.7; II 39°.2. 28 October 1964, 18^h40^m; $B_0 = +3°.4$. Seeing exceptionally steady; $t = +4°C$. The STeB breaks off at II 79° and tapers down at an angle. The Red Spot shows a reddish-pink coloration. The new S-region in the EG is a dense brick-brown with a bluish irridescence. The lightest region is the STeZ; the light areas in the middle of the EG are much darker; the N-hemisphere is yellowish-brown.

97. I 206°.4; II 207°.6. 8 November 1964, 17^h22^m; $B_0 = +3°.3$. Seeing occasionally good; $t = 0°C$. The south regions of the EG are a brownish-brick color, while the north region, which is extremely disturbed, is a bluish-grey. The whole northern hemisphere is yellowish-brown and darker than the southern, which is bluish-white. The western boundary of the STeB is at about II 200°.

98. I 25°.4; II 18°.7. 9 November 1964, 17^h57^m; $B_0 = +3°.3$. Seeing good; $t = -3°C$. The sharp shadow of Io together with the satellite itself are at the western limb, on the South Tropical Belt which is very dark. The Red Spot is a bright pink. The south and north dark regions of the EG are brick colored with a bluish-grey tinge. The thin N-tropical belt, the NTeB and NNTeB are clearly visible.

99. I 79°.3; II 165°.6. 10 November 1964, 17^h51^m; $B_0 = +3°.3$. Seeing poor, clearing up only for brief intervals; $t = +0°.5$. The whole N-hemisphere is distinctly yellowish, the S-hemisphere is light gray. The belt covering the S-tropical zone and bordering on the S-boundary of the EG, is distinctly bluish. The south region of the EG and the light area are a reddish tinge, different from the grayer coloration of the N-region of the EG. There is the impression that higher-lying formations of different nature are projected onto the equatorial zone. At 18^h31^m the western edge of the STeB crosses the CM.

100. I 151°.8; II 96°.4. 14 November 1964, 19^h30^m; $B_0 = +3°.3$. Sky hazy, but seeing satisfactory. The whole N-hemisphere is tinged with brown and darker than the S-cap. The belt above the S-boundary of the EG is darkish brown, while the dense south region of the EG and the whole central zone are brick-red. The eastern end of the STeB can be seen, and at other longitudes traces of it are barely visible. The dark part of the STeB must become shorter, because the CM is now only at II 40°.

101. I 59°.9; II 359°.6. 16 November 1964, 18^h10^m; $B_0 = +3°.3$. Sky hazy, seeing only occasionally steady; $t = +5°C$. At 18^h35^m the center of the Red Spot crosses the CM. The shadow of Io overtakes the planetary rotation and moves across the Red Spot. The bulge in the N-region of the EG crosses the CM at 18^h20^m. The whole N-hemisphere is still foggy, but the NTB, NTeB, and NNTeB show up clearly. The S-cap is almost as dark as the N-cap. There is a brown darkening in the north and south of the EG; the central regions are brick colored. The satellite shadow crosses the CM at 18^h45^m.

102. I 241°.0; II 141°.5. 21 November 1964, 21^h13^m; $B_0 = +3°.3$. Seeing poor, improving only occasionally; $t = -4°C$. The N-hemisphere is slightly browner and darker than the S-hemisphere. Of the STeB there remains just barely visible traces; the STeZ is obscured. The northern region of the EG is strongly disturbed.

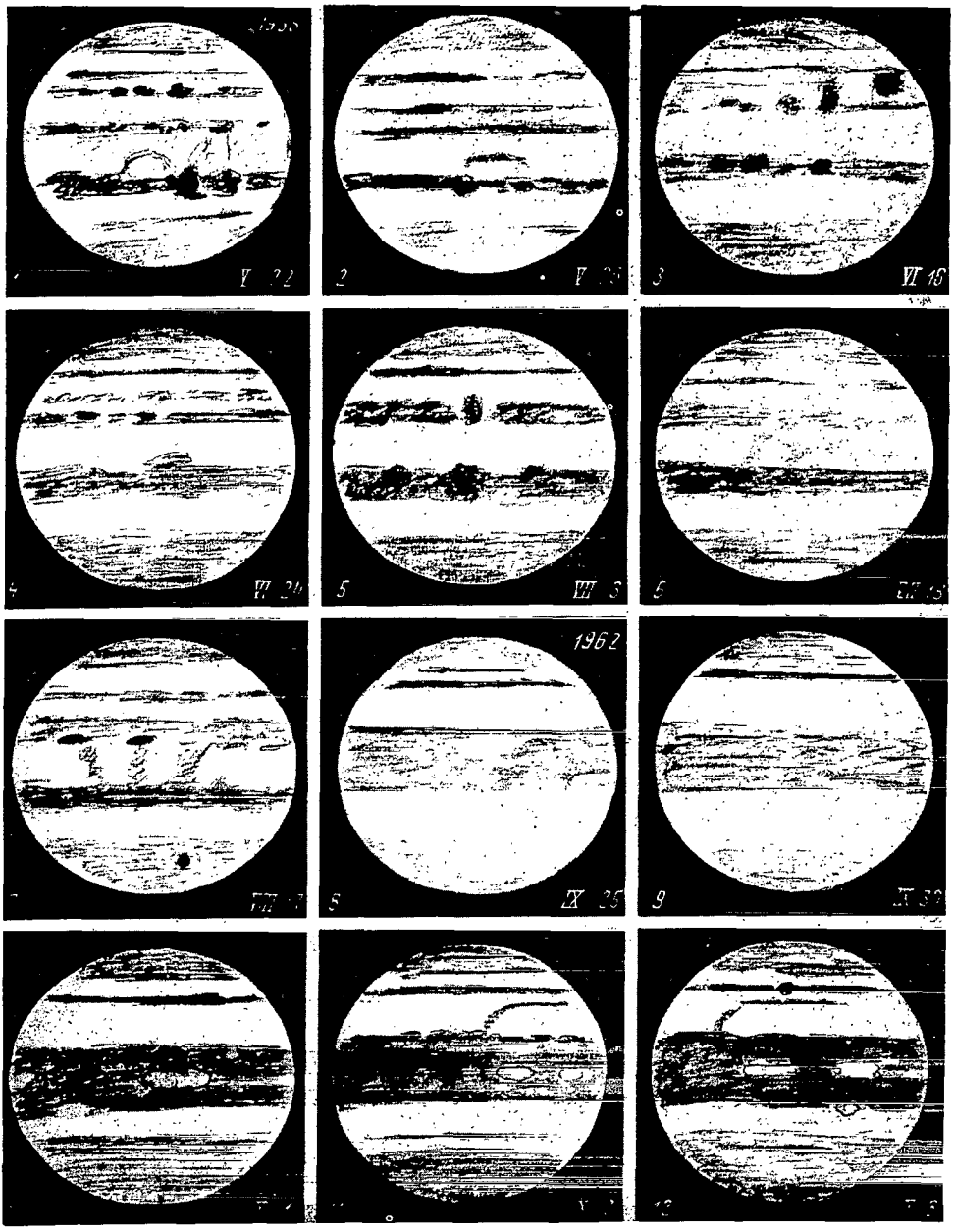
1962

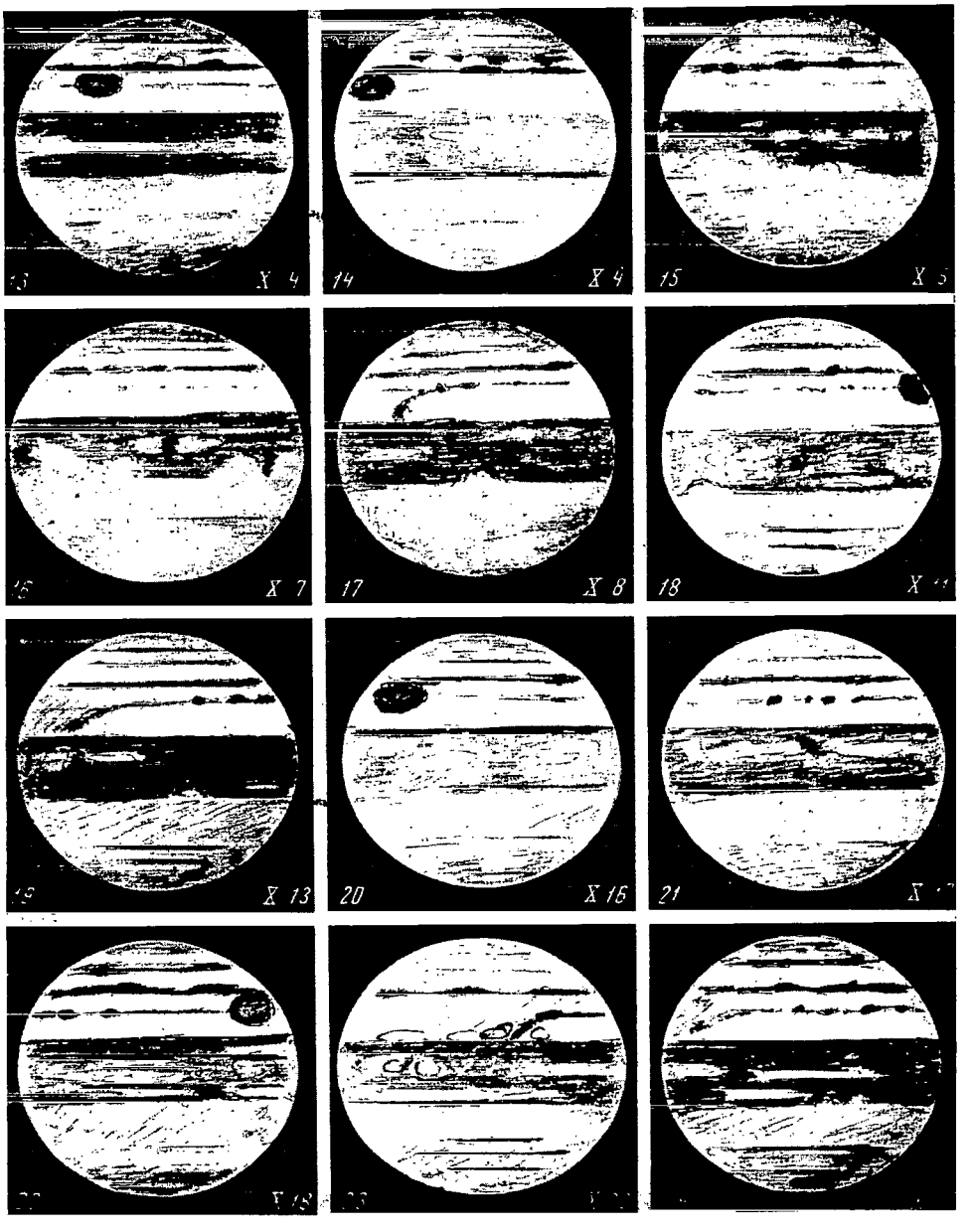
13 X 4
14 X 4
15 X 5
16 X 7
17 X 8
18 X 11
19 X 13
20 X 16
21 X 17

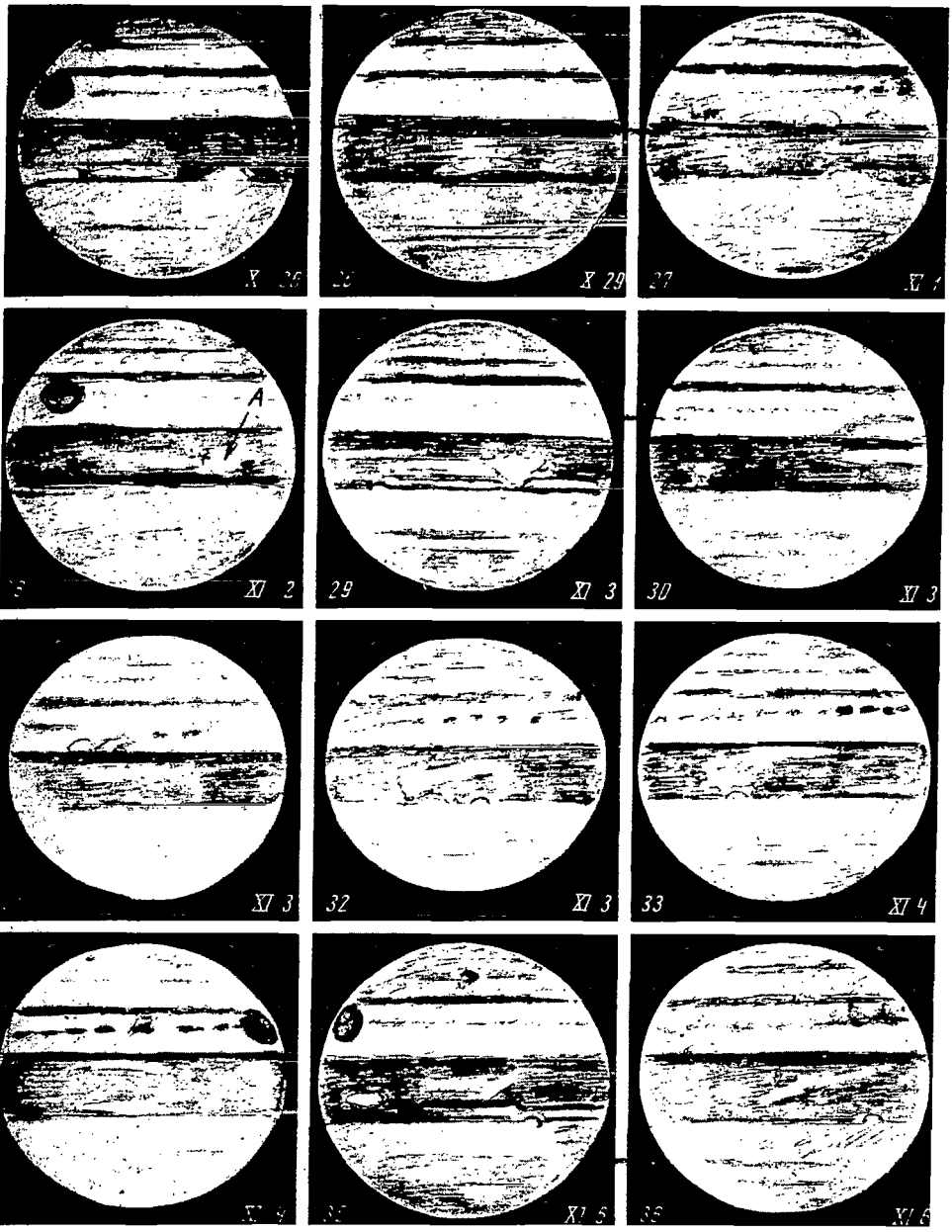
A

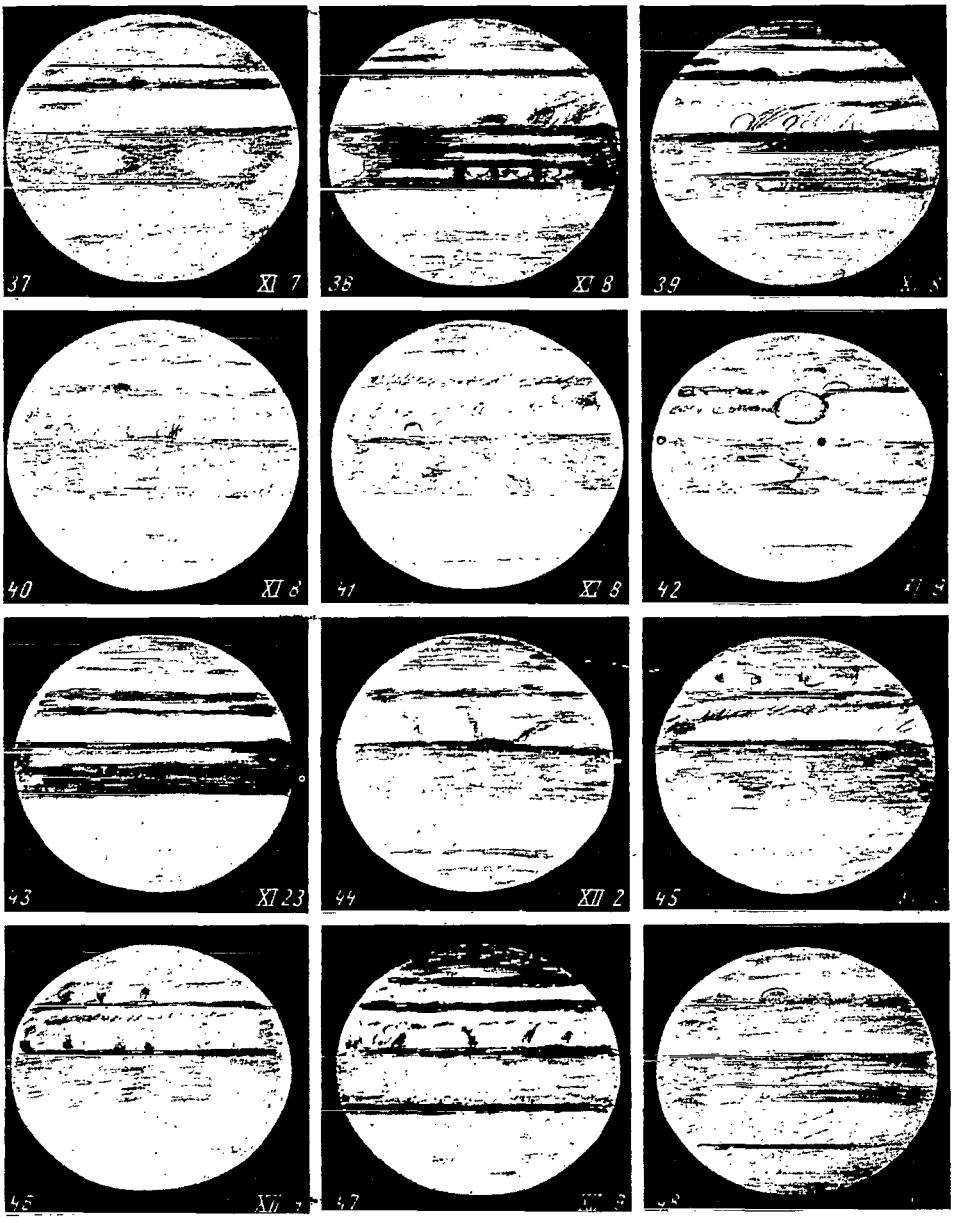
37 XI 7
36 XI 8
39 X. 8
40 XI 8
41 XI 8
42 XI 9
43 XI 23
44 XII 2
45
46 XII 3
47 XII 3
48

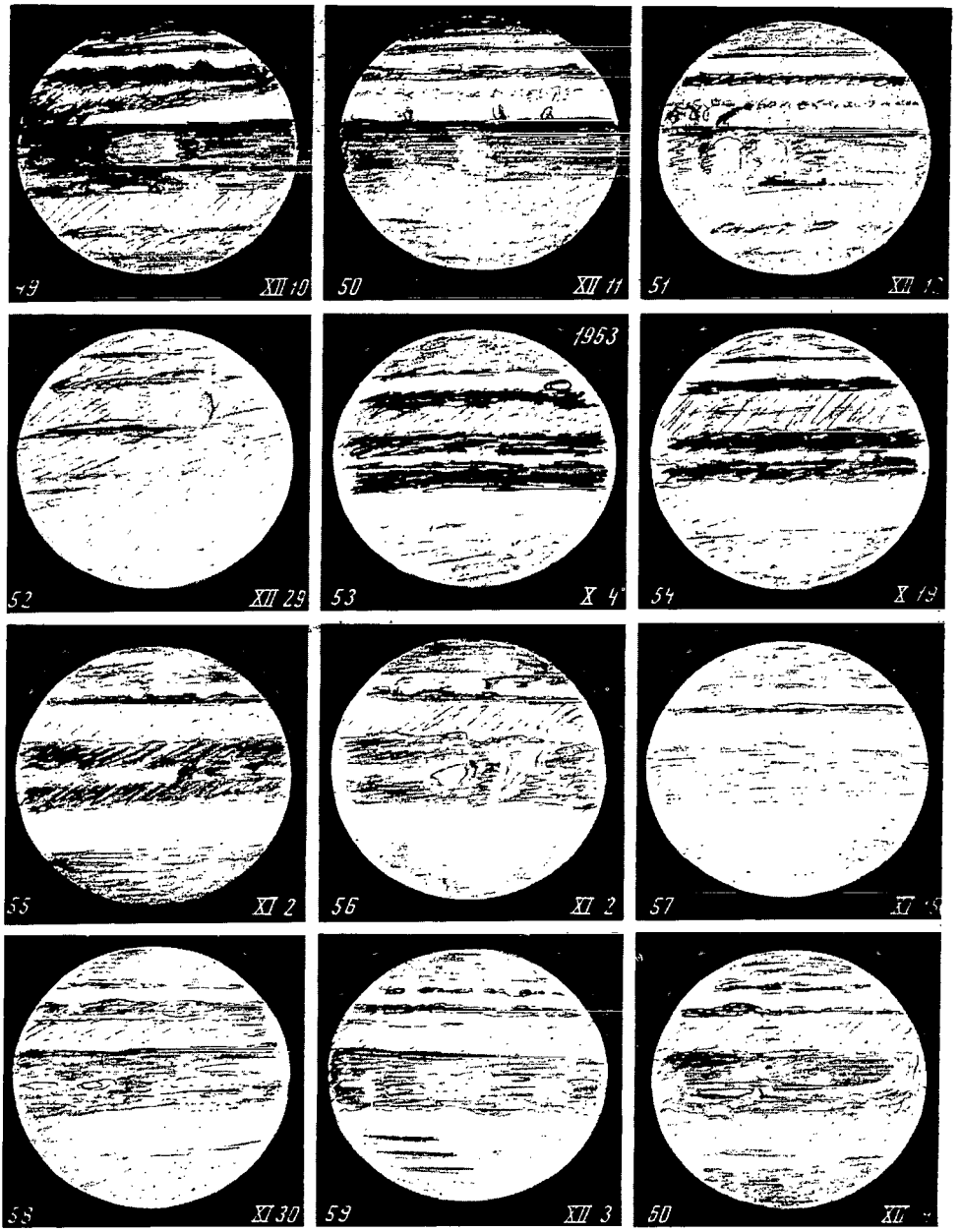
49 XII 10
50 XII 11
51 XII 12
52 XII 29
1953
53 X 4
54 X 19
55 XI 2
56 XI 2
57 XI 8
58 XI 30
59 XII 3
60 XII

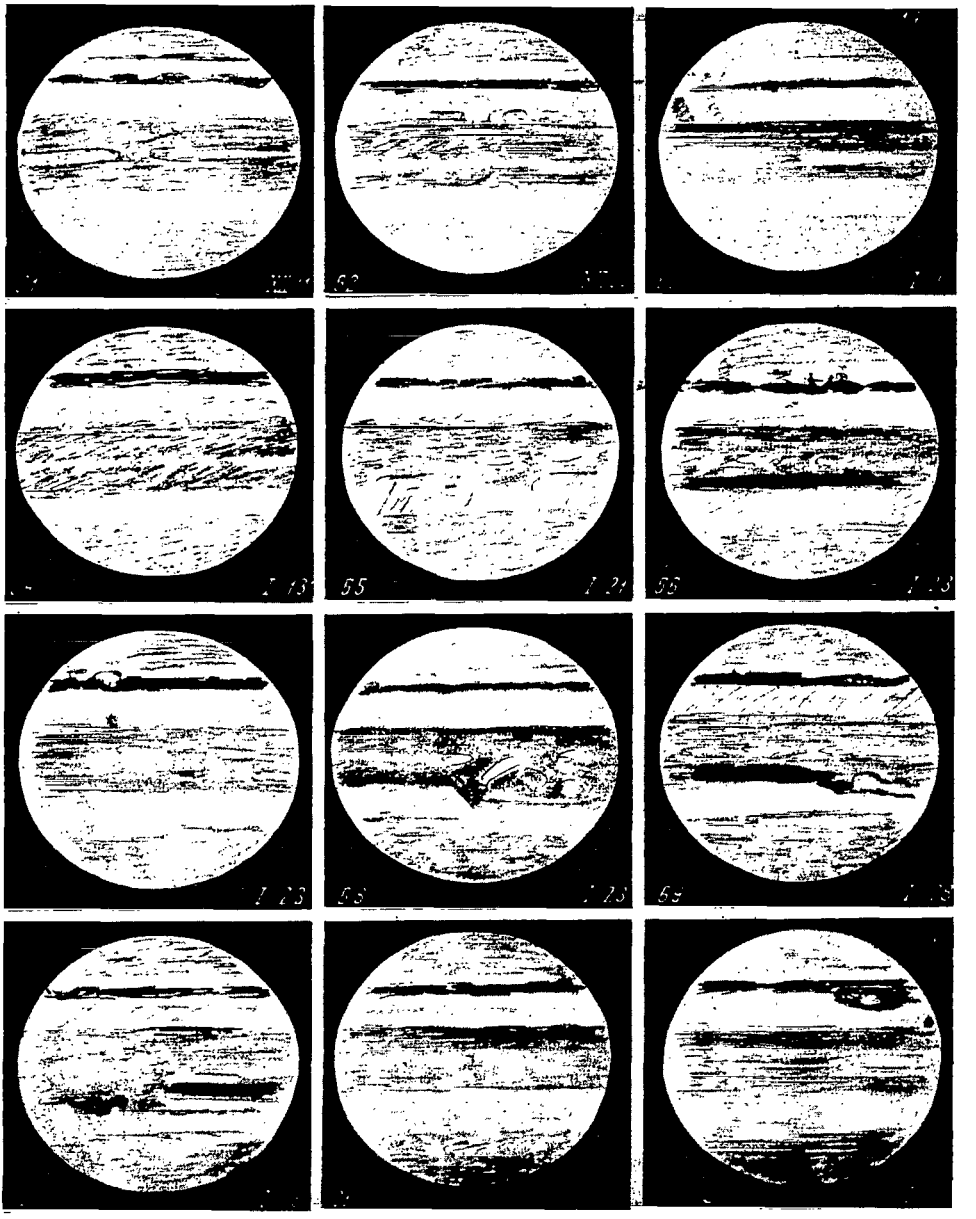

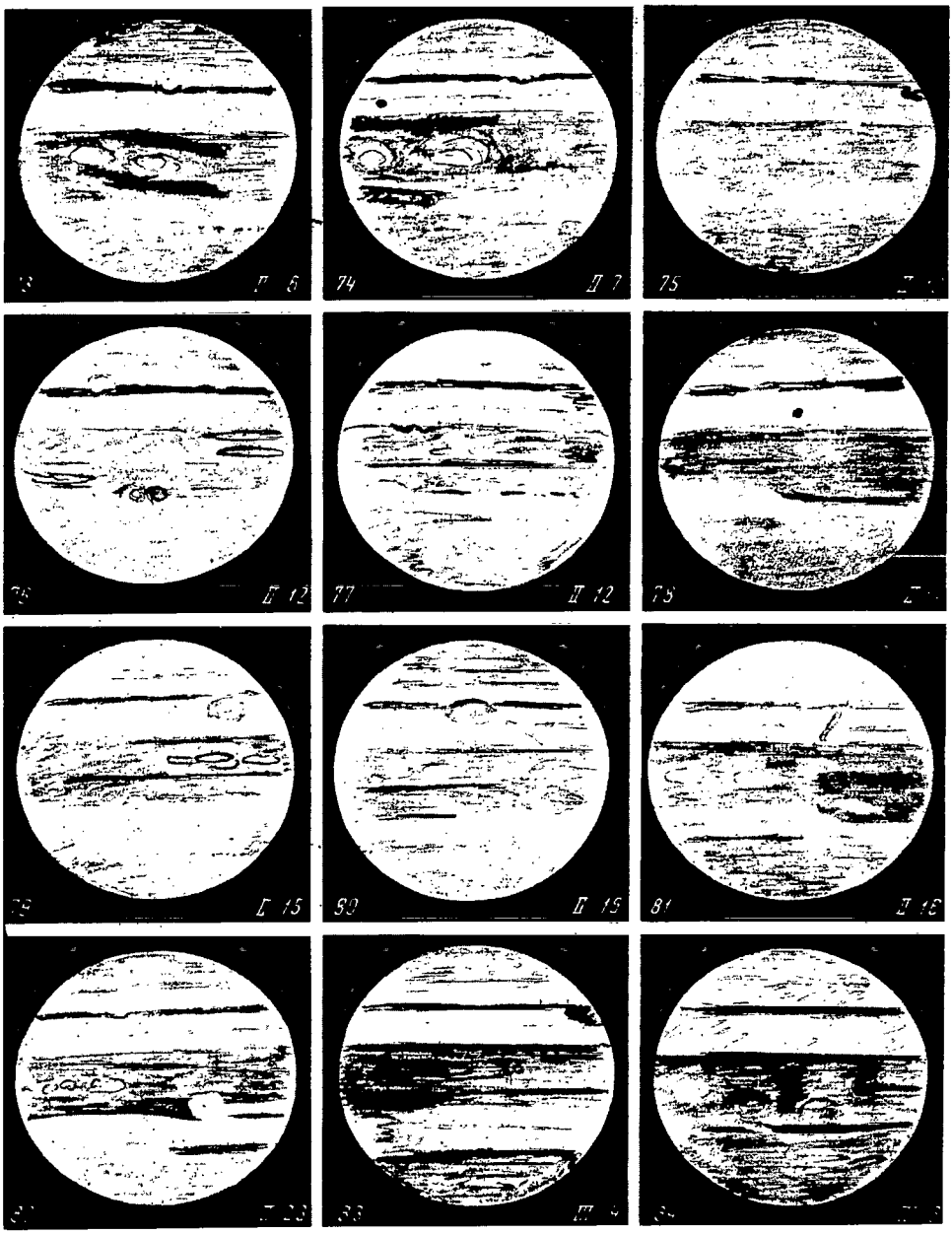

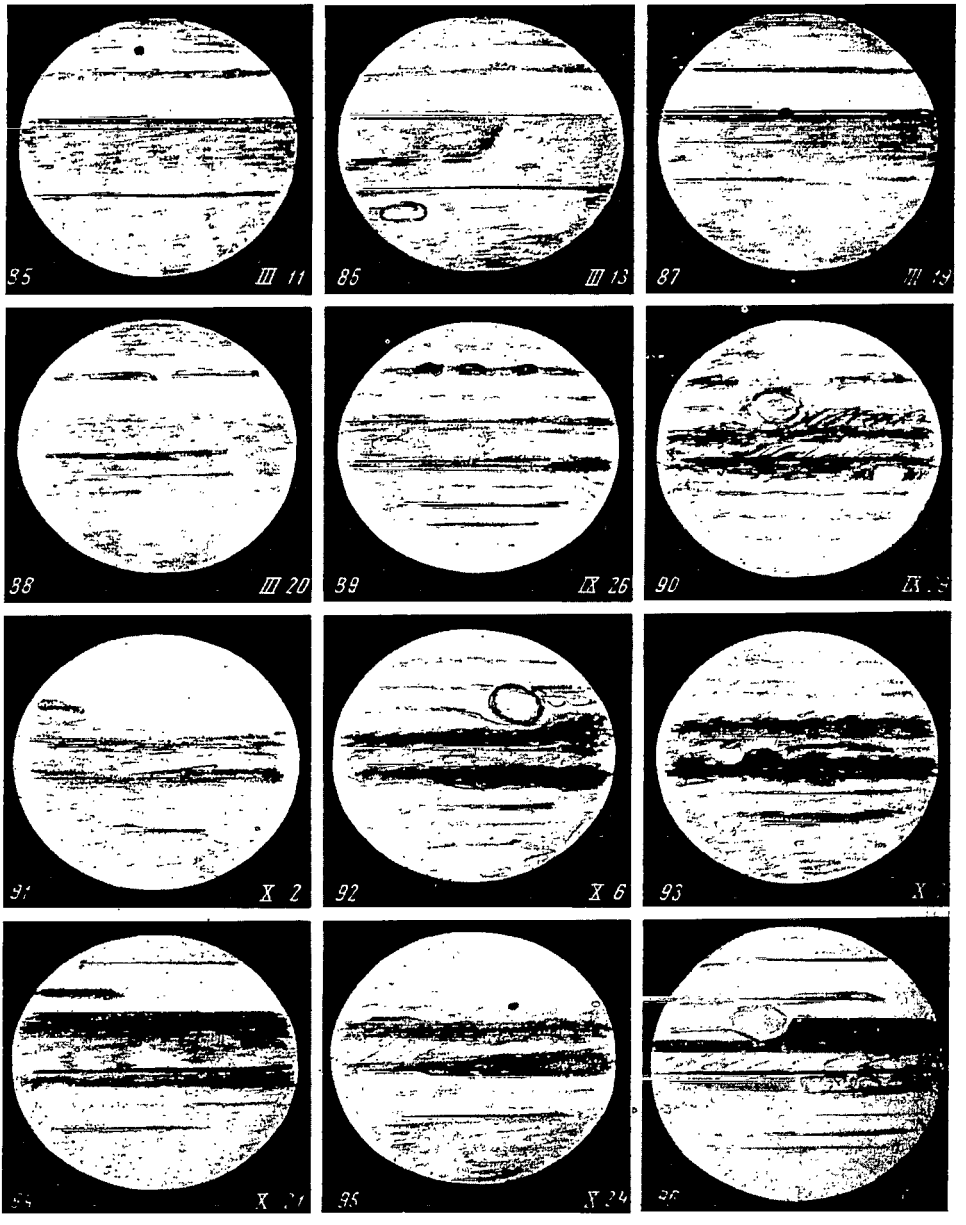
85 III 11
85 III 13
87 III 19
88 III 20
89 IX 26
90 IX
91 X 2
92 X 6
93 X
94 X 21
95 X 24
96

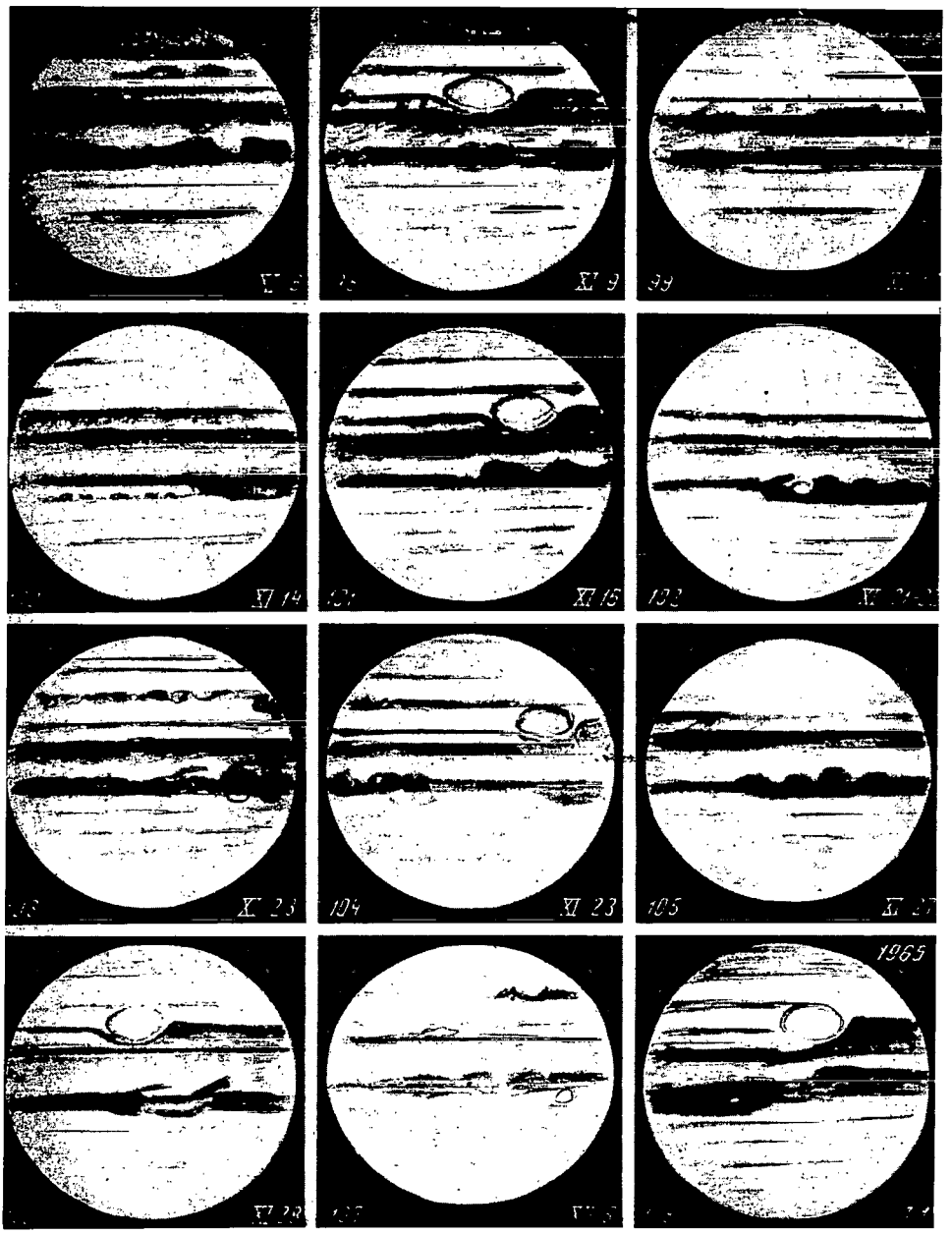
1965

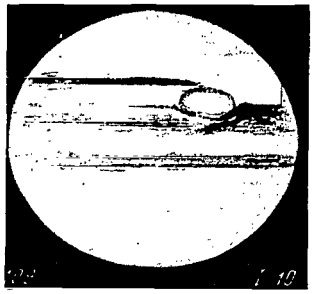

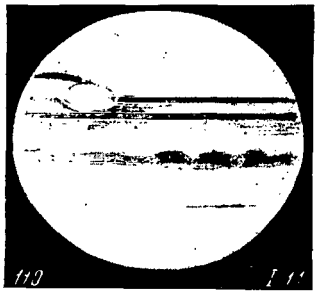

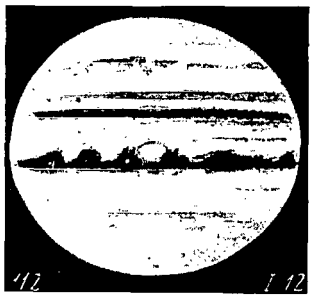

103. I 37°.4; II 284°.2. 23 November 1964, 16^h50^m; $B_0 = +3°.3$. Seeing good, observed through a haze which soon dissipated; $t = -3°C$. There are large inhomogeneities in the STeB, and a bright area which crossed the CM at 17^h28^m. The light intrusion in the N-region of the EG crossed the central meridian at 17^h31^m. The whole N-hemisphere is light yellowish-brick in color. The STeB is wide, and possibly double. The STZ and the STeZ are the lightest. The STB seems to grow fainter. A darkening is discernible on the eastern limb, preceding the appearance of the Red Spot.

104. I 104°.5; II 350°.7. 23 November 1964. 18^h40^m; $B_0 = +3°.3$. Seeing fair, only occasionally improving; $t = -4°C$. The N-region of the EG is widened in the area of disturbance east of the Red Spot. It may be clearly seen that the STB does not go into the Red Spot, but skirts it on the north. The N-hemisphere remains darker than the S-hemisphere.

105. I 293°.8; II 150°.2. 27 November 1964, 16^h25^m; $B_0 = +3°.3$. Seeing good; $t = +0°.5C$. The N-region of the EG is strongly disturbed. There remain barely visible traces of the STeB. The STZ above the STB is the lightest on the disk. The S-cap comes almost up to the STeB, but remains considerably lighter than the N-cap. The S-region of the EG is brick-red; the N part is a dark brown; the STB with the fringe is bluish-gray. Again there is the impression that the S-region of the EG might be the projection of a formation lying much higher than the other features of the disk.

106. I 181°.3; II 29°.2. 28 November 1964, 18^h52^m; $B_0 = +3°.2$. Seeing excellent; $t = +1-2°C$. The center of the Red Spot crossed the CM at 18^h37^m. There is a sharp border on the S-region of the EG, where the brick-red color terminates. The area beyond the border is blurred, and the disturbance east of the Red Spot is darkish brown. The N-region of the EG has the same brown color. Possibly this is the projection of an equatorial cloud forming into a ring.

107. I 111°.7; II 267°.0. 5 December 1964, 16^h15^m; $B_0 = +3°.2$. Seeing very poor, features detected with great difficulty; $t = +4°.5$ C. An indentation is visible on the STeB, which has appeared again. The belts sharply differ in color; the arched boundary of the EG is reddish, and further south the blurred area and the STB have a clear bluish tinge. The red color appears to be extrinsic to the whole EG.

108. I 65°.4; II 14°.5. 1 January 1965, 16^h30^m; $B_0 = +3°.1$. Seeing occasionally steady. Observations performed without clockwork drive, which broke down; $t = 0°C$. There is a further intensification of the processes in the EG, which looks wider and darker than earlier. The N-hemisphere is darker, as before. The NTB, NTeB, NNTeB can be seen with difficulty.

109. I 120°.7; II 1°.1. 10 January 1965, 18^h32^m; $B_0 = +3°.0$. Seeing poor, only occasionally steady. The N-hemisphere is darker than the S-hemisphere. The lightest area on the disk is the STZ; the darkest is the STeB. The light equatorial area has widened; the S-region is brownish, and the N-region is a dark brown. The NTeB can be seen with difficulty.

110. I 176°.6; II 50°.5. 11 January 1965, 15^h45^m; $B_0 = +3°.0$. $t = -11°.3$ C. Seeing exceptional. The disturbances near the Red Spot show interesting details. The N-region of the EG has a complex structure. The whole equatorial girdle is tinged with brown. The S-hemisphere is white; the N-hemisphere is yellowish-brown.

111. I 249°.9; II 123°.0. 11 January 1965, 17^h45^m; $B_0 = +3°.0$. $t = -12°C$. Seeing deteriorates, but features still clearly visible. The S-hemisphere is unusually white and the N-cap is dark; the central region of the EG has a bright reddish tinge. There are appreciable changes as compared with 110.

112. I 29°.5; II 255°.1. 12 January 1965, 17^h15^m; $B_0 = +3°.0$. $t = -10°C$. Seeing excellent. The whole EG and the N-hemisphere have a brick-brown coloration and are darker than the S-hemisphere. The South Cap is grayish-white. There are inhomogeneities in the STeB.

Bibliography

1. Vsekhsvyatskii, S. K. — Astronomicheskii Tsirkulyar, No. 232. 1962.
2. Focas, J. H. and C. Banos. — IAU Circ., No. 1809. 1962.
3. Jakashi, Sato. Soobshcheniya ob izmeneniyakh na Yupitere v pis'me ot 15 avgusta 1962 (Communications on the Changes of Jupiter in the Letter of August 15, 1962), Hiroshima.
4. Focas, J. H. La physique des planètes. — Univ. Liège, p. 535. 1962.
5. Hemert, J. L. and M. Marin. — Astronomie, 75:171. 1961.

6. Pearce, T.—Sky and Telescope, 21(2):97. 1962.
7. Anderson, Ch. M.—Sky and Telescope, 22(4):210. 1962.
8. Allen, G. (Dzh). Astrofizicheskie velichiny (Astrophysical Elements).—Fizmatgiz. 1960.
9. Kuiper and Middlehurst (editors). Collection Planets and Satellites [Russian translation. 1963].
10. Becker.—Sitzber. Preuss. Akad. Wiss., phys. mat. kl. 28:839. 1933.
11. Karlov, N.—Priroda, Nos. 4, 54. 1951.
12. Dolfus, O.—In: Planets and Satellites, edited by Kuiper and Middlehurst [Russian translation. 1963].
13. Hynek, J.A. Astrophysics. A Topical Symposium, p. 552, N.Y. 1951.

CHANGES IN JUPITER'S SYSTEM

S. K. VSEKHSVYATSKII
Department of Astronomy, Kiev State University

Observations conducted in Kiev in 1962—1963 and the analysis of other observational data suggested that the formation of the dark equatorial belt on Jupiter in 1961 was due to an outburst of volcanic activity and the ejection of large amounts of ash (10^{21} g) above the cloud layer /1/. In 1962 and 1963 the development of large-scale processes was recorded both in the Southern and the Northern hemispheres; particularly prominent was the appearance of a dense fog, which covered large areas in the Northern Hemisphere (first half of October 1962). The entire Northern Hemisphere grew darker and the northern boundary of the equatorial belt and other features became blurred; this effect intensified toward the end of 1962. In 1963 and 1964 the Northern Hemisphere invariably was of darker and redder coloration than the Southern Hemisphere. A tremendous disturbance was seen developing on the northern boundary of the equatorial belt at the beginning of November 1963 ($\lambda_{II} = 80-200°$). At about the same period (September 1963— February 1964) rapid changes were noted in the south temperate belt, and the Red Spot, previously quite prominent, became almost completely indistinct. In 1962 the equatorial belt was slightly displaced to the north of the equator, and in 1963—1964 it moved to the south of the disk center, apparently through an angle larger than that between the actual position of the planet's equatorial plane and the line of sight.

In the last months of 1964 the visual density (darkness) of the equatorial belt slowly decreased, but photographically it still remained appreciable. The central part of the equatorial belt, which stands out as a narrow darker fringe on the southern side, retains a brick-red color, quite distinct from the northern and the southern equatorial belts, which seem to be showing through the equatorial formation.

These observational data suggested that the equatorial belt was produced by large masses of ash particles and gas which rose above the cloud layer and formed a wide ring around the planet. It is possible that the heavier ash particles gradually settle to the surface and at the same time the ring contracts.

This assumption appears to be borne out by the results of radar observations of Jupiter (the equatorial diameter of the radar image is three times the polar diameter /2, 3/).

In order to verify the ring hypothesis, observations were made in Kiev on the occultation of the satellites at the western limb. On 16 January 1965 the brightness of Io was determined by comparison with Europa and Callisto, for which m_{vis} was taken as $5^m.52$ and $6^m.31$, respectively. From 19 hrs 00 min to 20 hrs 30 min UT (occultation at 21 hrs 05 min UT), Io decreased

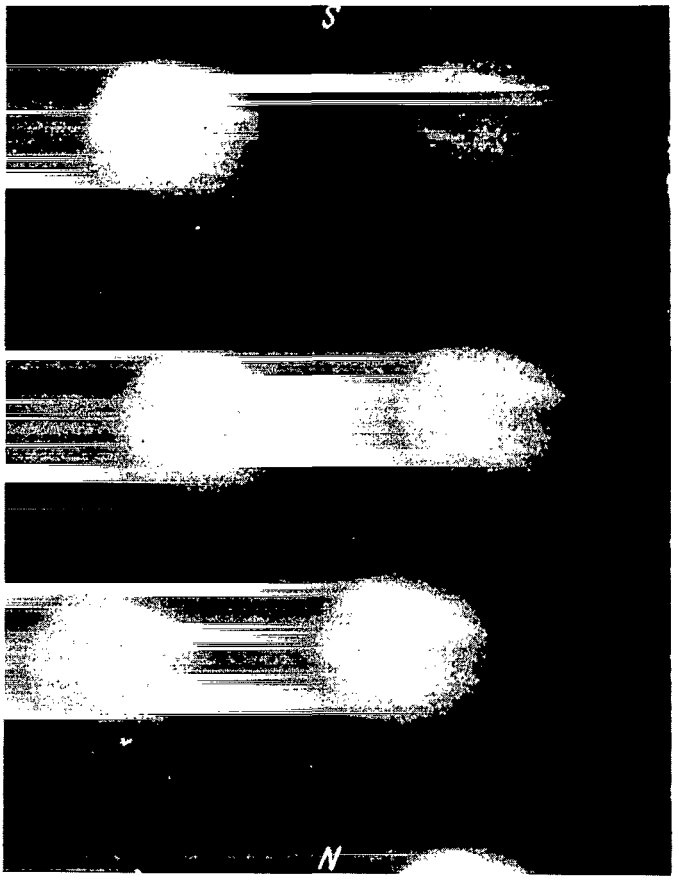

FIGURE 1. Photographs of Jupiter on 12 January 1965, 17 hrs 25 min UT (Kiev, the large astrograph, photographic attachment 3.5×; enlarged 9 diameters from negative):

$\lambda_I = 35°$; λ_{II} 261°.

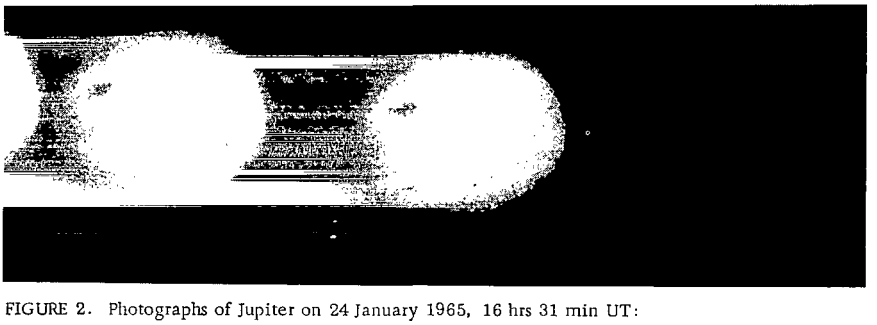

FIGURE 2. Photographs of Jupiter on 24 January 1965, 16 hrs 31 min UT:

Photographed under the same conditions as in Figure 1. Enlarged 12 diameters from negative.

in brightness from $5^m.72$ to $6^m.20$, and during the next 20 min almost by another 2^m. There proved to be a considerable drop in brightness as compared with Harris's findings, both in visual and photographic observations: 14 Jan $\Delta m_{I-II} = 0^m40$; 16 Jan $\Delta m = 0^m34$; 24 Jan $\Delta m = 0^m25$. From films taken on 4 February 1965 at the Astrophysical Institute of the Kazakh Academy of Sciences on the Kamenskoe Plateau with an AZT-8 70-cm telescope pointed at the Pleiades, the following magnitudes were found in the B system (taking $5^m.72$ for Ganymede):

	I	II	III	IV
3 February, 14 hrs 27–34 min (UT)	$6^m.79$	$6^m.27$	$5^m.72$	$7^m.11$
4 February, 14 hrs 36–46 min (UT)	6.62	6.09	5.72	7.22

The decrease in Io's brightness (on the average by $0^m.4$) may be due either to the screening effect of ash clouds moving around Jupiter or to a change in the albedo of the satellite produced by the precipitation of volcanic ash on its surface.

Intensive observations of Jupiter's system are required in order to study thoroughly this outburst of eruptive activity; of special interest is the photoelectric recording of the brightness, both of the planet and the satellites, and the study of the spectra of the various formations on the planet. The spectra of the satellites should also be investigated, as CH_4 and NH_3 absorption bands may be detected.

The author is greatly indebted to the astronometers of the Alma-Ata Observatory, D. A. Kalinenkov and V. G. Teifel', for their assistance in satellite observations.

Bibliography

1. Vsekhsvyatskii, S. K. – Astronomicheskii Zhurnal, 42(3):639. 1965. (see also the previous article in this collection).
2. Kotel'nikov, V. A. et al. – Doklady AN SSSR, 155(5):1037. 1964.
3. Kotel'nikov, V. A. et al. – Doklady AN SSSR, 157(3):554. 1964.

THE FEATURES OF JUPITER

V. A. ZINOV'EV
All-Union Astronomical and Geodetic Society, Volgograd Branch

Observations of Jupiter were carried out at the Volgograd Planetarium Observatory from October 1963 to February 1964. A 30-cm Zeiss refractor was used with 312× principal magnification, 200× for low-contrast features, and 500× for the observation of fine details. The seeing was good, and at times even excellent. The drawings given here were taken under very good seeing. During the five months 75 drawings were made, as well as several sketches of individual features and formations. About one quarter of the drawings were taken through different light filters.

During the period of observations Jupiter's equatorial belts showed a brownish color and merged into a single girdle about 30° wide. The Red Spot was bright red, the North Polar Cap was brown, and the South Polar Cap was a very faint gray. The uncolored South Temperate Belt was the strongest. The zone of the equatorial belts showed strong dark currents and various cloud groups.

The appearance of the planet changed frequently, and usually after a period of turbidity the surface would clear up and the features would stand out in sharp contrast.

Figure 1 shows the main formations on Jupiter during 1963—1964 (a, b, c, d, e—dark areas; I, II, III, IV—light zones; 1—edge of the SPC, 2, 3, 5—narrow belts, 4—equatorial fringe).

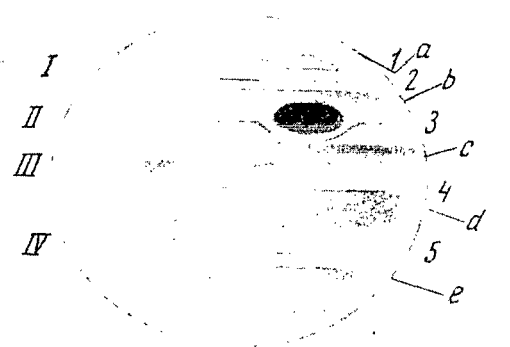

FIGURE 1. Distribution of zones and bands on Jupiter in 1963.

The South Polar Cap (a) showed in the fall of 1963 as a low-contrast grayish zone; on 11 November two reddish clouds appeared and the reddish tint then continued expanding. The onset of activity was most apparent in the lowest latitudes of the Polar Cap, where also a number of interesting features were noted (Figure 2). The South Polar Cap showed a light zone (Figure 2, 27*), which sometimes appeared as an aggregate of clouds (Figure 2, 38).

The Polar Cap was separated from the light zone (Figure 1, I) by a dark edge 1, which often changed its configuration and split into two in December. If it lay over a light area or a light cloud, the edge always curved around these formations; even when split, its two parts remained parallel where it curved.

The edge mostly appeared with short projections which divided the zone I into clouds (36). Figure 3 (2 November 1963) shows the edge with a cloud crossed by a dark bridge; it may be seen that this is one divided cloud and not a double one. The whole cloud has a regular oval shape. Over it lay a high-intensity belt, whose right-hand part was joined to the bridge. The clouds of 11 November, at $L_{II} = 40$ and 80° were the brightest parts of the light zone in the polar cap. The drawings of 2 November (37—39) showed that the area at the longitude $L_{II} = 180°$ was the most active of the Polar Cap, and diametrically opposite to it there was also a high-activity area, though weaker (36). There actually occurred no other such active, or clear, areas in the Polar Cap. That same evening the North Polar Cap was also clearly visible (39). The area of the South Cap at $L_{II} = 190°$, i.e., very close to the zone of activity, was observed under excellent seeing conditions on 4 December, but no particular details were noted (64).

The light zone in the South Polar Cap is situated between - 50 and - 60°.

The South Temperate Zone (I). Its structure is clearly visible on the disks (38) and (66). The zone contains a dark belt which was not always apparent, but normally stayed over the areas of disturbance (the Red Spot, white clouds). This belt was often broken up by white clouds (26, 65). The zone sometimes presented a blurred appearance (60). From the disks (64)— (66) the zone may be seen to be narrow at first (64), and later on, very wide and split in the area of $L_{II} = 17°$ (66). The inclination and discontinuity of the bridges in zone I are indicatory of fast proper motion of the zone. In its widest part the motion is differential, leading to the formation of the intermediate belt 2.

The South Temperate Belt (b) is distinguished by two bright clouds and the Red Spot. This is Jupiter's most intense belt, and only the dark currents in the North Tropical Belt are comparable to it. The belt was at its widest on 11 November, when it was almost as wide as one of the tropical belts. In October 1963 the belt showed a high intensity only in its upper part, and unlike the equatorial belts it had no color at all. Some color was noticeable only on 5 December, slightly to the right of the Red Spot. This is associated with a general reddening of Jupiter's southern part, due to some changes which occurred over the entire planet. On 4 December the temperate belt appeared strongly disturbed (65), with many dark spots and gaps dispersed over it. On 20 November there appeared an elongated gray spot (seen ascending in (65)), which could not be studied because of poor weather. The belt was subsequently fragmented by small

* Here and in the following the numbers in parentheses correspond to the numbers of the drawings of Jupiter in Figure 2. Data on the drawings are given in the table.

clouds and areas of lower intensity, and on 7 January (68) it appeared as if twisted. In the protrusions of the belt near the white spot and the Red Spot there were formations of lower intensity, resembling clouds (Figures 3, 4). As may be seen on many of the drawings, the white clouds themselves exert a strong influence on the adjacent regions. A comparison of drawings taken at large intervals of time shows that the white clouds move faster than the Red Spot (35, 70). At the beginning of October the Red Spot was still near one of the white spots, or clouds. On (32) and (60) (from 31 October to 29 November) another white cloud is seen emerging from a small recess in the belt.

List of drawings reproduced in Figure 2.

Drawing No.	Date	Time (UT)	Longitude of CM L_I	Longitude of CM L_{II}
		1963		
26	23/X	17^h55^m—18^h25^m	41°6	77°5
27	23/X	18^h45^m	98 7	133.8
32	31/X	17 15	228.4	203.2
34	1/XI	16 45	8.1	335.4
35	1/XI	17 45	44.6	11.6
36	1/XI	18^h05^m—18^h35^m	66.0	32.8
37	2/XI	17 00—17 30	184.2	143.7
38	2/XI	18 00—18 25	220.8	180.0
39	2/XI	18 40—18 45	236.0	195.1
45	11/XI	16 10—16 25	132.0	23.4
60	29/XI	16^h15^m	91.4	205.0
64	4/XII	14^h50^m—15^h10^m	114.1	190.8
65	4/XII	16 00—16 20	157.5	233.1
66	5/XII	15 45—16 05	309.3	17.3
		1964		
68	7/I	15^h00^m	77.9	254.5
70	7/I	17 15	160.1	336.0
71	7/I	17 40	175.4	351.2

The South Tropical Zone (II). This zone shows the lowest contrast, and it is exposed to the influence of the temperate and the tropical belts. It could be drawn in some detail only on 4 December, probably only as a result of a strong disturbance from the South Tropical Belt (64). When the seeing was good, the zone almost always showed the belt 3, which also revealed the effects of the adjacent regions or the Red Spot. On 7 January 1964 an indentation was observed on the belt (70), exactly similar to an indentation in the disturbed part of the South Tropical Belt, which was only slightly farther to the east. Observations could be made of the belt where it bent near the Red Spot. On 1 November 1963 (34—36) the left-hand part of the belt was fairly distinct and bent near the Spot, but it was broken along the middle. On the right the bend could not be clearly seen, as the belt was quite indistinct. The appearance of the belt was completely different on 11 November (45); it made a clean uninterrupted circuit around the Spot, coming close to the lower right-hand part of the Spot, and the right-hand part of the belt lay appreciably higher than its left-hand part. At a latitude $L_{II} = 143°$ ($L_I = 184°$) there was a large indistinct gray formation

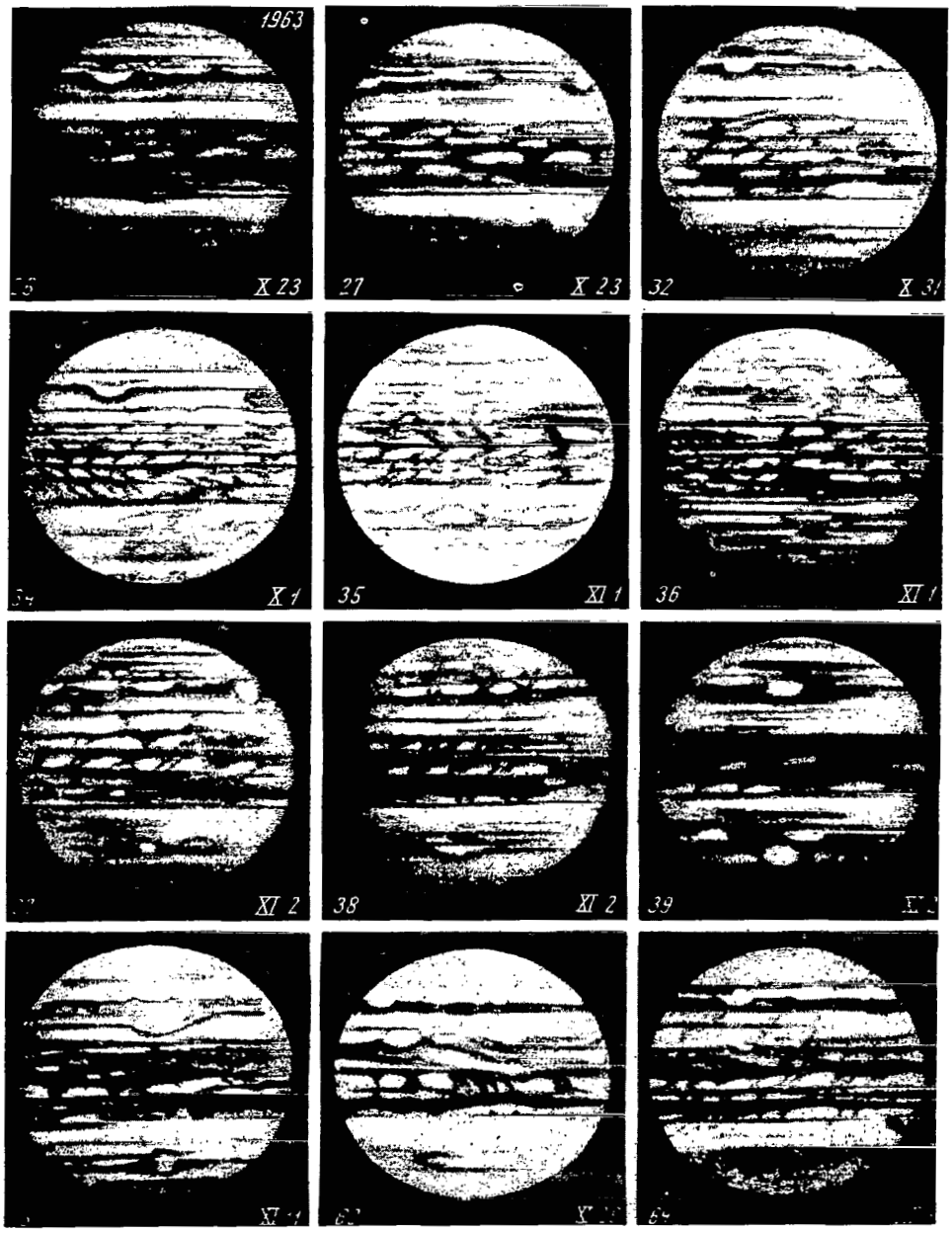

FIGURE 2. Drawings of Jupiter (see table)

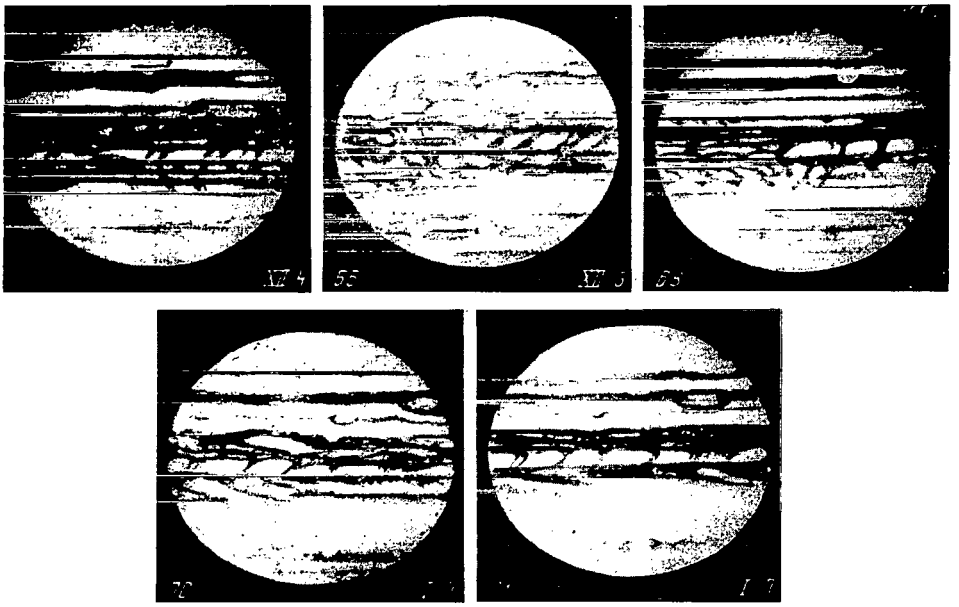

FIGURE 2 (continued). Drawings of Jupiter.

which was often invisible, but which enhanced the intensity of the belt (37, 27). The observation of this zone leads to the conclusion that all the light zones on Jupiter might be cloud formations of very low contrast.

The Red Spot, Longitude $L_{II} = 23-24°$. In October 1963 the Red Spot was suffused by an unusually bright red color, which even crept over the temperate belt. During that time the Spot showed a uniform red color and appeared slightly larger than it did in later observations, when it gradually darkened around the edges (Figure 4). In October the temperate belt showed an appreciable drop in intensity toward its lower edge, while the Red Spot was of uniform intensity; this created the false impression that the Spot lay above the belt and the zone, and its bright red color suggested that the Spot was transparent, the dusky temperate belt showing through. On 5 December two light areas in the form of small clouds formed on the Red Spot (66). These formations did not have clearcut boundaries and was dead white at the center.

The equatorial girdle consists of two equatorial belts separated either by the narrow equatorial fringe 4, or by the cloud zone III in which a cluster of four bright clouds persisted (66). The first cloud was divided by a faint bridge and separated from the second by a double bridge. Double bridges are a common occurrence at all latitudes on Jupiter. On 31 January an interesting formation was observed on this quadruplet: a fairly clear narrow horizontal band cutting across the clouds. The equatorial belt 4 was almost constantly visible but quite diffuse, and it became clearly defined only on 1 November 1963. At that time it showed the highest contrast and intensity, which made Jupiter look very similar to Saturn when its rings disappear. The fringe 4 was very narrow and lay over a wider belt of lower intensity, on which bridges running toward the equator and various protrusions were seen. The equatorial fringe looked perfectly straight, and only in the vicinity of the cloud quadruplet was it deflected to the north (36). The northern part of the equatorial girdle showed a strong dark streak which curved toward the equator in two places (36, 37). The central part of the streak may be seen in (38, 39) and some others. The equatorial belts became frequently blurred; on 7 January there was a particularly strong blurring of the north belt, which showed as indistinct stripes running at an angle to the equator (71). The belt did not have clearcut boundaries on the north, where the belt 5 normally occurs, and merged with the North Tropical Zone.

The South Belt was usually obscured, and if any features showed on it they were usually less distinct than in the North Belt. Its cloud structure was clearly visible at the beginning of the observation period in 1963; subsequently the intensity increased and the contrast appreciably decreased.

After the blurring on 7 January, the formations in the North Belt showed up with exceptional clarity; a strip detached itself from the equatorial fringe and traveled across the cloud quadruplet, but its intensity was insufficient and it faded out before reaching the limb. It evidently originated in the fringe 4, its left-hand part being more intense than the right; at its point of emergence a dark nodule could be seen on the fringe. The South Tropical Belt remained very dark and obscured.

On the equator there was a large number of bridges dividing the zones between the belts into clouds. The bridges characteristically slope in the direction of Jupiter's rotation. They thus seem to emphasize the fact that the equatorial regions move with a higher velocity. The south and north

FIGURE 3. White cloud cut by a bridge on the edge of the Red Spot, 7 November 1963, 17 hrs 30 min UT.

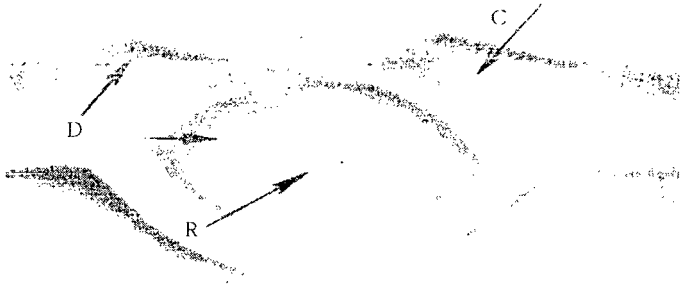

FIGURE 4. The Red Spot on 1 November 1963, 17 hrs 30 min UT:
D—dark color; R—red; C—cloud in the STeB.

bridges meet on one line at the equator (on the equatorial fringe) and form a "herringbone" pattern pointing to the east (34). The distribution of dark areas and the slope of the bridges is sometimes the same in the south and north equatorial belts (only shifted to the east in the north belt). Often bridges inclined in the opposite direction are seen, especially in regions of strong dark streaks. The drawings (36, 66) show a current running through the equator in front of the clouds. This may be accidental; the point is that the persistent cloud clusters are streamlined—the leading cloud is wide and the others taper down. The cluster has dark upper border, which curves down to the equator beyond the cluster and looks like a reversed bridge. In (36, 66) this feature may be seen at the tail-end of a narrow group of clouds preceding the quadruplet, while (45) shows short clusters creeping one on top of the other ($L_I = 160°$). The current crossing the equator could possibly be the dark streak ejected from the equatorial fringe on 31 January, which may have moved on (or, rather, lagged behind) and projected against the quadruplet. On the other hand, though, the streak was observed at the boundary between the first and second clouds of the quadruplet, at the point where the dividing double bridge met the equatorial band. It thus seems more likely that the streak is an independent formation; it will be noted that this streak was located at the same place on 1 November and 5 December, and it could not have moved so far back by 31 January, besides the fact that, being located on the equator, it should have been displaced to the east and not to the west.

Between the North Equatorial Belt and the North Polar Cap there is a light zone, on which very faint narrow belts could sometimes be seen (36).

The North Polar Cap. Its structure clearly shows on the drawing of 2 November 1963 (39), taken under 200 × magnification. Unlike the other zones, the Cap did not have a regular edge, and its surface was marked with immense puffs of brown smoke. The Cap normally showed a flocculent appearance, with indistinct dark riges running through. Occasionally the cap was divided into two parts, more intense in the high latitudes. This may be due to the effect of a belt combined with limb darkening. The features were generally arranged in an almost straight row at the same latitude. Bridge-type formations could be seen, sloping slightly in the direction of Jupiter's rotation.

Another interesting aspect was the asymmetry of the North Polar Cap (27, 37). At a longitude $L_{II} = 130-140°$ there occurs a sharp dip to the right, while at $L_{II} = 30-40°$ the edge reaches its lowest latitude. A dip to the left was never observed, while on the far right it must have been offset by the darkening of the western limb.

The January observations showed that chromatic aberration had a more pronounced effect on Jupiter's disk when it grew smaller, thus the polar part of the North Cap became tinged with green, while its lower part remained brown, as before. The faint reddish color of the South Cap also could be the result of climatic aberration. This effect was probably responsible for the northward reddening observed at the boundaries between the dark and light formations.

General remarks. Some of the processes observed on Jupiter bear conflicting aspects: two types of dark bands, and three types of clouds. Thus, if it is assumed that the dark bands are produced by zonal velocity differences, it is hard to explain the presence of dark formations on the

clouds; furthermore, the darker parts of the equatorial belts are usually redder, and the disappearance of the red color in the North Polar Cap reveals two dark belts, while the high-contrast feature on the South Temperate Belt is not colored red (there is no noticeable coloring of the light zone further below by chromatic aberration, either). Some clouds on Jupiter appear as bright spots (South Temperate Belt), and in other regions there are none of this type; on the equator, though, there are lighter areas either against a light background, or just thrown into contrast by bridges. The clouds of the second type sometimes appear expelled from within; it may be that they are simply outlined by bridges which are obscured to a varying extent. As to the possible existence of a ring, the disk did not show any ears, and there was no limb darkening of the belts. The apparent equatorial belts could hardly be taken as a ring shadow—at times there are many of them and it is difficult to tell which are equatorial. Besides, the shadow should have been perfectly visible on any fog, and this was never observed. There is, however, an interesting intersection of the curved streak passing through the equator, which may be seen in (65). The streak is cut exactly at the point where the straight sections of the equatorial fringe terminate.

JUPITER IN 1964

V.A. ZINOV'EV
All-Union Astronomical and Geodetic Society, Volgograd Branch

The observations of Jupiter were begun at the end of May 1964, at the observatory of the Volgograd Planetarium, using the 30-cm refractor (cf. preceding article).

There were some changes in the appearance of the planet compared with 1963: the brightness of the south tropical zone strongly increased, the equatorial zone became more sharply defined, the narrow belts in the tropical zones increased in intensity, and a red coloration showed only in the Red Spot and the South Equatorial Belt. The South Tropical Belt partly blended with the wide girdle of equatorial belts, and over the North Equatorial Belt persistent clouds and strong dark currents developed. Radical changes took place in the North Equatorial Belt below the Red Spot, resulting in the appearance of a stable cloud formation. There was an unusual rise in the intensity of the two belts in the North Polar Cap, while the South Temperate Belt showed areas of extremely low intensity.

THE PASSAGE OF A WHITE SPOT ABOVE THE RED SPOT

In July 1964 one of the white spots in the South Temperate Zone overtook the Red Spot, skirting it on the south. Outwardly this passage did not attract particular attention, but the curves of motion of the spots showed that at the time of passage the features clearly interacted (Figure 1).

It may be seen from Figure 1 that the white spot "shifted" the Red Spot from its normal position, $L_{II} = 16°$. During the overtaking the white spot slowed down due to interaction with the Red Spot. After the passage the motion of the two features became regular again, and the Red Spot resumed its normal position.

Analysis of the motion of the white spot which passed above the Red Spot (I) has shown that the white spot had different velocities at different times. Thus, after the conjunction its velocity was 0.67 deg/day, and in July-October it was 0.58 deg/day. In October 1963 the position of the white spot was near $L_{II} \approx 200°$, and at the end of August 1964 it crossed the zero meridian. The white spot accordingly traverses the entire South Temperate Belt in about 20 months.

OTHER WHITE SPOTS, OR CLOUDS, IN THE SOUTH TEMPERATE BELT

The second white spot is a young formation which developed into a separate cloud at the end of November 1963, at about $L_{II} = 250°$.

The third white spot was observed, like the first, in October 1963 at $L_{II} = 90°$.

Analysis of the changes in these spots and their motion along the South Temperate Belt has shown that the white spots are not permanent formations; they apparently originate in the southern part of the South Temperate Belt, at its boundary with the South Temperate Zone. These spots move at roughly the same speed, 0.57—0.59 deg/day.

With the formation of the second spot, an elongated gray feature, extending to the right of the spot, appeared on the South Temperatre Belt. It is here, between white spots II and III, that the veiled part of the South Temperate Belt observed in the fall of 1964 was located.

This region is distinguished by three factors: heavy fog, a sharp dip in the latitude of the northern edge of the South Polar Cap, and low intensity of the South Temperate Belt.

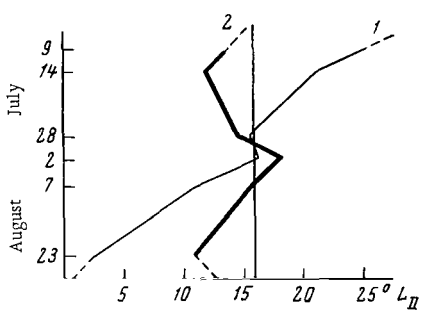

FIGURE 1. Variation of the latitude of the white spot (1) and Red Spot (2) during their meeting in June—August 1964.

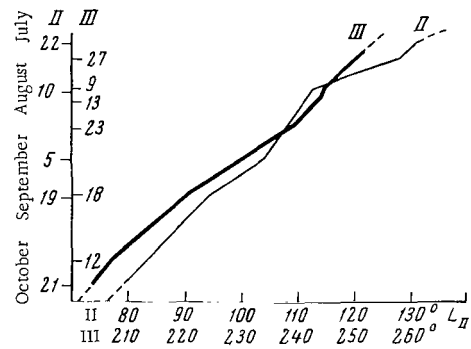

FIGURE 2. Variation of the latitude of the white spots (II, III) in July—October 1964.

Figure 2 shows for comparison the curves of motion of white spots II and III, i.e., of the end-points of the turbid area of the belt. We see that the width of this area varied, reaching maximum at the middle of August 1964.

The fog was observed to move together with the lowermost edge of the polar cap toward spot III, where the edge was joined with the temperate belt by diffuse bridges.

Before the appearance of the fog, the northern part of the split temperate belt was very distinct, and when the fog disappeared the southern part became stronger.

The variation in the intensity of the temperate belt may be explained by the displacement of gas masses in the polar cap, which affected its appearance. The position of the edge of the polar cap at different longitudes suggests that Jupiter's polar axis does not coincide with the axis of rotation, since the asymmetry of the North Polar Cap observed in 1963 is closely

correlated with deviations in the South Polar Cap. The South Pole is displaced from the Red Spot; the northern polar boundary is lowest at the longitude of the Red Spot, whereas the southern polar boundary is highest.

NORTH EQUATORIAL BELT

This belt is formed by a highly complex system of light spots, dark currents, and strong disturbance regions, where the dark belts are directed toward the equator. Perhaps the most interesting formation in the belt are the two small bright clouds lying in the northern (high-latitude) part of the belt. They were observable not only because of their brightness, but especially because they always stayed under the Red Spot, in front of a strong dark current moving to the equator; this suggested that the clouds were eddies. Measurements of the difference in the times of passage of the white clouds and the Red Spot across the central meridian (Figure 3) have shown that the clouds move in the direction of Jupiter's rotation; over two months the difference was 25 min, which corresponds to $\Delta L = 15°.1$ in System II. The curve of motion shows that the clouds abruptly shift by 10° in about 37 days; the maximum displacement is observed at one third of the period.

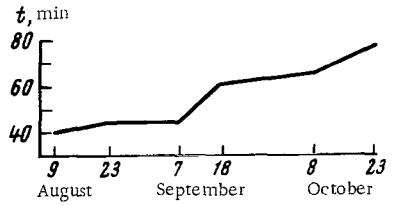

FIGURE 3. Difference in the times of central-meridian crossing of the Red Spot and the white clouds in the North Equatorial Belt.

The system of strong dark disturbances in the North Equatorial Belt was seen in the same places where they had been observed in 1963.

To the side and south of the disturbances (very close to the equator) the belt shows light archlike clouds; a study of their position indicates that the clouds move in System II. These clouds gradually stretch out in longitude and are intersected by thin bridges. Some of the clouds cover the entire width of the belt and are usually bisected by a curved dark strip which links the two parts of the split belt.

NORTH POLAR CAP

The considerable intensity of the belts in the high northern latitudes of Jupiter facilitates observation of the features of the North Pole, which faces the Earth. The high-latitude belt was the wider and stronger of the two. The belts were joined by a set of bridges and arms. As in the equatorial zone, the bridges are deflected in the direction of rotation, and the dark formations in the belts are inclined in the opposite direction.

Like the other zones of Jupiter, these latitudes display a variety of bright formations.

On 21 October favorable conditions prevailed and the features of the North Polar cap were observable right up to the pole. Two more spots

were observed at higher latitude above the belts; irregular fields of spots—oval light formations and dark formations in the form of winding trails which issue from the pole and skirt the light areas—were observed above 70° latitude. Next to the pole a faint banded structure was observed, and two light spots off-center from the pole.

The variation in the longitude of the bright formations in Jupiter's North Polar Cap reveals them to have the rotation period of System II. One of the light spots was seen in 1963 at $L_{II} = 190°$, and in 1964 a light spot was observed in the same region, at $L_{II} = 200°$.

CONCLUSION

Even with frequent and systematic observation of Jupiter, many changes on the planet are inevitably missed. It was nevertheless obvious that, after subsiding somewhat in the middle of the summer, the activity on Jupiter rose by the end of August 1964 to an anomalous two-year high (1963—1964). The planetary disk was lamost completely veiled by reddish-gray fog, except for the South Tropical Zone and part of the Temperate Zone. The fog was particularly dense over the equatorial zone, where it was very nonuniform, with many gaps and clear patches.

At the beginning of September, Jupiter literally started boiling, and long chains oi very bright clouds could be seen at all latitudes (up to 70°). In the fall of 1964 a deep red North Tropical Belt suddenly developed and became progressively wider. A strong turbulence was observed not only in the equatorial and tropical belts, but also in the high-latitude regions.

The processes obsevable on Jupiter are apparently characterized by vertical atmospheric mixing. Together with dark currents there are seen very bright formations in the shape of round clouds. There is evidently a downward motion of gases which subsequently rise, producing various light formations. It is worth noting that the apparent processes (however varied and complex) consistently present the same aspect. The only difference is in the intensity and the speed of these processes and in their interaction.

The observation of Jupiter at the time of highest activity provides us with a fairly good picture of the Jovian processes in all their complexity and interdependence.

OBSERVATIONS OF JUPITER DURING THE OPPOSITION OF 1964

N. K. ANDRIANOV
All-Union Astronomical and Geodetic Society, Chelyabinsk Branch

ORGANIZATION AND OBSERVATION PROGRAM

In 1964 the author undertook systematic visual observations of Jupiter, using a 165-mm reflector on an equatorial mounting of his own design. Depending on atmospheric conditions the magnification was 190× or 285×. A yellow (ZhS-17), an orange (OS-12), or a green (ZhZ-5) filter was used. Drawings of the planet were made, as usual, on an oval template of standard size /1, 2/.

During the period from 1 September 1964 to 31 January 1965, a total of 114 drawings were made, all of which were processed. Observations were carried out at such times when atmospheric conditions were fair. The seeing averaged 3.6 (out of maximum 5) over the period of observations. More than 40 drawings were made under good or excellent seeing.

Besides drawings of the telescopic images of the planet, the observation program also included systematic evaluations of the intensity of the belts and polar caps on the current six-point scale /1/.

The observations were aimed at studying the distribution of the features on the planetary disk, the latitudinal motion of the belts, and the variation of their intensity during the relevant period. The proper motion of the Red Spot over the planetary disk was also investigated. Whenever the Red Spot was visible, particular care was taken to record its exact position. During the entire period of observations, 46 drawings of Jupiter showing the Red Spot were made. From these, 34 drawings were picked out for processing; they had been made under very good atmospheric conditions and with the Red Spot sufficiently far from the limb.

PROCESSING OF THE OBSERVATIONAL MATERIAL AND SOME FINDINGS

The observational data were processed by the usual methods /1– 3/. For the calculation of the mean latitude of the belts and their mean intensity, the observations were divided into five groups. The drawings were measured with a standard reticule, and in each group the mean latitude of the belts and the polar caps was calculated for the mean data of the particular group.

In addition, the mean square error was calculated by sampling different latitudes /1, 2/. The resultant error is roughly the same as in earlier publications /3, 4/, and tends to decrease from 0°.9—0°.8 at high latitudes to 0°.3—0°.2 in the equatorial zone.

The variations in the latitude of the edges of the belts and polar caps with time are listed in Table 1, where the conventional notation has been adopted: SPC—South Polar Cap; STeB—South Temperate Belt; STB—South Tropical Belt; NTB—North Tropical Belt; NTeB—North Temperate Belt; NPC—North Polar Cap. Another four fainter belts were also observed: the South-South Temperate Belt (SSTeB), located near the SPC; the South-South Tropical Belt (SSTB), very narrow but quite intense; the North-North Tropical Belt (NNTB), very narrow and faint; and, finally, the North-North Temperate Belt (NNTeB), located near the NPC. The mean latitudes of the edges of these belts are also given in Table 1.

TABLE 1. Variation of latitudes with time

Group	No. of drawings	Mean date	SPC	SSTeB		STeB		SSTB		STB	
				S	N	S	N	S	N	S	N
1	18	15 Sept.'64	−43°.6			−33°.4	−27°.3	−21°.2	−18°.5	−15°.0	−3°.1
2	23	20 Oct. "	−51.2	−47°.7	−46°.2	−37°.6	−30.3	−21.4	−19.6	−17.0	−3.4
3	20	19 Nov. "	−52.5	−46.6	−44.9	−35.8	−28.8	−21.9	−20.5	−17.4	−4.0
4	26	11 Dec. "	−49.0	−46.3	−45.6	−37.9	−29.8	−22.2	−20.8	−18.7	−3.7
5	27	17 Jan. '65	−50.0	−49.1	−47.6	−37.6	−30.0	−21.9	−20.8	−19.4	−4.6

Group	No. of drawings	Mean date	NTB		NNTB		NTeB		NNTeB		NPC
			S	N	S	N	S	N	S	N	
1	18	15Nov.'64	2°.0	13°.5			28° 1	32°.6	37°.9	38°.7	40°.2
2	23	20 Oct. "	2.8	13.1			31.4	33.8	36.6	37.7	41.6
3	20	19 Nov. "	4.0	12.7	21.2	22.5	30.7	33.6	37.2	38.6	43.5
4	26	11 Dec. "	4.6	13.9	22.5	23.8	32.0	36.7	39.2	40.7	46.3
5	27	17 Jan.'65	4.6	12.4	21.0	22.3	31.1	35.6	38.0	40.0	46.7

The data of the table are plotted in the diagram of Jupiter's belts in Figure 1. Examination of the diagram yields the following results:

1. On the whole the latitude and the width of the belts varied little during the period of observations.

2. The SSTeB became observable approximately in the second half of October 1964, and the NNTB appeared in the second half of November.

3. There was a gradual drift of the STB to the south and the NTB to the north; the width of the STB slightly increased in the process, and that of the NTB decreased.

4. The distance between the STB and NTB slowly increased and reached a maximum at the end of the observational period.

5. There was a certain decrease in the SPC in November, and a steady but very small decrease in the NPC during the entire observational period.

6. In October the STeB migrated to the south, its position and width remaining virtually constant thereafter.

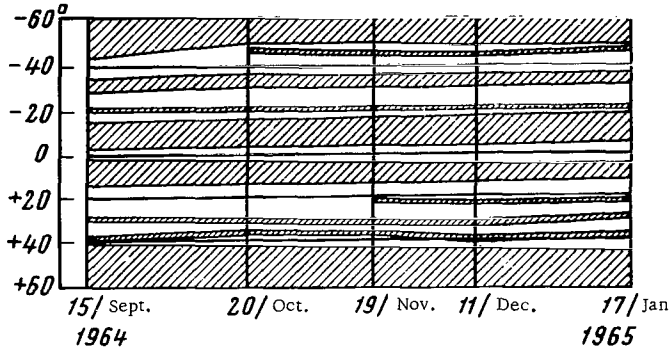

FIGURE 1. Diagram of latitudinal motion of Jupiter's belts (September 1964—January 1965).

The average intensity of the belts and polar caps in each of the five groups is given in Table 2. The table shows the following results:

1. On the whole, the STB, NTB, SSTB, and the active zone in the STeB showed the highest intensity during the period of observations, whereas the intensity of the SPC and NPC was fairly low and constant.
2. The intensity of the STB and NTB became highest by the end of the observation period. The intensity of the NTB was a little higher than that of the STB almost all the time.
3. The lowest intensity was observed in the SSTeB and the NNTB.

TABLE 2. Average intensity of the belts and polar caps

Group	SPC	SSTeB	STeB	SSTB	STB
1	0.5	—	0.9	2.4	2.6
2	0.6	0.7	1.2	1.1	2.7
3	0.7	0.8	1.2	1.4	2.6
4	0.5	0.6	1.1	2.5	2.7
5	0.5	0.5	0.6	1.8	2.8

Group	NTB	NNTB	NTeB	NNTeB	NPC
1	2.6	—	0.9	—	0.6
2	2.8	—	0.9	0.5	0.6
3	2.7	0.4	0.7	0.3	0.5
4	3.1	0.5	1.2	0.9	0.7
5	3.3	0.2	0.9	0.7	0.6

MAPPING OF JUPTER AND THE VISIBILITY OF ITS FINE SURFACE FEATURES

A map of Jupiter was prepared for the mean date of 19 November 1964 from 27 drawings taken in the period from 26 October to 7 December 1964.

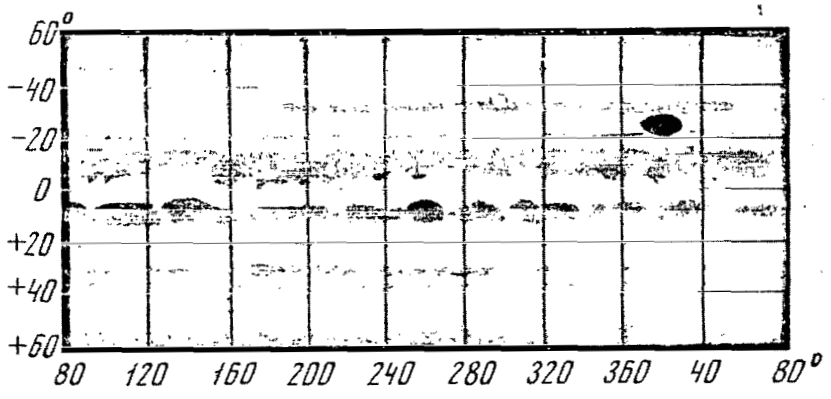

FIGURE 2. Map of Jupiter on 19 Nov. 1964.

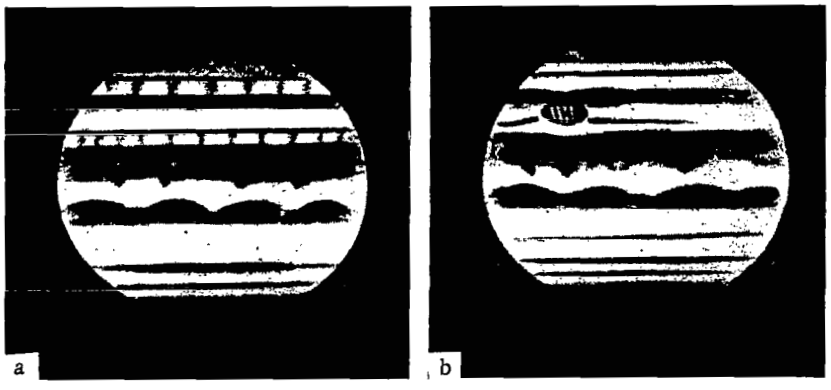

FIGURE 3. Drawings of Jupiter:

a—23 Sept. 1964, 21 hrs 10 min UT; b—23 Nov. 1964, 20 hrs 15 min UT.

A coordinate reticule and a table of Jupiter's physical coordinates /5/ were first used to determine from the drawings the joviographic coordinates of the 28 most prominent features which were observed at least twice. The measurement results are summarized in Table 3. The longitude of most features was calculated in System II. On the basis of the table a map of Jupiter was compiled for 19 November 1964 (Figure 2). The map was drawn in the Lambert equigraphic cylindrical projection /1, 2/, which is very convenient for the mapping of Jupiter, as essentially all the belts and other characteristic features lie at latitudes between - 40 and + 40°. The most active zones in the latitude ranges of 20, 140, 260, and 350° are easily discernible on the map. Many active areas in the NTB and the active zone in the STeB are also clearly visible.

TABLE 3. Catalogue of features observed at least twice (mean date 19 November 1964)

No.	Description	n	λ	φ	No.	Description	n	λ	φ
1	Indentation in the NTB	3	17°	+ 5°	15	Protrusion in the STB	2	188°	−4°
2	Indentation in the STB	3	19°	−35	16	Dark spot in the STB	2	198	−4
3	Red spot	13	8(W) 31(E)	−29(S) −20(N)	17	Protrusion in the STB	3	216	−3
4	Dark spot in the STB	2	24	−1	18	Indentation in the NTB	5	220	+ 8
5	Indentation in the NTB	4	49	+ 8	19	Dark spot in the NTB	4	261	+ 7
6	Protrusion in the STB	3	53	−2	20	Protrusion in the NTB	4	284	+ 4
7	Intensity drop in the STeB	5	58	−32	21	Narrowing of the NTeB	2	291	+ 33
8	Protrusion in the STB	3	69	−1	22	White spot in the STeB	3	298	−37
9	Indentation in the NTB	3	95	+ 8	23	Indentation in the NTB	2	300	+ 8
10	Dark spot in the NTB	3	144	+ 7	24	Dark spot in the NTB	3	309	+ 6
11	Protrusion in the STB	2	160	−3	25	Indentation in the STB	6	310	−7
12	Widening of the NTeB	2	172	+ 35	26	Indentation in the NTB	2	341	+ 8
13	Indentation in the NTB	3	173	+ 7	27	Dark spot in the STB	2	358	−2
14	Intensification in the STeB	3	183	−31	28	Protrusion in the STB	2	359	−4

Occasionally, but only under excellent atmospheric conditions, it was possible to observe on Jupiter's disk some fine surface features which were normally undetectable. Figure 3a shows Jupiter as viewed through the 165-mm reflector under excellent seeing. This drawing, made at a 285 x magnification, displays a fine network of delicate grayish bridges joining the SSTB with the STB and the SPC with the STeB. Figure 3b, which was also made under excellent seeing with 285 × magnification, clearly shows

the fine traces of the SSTeB, SSTB, NNTB, NTeB, and NNTeB; also evident are the Red Spot, the drop of intensity in the STeB, and a number of fine features in the two tropical belts.

STUDY OF THE MOTION OF THE RED SPOT AND THE ACTIVE ZONE IN THE STeB

For the study of the proper motion of the Red Spot over the planetary disk, the 34 best drawings of Jupiter were selected, showing the Red Spot sufficiently far from the limb. The drawings were divided into 5 time groups, covering the period from 14 September 1964 to 30 January 1965. Reticule measurements combined with tables of the physical coordinates of Jupiter /5, 6/ gave the planetographic coordinates of the northern, southern, western, and eastern edges of the Red Spot. From these the coordinates of the Spot's center were calculated, and the results were averaged for the mean date of each group. The mean rate of migration of the Red Spot in latitude, longitude, and along the tangent to its trajectory was also calculated over the periods between the mean dates of the 5 groups. The results are listed in Table 4.

TABLE 4. Proper motion of the Red Spot (observations from 14 Sept. 1964 to 30 Jan. 1965)

Group	No. of drawings	Mean date	Averaged planetographic coordinates		Time interval	Mean velocity of proper motion, deg/day		
			λ_{II}	φ		longitudinal	latitudinal	along trajectory
1	4	20 Sept. '64	27°.2	−24°.5				
2	8	10 Oct. "	25 .0	−27 .1	20 Sept. — 10 Oct. '64	−0.11	+ 0.13	0.17
3	8	13 Nov. "	19 .3	−25 .3	10 Oct. — 13 Nov. '64	−0.17	+ 0.05	0.18
4	7	11 Dec. "	24 .3	−26 .3	11 Dec. — 11 Dec. '64	+ 0.18	− 0.04	0.19
					11 Dec. '64	−0.11	−0.04	0.12
5	7	18 Jan. '65	20.0	−27 .9	18 Jan. '65			

The data of the table are plotted in Figure 4, which shows graphically the apparent displacement of the Red Spot over the planetary surface during the observation period. From the diagram and the table we conclude the following:

1. During the observation period, the latitude of the Red Spot decreased by approximately 8°. The retrograde motion (West to East) lasted just about one month, from 13 Nov. to 11 Dec. 1964.

2. During the observation period the Red Spot moved toward the SPC by almost 5° latitude.

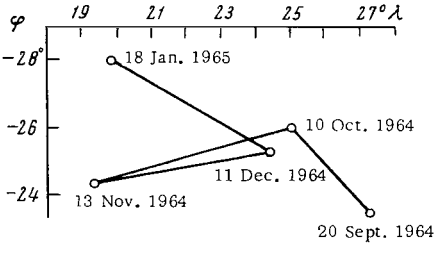

FIGURE 4. Proper motion of the Red Spot.

3. The rate of motion along the trajectory increased somewhat at the end of November and the beginning of December 1964, and then fell off rapidly after that (from 11 Dec. 1964 to 18 Jan. 1965).

a *b* *c*

FIGURE 5. Migration of the boundary of the active zone in the STeB:

a—18 Oct. 1964, 21 hrs 13 min; b—12 Dec. 1964, 20 hrs 05 min; c—22 Jan. 1965, 19 hrs 25 min UT.

In conclusion it remains to mention the high-intensity active zone which was clearly observed in the STeB. In November this zone extended over a longitude range of 125°. Its intensity averaged about 3.1 on the 6-point scale, while the remaining part of the STeB showed an intensity of about 0.1—0.2 and was barely discernible at times.

On 9 drawings the western boundary of the active zone could be seen to move very rapidly to the east (Figure 5), with a mean velocity of about 0.7° per day. This is an uncommonly high rate of migration, even for Jupiter's surface. Further confirmation of this phenomenon would no doubt be of considerable interest.

Bibliography

1. Bronshten, V.A. Planety i ikh nablyudenie (Planets and their Observation).—Gostekhizdat. 1957.
2. Bronshten, V.A. Instruktsiya dlya nablyudenii planet (Instructions for Observation of Planets).—Izdatel'stvo AN SSSR. 1961.
3. Rutkovskaya, M.Ya. Yupiter v 1955g. (Jupiter in 1955).—Byulleten' VAGO, No. 25 (32). 1959.
4. Tsvetkov, V.I. Osnovnye polosy i detali na Yupitere v 1959g. (Main Belts and Other Features on Jupiter in 1959).— Byulleten' VAGO, No. 34. 1963.
5. Astronomicheskii kalendar' na 1964g. (Astronomical Calendar for 1964).—VAGO, Fizmatgiz. 1963.
6. Astronomicheskii kalendar' na 1965 g. (Astronomical Calendar for 1965).—VAGO, Fizmatgiz. 1964.

JUPITER IN 1963—1964

I. N. POTAPOV
All-Union Astronomical and Geodetic Society, Kazan Branch

In 1963—1964 the Kazan Branch of the All-Union Astronomical and Geodetic Society conducted a series of observations of Jupiter. The observations were carried out at the Kazan Astronomical Observatory on a 225-mm Merz refractor with 330× magnification. By 31 December 1964, 277 drawings were made (164 in 1963 and 113 in 1964). Jupiter was under constant observation: in 1963, by I. N. Potapov (43 drawings), A. M. Vasil'ev (27), E. G. Galeeva (21), V. P. Merezhin (20), V. S. Simonov (16), V. M. Popov (12), S. M. Valisheva (10), and Yu. Voroshilov (7); in 1964, by I. N. Potapov (30 drawings), V. Kasatkin (16), A. Shavrina (13), V. S. Simonov (11), E. Kolotilov (7), Yu. Voroshilov (6), and T. N. Zelenkova (5).

The material for 1963 was processed by V. M. Popov, V. P. Merezhin, and I. N. Potapov, and that for 1964, by I. N. Potapov. The processing was done by the method of groups /1/.

The observations cover the period from 14 October 1963 to 28 February 1964, and from 6 September to 31 December 1964.

In the fall of 1963 (14 October—31 December) the following features were constantly observed on Jupiter: the North Polar Cap, the North Temperate and Tropical belts, the South Tropical and Temperate belts, the South Polar Cap, and the Red Spot. The mean latitudes of the edges of the belts and caps are given in Table 1 and in the diagram in Figure 1. A map of Jupiter's surface was drawn for the date of 15 December 1963 (Figure 2). An attempt was made to find a correlation between the intensity of the belts and their width. The results are listed in Tables 2 and 3.

TABLE 1. Mean latitudes of the belts in 1963

Group	No. of drawings	Mean date	NPC	NTeB		NTB		STB		STeB		SPC
				N	S	N	S	N	S	N	S	
1	18	15 Oct.	38°.6	36°.8	29°.7	13°.8	3°.2	−1°.1	−15°.9	−26°.1	−34°.8	−43°.5
2	25	26 Oct.	36 .7	35 .9	32 .5	14 .6	3 .4	−1 .1	−14 .7	−28 .5	−37 .9	−43 .4
3	14	26 Nov.	38 .8	37 .9	33 .2	16 .4	3 .7	−0 .8	−16 .9	−28 .9	−37 .5	−44 .9
4	20	4 Dec.	38 .1	37 .0	31 .1	16 .4	3 .3	−0 .7	−14 .8	−26 .7	−35 .4	−45 .4
5	12	11 Dec.	38 .0	37 .6	31 .6	17 .4	4 .2	−0 .8	−17 .8	−31 .2	−39 .0	−49 .9
6	17	14 Dec.	35 .9	33 .7	31 .9	14 .8	3 .1	−1 .2	−16 .5	−28 .2	−35 .0	−42 .1
7	18	21 Dec.	36 .8	36 .2	29 .4	15 .2	3 .1	−1 .2	−14 .4	−26 .4	−32 .7	−37 .5
8	21	26 Dec.	35 .1	34 .0	30 .4	15 .3	3 .5	−1 .3	−15 .1	−27 .0	−34 .0	−39 .1

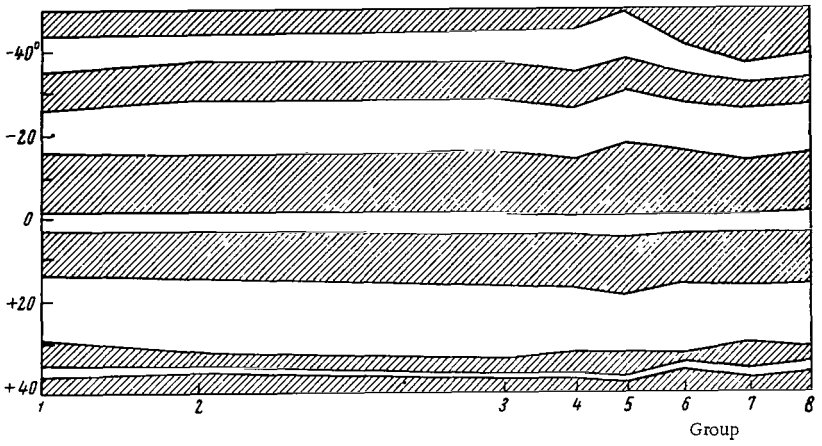

FIGURE 1. The latitudes of the belts and caps on Jupiter in 1963.

In 1964 (1—28 February, 6 September—31 December) additional features became visible on Jupiter's surface. In the Northern Hemisphere the NNTeB appeared, and the NTeB was better observable. The Southern Hemisphere showed the formation of the SSTeB, which merged with the STeB near the Red Spot.

The Red Spot itself showed a number of changes. Its size increased and it occupied almost the entire width of the South Tropical Zone. There was an enhancement in the intensity of the Red Spot, and it displayed a distinctly pink color. The STB also changed color and its southern edge deepened to brick red. The northern edge was not clearly marked and it faded evenly into the equatorial zone.

TABLE 2. Mean width of the belts in 1963

Group	NTeB	NTB	STB	STeB
1	7.1	11.6	14.8	8.7
2	3.4	11.2	13.6	9.4
3	4.7	12.7	16.1	8.6
4	5.9	13.1	14.1	8.7
5	6.0	13.2	17.0	7.8
6	2.6	11.7	15.3	6.8
7	5.8	12.1	13.2	6.3
8	3.6	11.8	13.7	7.0

The mean measured latitudes of the edges of the belts and caps on Jupiter in 1964 are given in Table 4 and Figure 3. A map of Jupiter's surface for 15 December 1964 was drawn (Figure 4). The map shows a bending of the belts, within the latitude range from 60 to 210° in the Southern Hemisphere, and from 60 to 300° in the Northern. The asymmetric bending of the belts with respect to the planetary equator may be attributed to the presence of

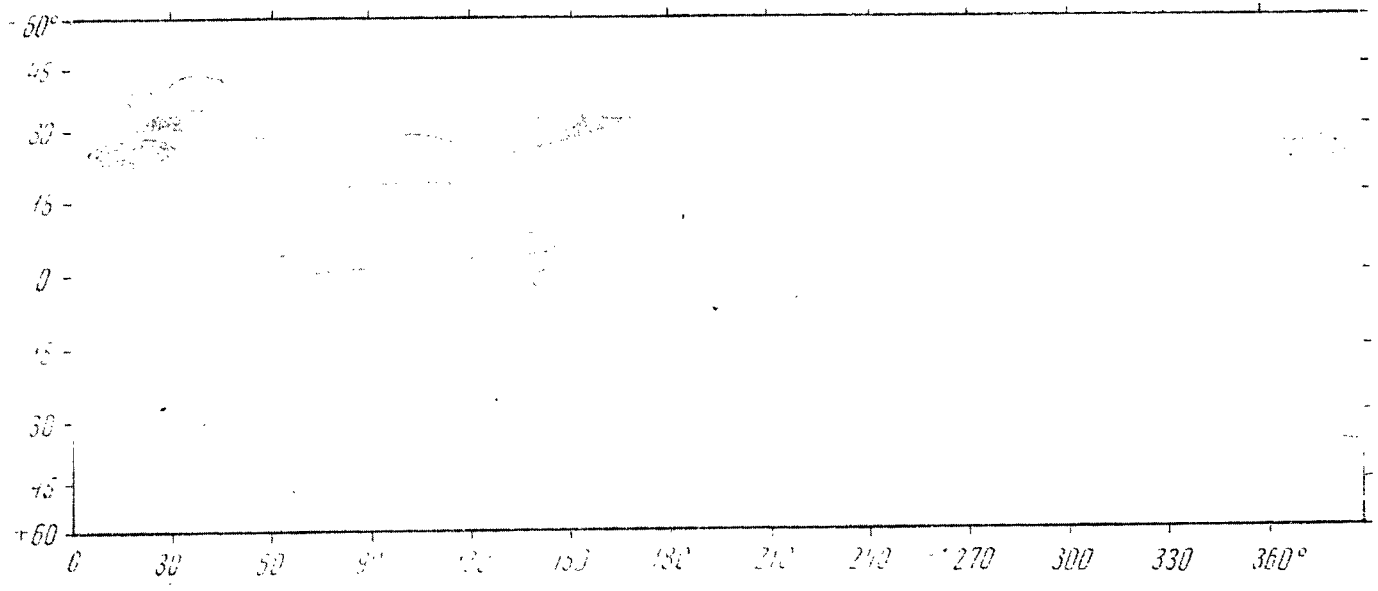

FIGURE 2. Map of Jupiter's surface, 15 December 1963.

the Red Spot in the Southern Hemisphere. If such bending is significant (this is supported by the bends appearing in the drawings we have taken, see Figure 5, and in Lose's drawings /2/), its existence might be associated with meridional currents extending over a wide range of latitudes.

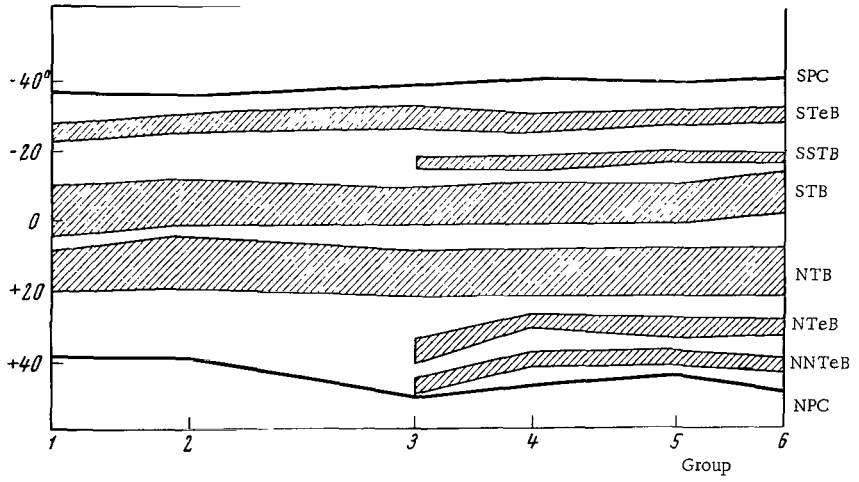

FIGURE 3. The latitudes of the belts and caps on Jupiter in 1964.

TABLE 3. Mean intensity of the belts and caps in 1963

Group	SPC	STeB	STB	NTB	NTeB	NPC
1	2.0 (11) *	3.8 (13)	3.2 (14)	3.4 (14)	2.3 (12)	2.2 (11)
2	1.9 (14)	3.6 (16)	3.4 (16)	3.0 (16)	2.6 (16)	2.3 (15)
3	1.5 (6)	3.8 (8)	2.8 (8)	2.7 (7)	1.3 (6)	1.3 (6)
4	1.3 (11)	3.9 (12)	3.5 (12)	3.3 (12)	2.1 (11)	2.2 (11)
5	1.3 (7)	3.4 (8)	3.3 (8)	3.4 (7)	1.9 (7)	1.9 (7)
6	1.6 (16)	3.5 (14)	3.5 (14)	3.5 (13)	1.7 (14)	1.6 (14)
7	1.3 (13)	3.0 (12)	3.1 (14)	3.1 (14)	1.6 (14)	1.6 (14)
8	1.2 (14)	3.4 (13)	2.8 (16)	3.1 (15)	1.5 (14)	1.5 (14)

* The figures in parentheses indicate the number of drawings from which the mean intensities were calculated.

In 1962 an unusual phenomenon took place on Jupiter: the NTB and the STB merged into an equatorial girdle. This was recorded only once before, in 1876—1878 (drawings of that period were published by the Potsdam Observatory /3/), and it occurred simultaneously with an enhancement in the brightness of the Red Spot. In our observations there was also a rise in the activity of the Red Spot, which in 1964 was the most prominent feature on Jupiter's surface. The equatorial girdle formed in the fall of 1962 (September—October /4/) and persisted at least for two months /5/ but not more than a year, since in the fall of 1963 the equatorial zone was observable; after the girdle had split up, the South and North Tropical belts drifted slowly toward the poles (according to the observations of 1963—1964). On the basis of data of the Dnepropetrovsk Department of the Kharkov branch of the Astronomical and Geodetic Society /5/ on the

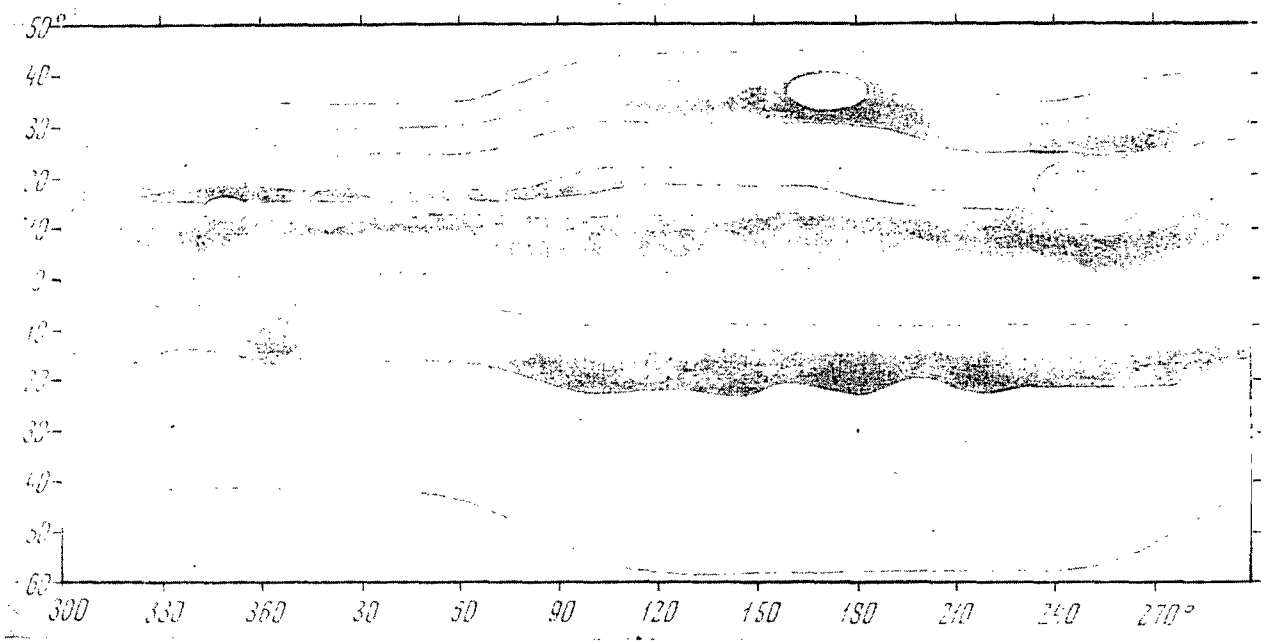

FIGURE 4. Map of Jupiter's surface, 15 December 1964.

TABLE 4. The latitude of Jupiter's belts in 1964

Group	No. of drawings	Mean date	NPC	NNTeB		NTeB		NTB	
				N	S	N	S	N	S
1	7	21 Jan.	39°.0					21°.0	9°.0
2	8	19 Feb.	40 .3					19 .6	4 .0
3	16	9 Sept.	51 .1	50°.5	44°.8	40°.0	34°.2	21 .9	8 .1
4	32	19 Oct.	46 .6	42 .2	38 .3	30 .8	27 .5	21 .2	7 .1
5	6	20 Nov.	43 .8	42 .4	37 .6	32 .5	28 .0	20 .6	7 .5
6	39	8 Dec.	48 .1	44 .2	39 .8	32 .5	28 .9	20 .2	7 .2

Group	No. of drawings	Mean date	STB		SSTB		STeB		SPC
			N	S	N	S	N	S	
1	7	21 Jan.	4°.0	−10°.0	—		−24°.0	−29°.0	−37°.0
2	8	19 Feb.	1 .3	−11 .3			−25 .3	−30 .8	−37 .2
3	16	9 Nov.	1 .1	−9 .8	−14°.8	−17°.8	−28 .1	−33 .6	−39 .5
4	32	19 Oct.	0 .8	−11 .2	−13 .8	−17 .6	−25 .8	−31 .0	−41 .2
5	6	20 Nov.	0 .1	−11 .1	−17 .0	−20 .0	−28 .1	−32 .5	−41 .3
6	39	8 Dec.	1 .6	−14 .1	−16 .8	−19 .6	−28 .6	−33 .1	−40 .9

TABLE 5. Measurement results on the width of Jupiter's equatorial zone in 1962−1964

Group	Year		
	1962	1963	1964
1	0°	4°.3	5°
2	0	4 .5	2.8
3	0	4 .5	7
4	0	4	6.3
5	0	5	7.4
6	0	4 .3	8.8
7	0	4 .3	
8	0	4 .8	
Average	0	4 .46	6.22

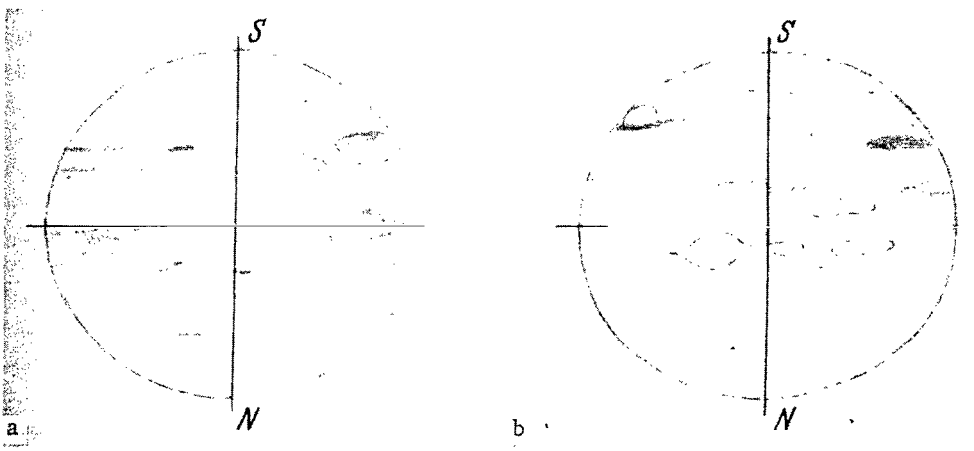

FIGURE 5. Drawings of Jupiter (9-inch refractor of the Kazan Astronomical Observatory, 330x): a—7—8 Sept. 1964, 1 hr 08 min (I.N. Potapov); b—9—10 Sept. 1964, 2 hrs 40 min (Yu. Voroshilov).

state of Jupiter's surface in the fall of 1962 and from our observations, we plotted the variations in the width of the equatorial zone for the period of 1962—1964 (Figure 6). The numerical values are given in Table 5. Here too, we probably have a case of meridional currents on a planetary scale.

Finally, the drawings in Figure 7 show typical configurations of Jupiter's surface in 1963—1964.

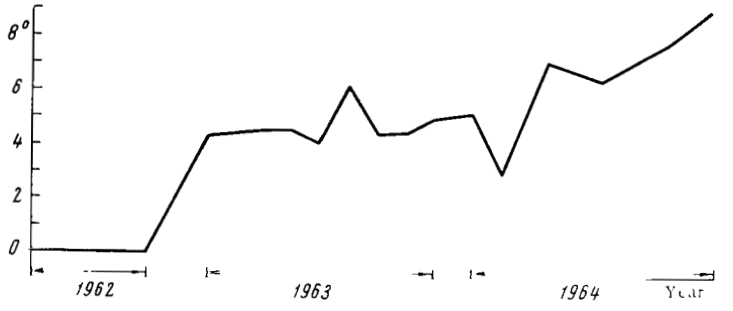

FIGURE 6. Variations in the width of the equatorial zone during 1962—1964.

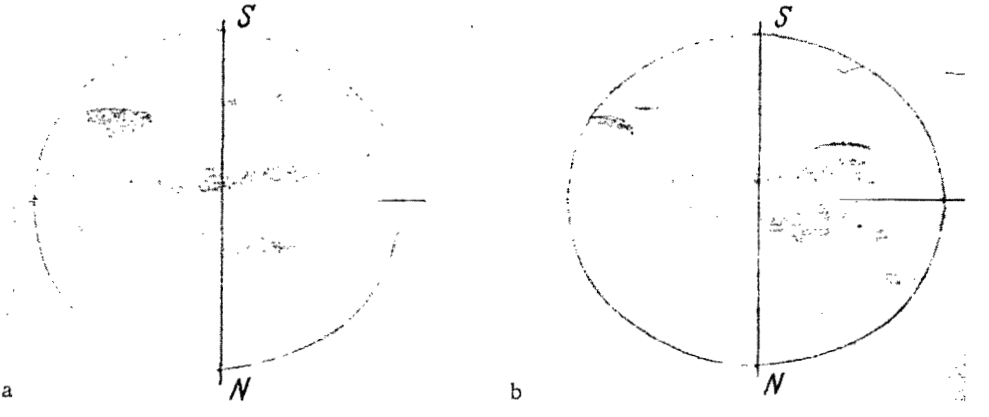

FIGURE 7. Drawings of Jupiter (9-inch refractor of the Kazan Astronomical Observatory, 330 x):
a—7—8 Dec. 1964, 19 hrs 45 min (V.M. Popov); b—9—10 Dec. 1964, 0 hrs 38 min (I.N. Potapov).

Bibliography

1. Bronshten, V.A. Planety i ikh nablyudeniya (Planets and their Observation).— Gostekhizdat. 1957.
2. Publikation des astrophysikalischen Observatoriums zu Potsdam, Vol. 21, Potsdam. 1911.
3. Publikation des astrophysikalischen Observatoriums zu Potsdam, Potsdam, 1878. 1883.
4. Vsekhsvyatskii, S.K. Burnye protsessy na Yupitere (Violent Processes on Jupiter).— Astronomicheskii Tsirkulyar, No. 232. 1962 (See also his article in this collection, p. 30).
5. Baranenko, V.A. Yupiter osen'yu 1962 goda (Jupiter in Fall 1962).— Byulleten' VAGO, No. 35. 1964.

THE THREE SYSTEMS CHARACTERIZING JUPITER'S ROTATION

I. N. POTAPOV
All-Union Astronomical and Geodetic Society, Kazan Branch

The rotation of Jupiter about its axis is described by three longitudinal systems: System I is derived from observations of the equatorial zone of of the planet and has a rotational period of $9^h50^m30^s.003$ /1/; System II has a period of $9^h54^m40^s.632$ /1/; System III was recently introduced, on the basis of radio-astronomical data, and it has a period of $9^h55^m29^s.37$ /1/. Since these periods are associated with actual objects in Jupiter's atmosphere, the relative altitude of these objects possibly can be found from consideration of the system to which they belong, but as yet there seems to be no general agreement concerning the vertical distribution of the various formations above the planet's surface /2/.

A rotating planet with a solid core and an atmosphere can be visualized as a sphere rotating in a viscous fluid. If the radius of the solid core is a and the angular velocity is ω_0, the linear velocity varies with the distance r above the solid surface according to the equation /3/:

$$v(r, \theta) = \frac{\omega_0 a^3 \sin\theta}{r^2}, \tag{1}$$

where θ (reckoned from the spin axis) varies from 0 to 180°. Equation (1) may be rewritten in the form

$$\omega(r) = \frac{A}{r^3}, \tag{2}$$

where A is a constant, equal to $\omega_0 a^3$.

Replacing ω by T, where T is the period of rotation, we get

$$r = a \sqrt[3]{T : T_0}. \tag{3}$$

In (3) T_0 is the rotation period of the solid core.

In order to calculate r by (3) we require the values of a and T_0, which are not directly available from observations. In our case we take for a the radius of the first density discontinuity in the Fesenkov—Masevich model of Jupiter's interior structure /4/, i. e., the outer radius of the intermediate layer consisting of hydrogen in a metallic state.

T_0 is obtained from the following empirical relation /5/ among the axial and orbital periods of planets:

$$T_2^{ax}\ T_2^{orb} = k\, T_1^{ax}\ T_1^{orb}, \tag{4}$$

where T^{ax} is the axial period of a planet, T^{orb} is the orbital period of the planet about the sun; T_2^{ax} is the axial period of the next planet from the sun whose orbital period is T_2^{orb}; k is a conversion factor, equal on the average to 2.75 for all the planets.

Let us write equation (4) for Jupiter, using the known values for Mars and Saturn:

$$T_{♃}^{orb} T_{♃}^{ax} = 2.75 T_{♂}^{orb} T_{♂}^{ax}, \quad (5)$$

$$T_{♄}^{orb} T_{♄}^{ax} = 2.75 T_{♃}^{orb} T_{♃}^{ax}. \quad (6)$$

From these equations we obtain two values for the period of rotation of Jupiter's surface, and the average result gives the unknown T_0. Admittedly, the value obtained in this way is only approximate, as it is difficult to fix the true value of k. However, even a rough approximation to T_0 can help to determine the vertical distribution of the various formations in Jupiter's atmosphere, according to the particular rotation system to which they belong; any correction in the value of T_0 would only affect the absolute altitudes obtained for the different systems.

From (5) and (6) we obtain for T_0 the value of 9^h84. Given now all the required data, we can calculate r_I, r_{II} and r_{III} by means of (3):

$$r_I = a, \; r_{II} = 5.7167 \cdot 10^9 \text{ cm}, \; r_{III} = 5.7163 \cdot 10^9 \text{ cm}.$$

These figures are obtained using the initial data

$$T_I = 9^h.84; \; T_{II} = 9^h.928; \; T_{III} = 9^h.925; \; T_0 = 9^h.84; \; a = 0.85 R.$$

These results identify the atmospheric layers responsible for the light zones, the dark belts, and the radio source used to define System III. System II is related to the outermost layers of Jupiter's atmosphere, while the motion of the deepest layers is represented by System I. System III occupies an intermediate position, but it is much nearer (by one order of magnitude) to System II than to System I. Since the dark belts belong in System II, it follows that the light zones lie deeper down in the atmosphere (assuming that they are cloud formations). However, if we take $r_I = a$, then the light zones actually ought to be areas of higher transparency which extend all the way down to the density discontinuity at the upper level of the intermediate layer. However the assumption ($r_I = a$) has to be taken with some reservation, as the factor k in equation (4) may be inaccurate.

The above results are comparable with the findings of other authors. Thus, from an analysis of the apparent changes on Jupiter's surface, Focas /6/ concludes that the belts are located in the upper layers of the atmosphere.

M. A. Klyakotko /7/ also concludes that the motion of the outer layers is described by System II, and that System I is associated with deeper layers. It is also suggested that the angular velocity of Jupiter's atmospheric layers decreases with increasing altitude above the planetary surface.

CONCLUSIONS

1. The angular velocity in Jupiter's atmosphere decreases with increasing altitude above the planetary surface.
2. The objects whose motion is described by System II are situated in the outer layers of Jupiter's atmosphere, higher than the formations which belong in Systems I and III.
3. System I associated with the motion of objects lying in the deepest layers of Jupiter's atmosphere.

Bibliography

1. Kurs astrofiziki i zvezdnoi astronomii (A Course in Astrophysics and Stellar Astronomy). 3.—Izdatel'stvo Nauka. 1964.
2. Sharonov, V. V. Priroda Planet (The Nature of the Planets).—Fizmatgiz. 1958.
3. Kochin, N. E. Teoreticheskaya gidromekhanika (Theoretical Hydromechanics).—Fizmatgiz. 1963.
4. Fesenkov, V. G. and A. G. Masevich.—Astronomicheskii Zhurnal, 28:317. 1951.
5. Tomchuk, L. G. Ob odnom neizvestnom empiricheskom zakone (On One Uncertain Empirical Law).—Byulleten' VAGO, No. 25. 1959.
6. Focas, J. H. Preliminary Results Concerning the Atmospheric Activity of Jupiter and Saturn. XI Internat. Astrophys. Colloq. The Physics of Planets, Univ. Liège, 9—10—11 July 1962.
7. Klyakotko, M. A. O stroenii atmosfery Yupitera (On the Structure of Jupiter's Atmosphere).—Byulleten' VAGO, No. 13(20). 1953.

[5442]

Printed in Jerusalem, Israel

TT 69-55026
NASA TT F-563